Journal of Molecular Spectroscopy **210,** 60–83 (2001)
doi:10.1006/jmsp.2001.8444, available online at http://www.idealibrary.com on IDEAL®

Comprehensive Evaluation and Compilation of H_3^+ Spectroscopy

C. Michael Lindsay and Benjamin J. McCall

Department of Chemistry, Department of Astronomy & Astrophysics, and the Enrico Fermi Institute, The University of Chicago, Chicago, Illinois 60637

Received May 10, 2001; in revised form September 4, 2001

Since its initial detection in 1980, there have been 17 laboratory studies of the H_3^+ infrared spectrum, reporting 895 transitions from a variety of fundamental, overtone, combination, and hot bands. The results of these two decades of labor, however, are difficult to utilize. There is no comprehensive list of the observed H_3^+ transitions, and the literature contains errors in frequency measurement and assignment due to the inherent difficulty of the measurements and the complexity of the spectrum. This paper resolves these problems while assembling all of the data into a single source. We have reviewed all reported transitions of H_3^+ for reliability in frequency measurement and have reassigned them based on a comparison with recent theoretical calculations. We have also developed a complete labeling scheme for all energy levels below 9000 cm^{-1}, which alleviates the confusion in assigning H_3^+ transitions that results from the difficulty of labeling the rovibrational energy levels of a molecule with such strong mixing. Our comprehensive linelist was then used to produce a set of 526 experimentally determined energy levels, which facilitates direct comparison with theoretical calculations and prediction of the "forbidden" pure rotation spectrum of H_3^+.

I. INTRODUCTION

H_3^+ plays important roles in many fields (*1*), including interstellar chemistry, the study of planetary ionosopheres, and theoretical calculation of rovibrational energy levels of polyatomic molecules. The detailed study of H_3^+ in these fields has only been possible because of the observation of infrared transitions of H_3^+ in laboratory discharges.

The laboratory detection (*2*) of the fundamental band $\nu_2 \leftarrow 0$ of H_3^+ opened the door to the detailed study of H_3^+ in astronomical sources. In dense interstellar clouds, spectra of H_3^+ have not only confirmed the general picture of ion-neutral chemistry but also allowed measurement of the physical conditions in the clouds (*3*, *4*). In diffuse clouds, H_3^+ has been observed (*5*) to be far more abundant than predicted by chemical models. H_3^+ has also been observed in emission from several planetary ionospheres (*6–9*) and has been used to image the plasma activity of the Jovian ionosphere (*10*).

Continued lab work on other vibrational bands of H_3^+ has allowed a detailed comparison with theoretical predictions of rovibrational energy levels from variational calculations. The variational approach is particularly well suited to H_3^+ because this simple system (consisting of only three protons and two electons) is amenable to detailed calculations.

Both astronomical spectroscopy and theoretical calculations of H_3^+ have advanced to the point where the quality of the existing laboratory database may soon hinder their progress. The state-of-the-art infrared spectrometers on large telescopes (*11*) have now achieved resolving powers of R $\approx$ 75000 (corresponding to a resolution of $\approx$0.03 cm^{-1} at 4 μm). Soon, this resolution may approach the precision of the existing laboratory data, and the ability of astronomers to accurately measure Doppler shifts (which measure the velocities of molecular clouds and the motions of planetary ionospheres) will be impeded. On the computational side, *ab initio* calculations have produced highly accurate potential energy surfaces for H_3^+ which take into account adiabatic and nonadiabatic corrections to the Born–Oppenheimer approximation, as well as relativistic corrections (*12–14*). Variational calculations of energy levels using these potentials are said to have an accuracy of a few hundredths of a wavenumber (*15*). Increasingly accurate laboratory frequencies (as well as reliable assignments of spectral lines) are essential to evaluate the quality of the newest theoretical calculations.

In order to provide transition frequencies of H_3^+ to theorists and astronomers, 17 laboratory spectroscopic studies (*2*, *16–31*) have been performed over the past two decades, resulting in the observation of over 800 different transitions. These experiments have probed a wide range of rotational and vibrational states in both emission and absorption using several different experimental techniques. The job of the laboratory spectroscopists has been a difficult one—many of the observations have been performed at the limits of sensitivity, making frequency measurements difficult. The assignment of H_3^+ transitions also poses a formidable task, due to strong mixing between rovibrational levels. Despite the best efforts of the spectroscopists, the literature still contains errors in frequencies as well as assignments.

Because the precision of theoretical and astronomical work is approaching that of the laboratory work, it is now important to correct these problems and produce a convenient and reliable

Supplementary data for this article are available on IDEAL (http://www.idealibrary.com) and as part of the Ohio State University Molecular Spectroscopy Archives (http://msa.lib.ohio-state.edu/jmsa_hp.htm).

collection of the laboratory data. In this work, we have reassigned all of the observed transitions, scrutinized the frequency measurements, and compiled a comprehensive list of transitions. Using this linelist, we have also calculated a set of experimentally determined energy levels for direct comparison with theory. This paper is intended to provide a convenient summary of H_3^+ laboratory spectroscopy and replaces the outdated lists of Kao *et al.* (*32*), Majewski *et al.* (*27*), and Dinelli *et al.* (*33*).

II. BACKGROUND

II.1. Theoretical Background

The quantum numbers, symmetry restrictions, energy level structure, and selection rules for H_3^+ have been discussed in detail elsewhere (*34, 35*). Here we provide a brief discussion of the basic concepts needed to understand the rovibrational spectroscopy of the ground electronic state of H_3^+.

II.1.1. Quantum Numbers

The total angular momentum (F) and the parity ($\pm$) are the only completely rigorous quantum numbers of any molecule, as a consequence of the isotropy and inversion symmetry of free space. For H_3^+, the total angular momentum F is the vector sum of the total nuclear spin angular momentum I and the angular momentum associated with the motion of the nuclei J. H_3^+ contains three spin 1/2 protons, so I is either 1/2 (referred to as *para*) or 3/2 (*ortho*). Because the interaction between the nuclear spin and nuclear motion is extremely weak, I and J can be considered good quantum numbers, along with $\pm$.

In addition to these good quantum numbers, there are several approximately good quantum numbers which help us understand the behavior of H_3^+ at low energies. These include v_1 and v_2, which specify the number of quanta in the ν_1 and ν_2 vibrational modes, as well as the vibrational angular momentum ℓ (associated with the degenerate ν_2 mode), which takes values of $v_2, v_2 - 2, \ldots, -v_2 + 2$, or $-v_2$.

For most molecules, the projection of J onto the molecular symmetry axis (k) is a good quantum number. In H_3^+, however, there is near degeneracy for levels with the same $|k - \ell|$ as a result of the form of the Coriolis interaction and the values of the B and C rotational constants.[1] These levels mix strongly by the l-resonance term, and it becomes useful to define a new quantum number $g \equiv k - \ell$ (*37*), which can be thought of as the portion of the projection of J onto the molecular axis that is due to the rotation of the molecular frame. Because the energy does not depend on the sign of g, $G \equiv |g|$ is usually used. G is a reasonably good quantum number at low energies.

[1] This near degeneracy is evident from the first three terms in the rotational energy expression, $E_{rot} \approx BJ(J+1) + (C-B)k^2 - 2C\zeta k\ell$. Consider the levels $|J, k, \ell\rangle = |J, g+\ell, \ell\rangle$ and $|J, g-\ell, -\ell\rangle$. In this approximation, the energy separation between these levels is $4g\ell(C - B - \zeta C)$, which is nearly zero because $B \approx 2C$ (due to the planarity of the molecule) and $\zeta = -1$ (for the triatomic equilateral triangle (*36*)). Because these levels have the same symmetry and a small energy difference, they will be strongly mixed (the mixing is particularly strong for $|\ell| = 1$ due to the ℓ-resonance term $q(q_+^2 J_+^2 + q_-^2 J_-^2)/4$).

II.1.2. Symmetry Restrictions and Energy Level Structure

The Pauli principle requires the total wavefunction to be antisymmetric with respect to (12) permutation of any two protons and symmetric upon cyclic permutation (123) of all three protons (i.e., the total wavefunction must belong to the A_2 representation). This requirement imposes a relationship between the nuclear spin modification and the quantum number G: when $I = 3/2$, only $G = 3n$ levels (and when $I = 1/2$, only $G = 3n \pm 1$ levels) have the proper symmetry. Additionally, certain $G = 0$ levels (most notably $J =$ even and $G = 0$ in the ground vibrational state) do not satisfy the symmetry requirement and therefore do not exist.

The energy level structure of H_3^+ is similar to that of a normal oblate symmetric top (when plotted versus G rather than k) except that certain levels come in pairs. These pairs are due to the two ways of forming the same G with different values of k and ℓ. Energy level diagrams for the ground and $v_2 = 2, \ell = 2$ vibrational states are plotted in Fig. 1.

II.1.3. Selection Rules

We first consider the electric dipole selection rules for the good quantum numbers I, J, and $\pm$. Because the dipole operator $\hat{\mu}$ does not operate on the nuclear spin wavefunctions, the nuclear spin must not change during a radiative transition, and thus the selection rule for I is $\Delta I = 0$. The total angular momentum F must obey the "triangle rule" for angular momentum addition [as $\hat{\mu}$ is a tensor of rank one and transforms as the spherical harmonics $Y_{1,0}$ and $Y_{1,\pm 1}$ (*38*)], and thus $\Delta F = 0$ or ± 1, and $0 \nleftrightarrow 0$. Since $\Delta I = 0$, the "triangle rule" also applies to J: $\Delta J = 0$ or ± 1, and $0 \nleftrightarrow 0$. The selection rule for the parity can be obtained by considering that the matrix elements of the dipole operator, $\langle \psi_f | \hat{\mu} | \psi_i \rangle$, must be totally symmetric. Since $\hat{\mu}$ changes sign with the inversion operation ($\vec{r} \to -\vec{r}$), the parity of the initial and final wavefunctions must be different ($+ \leftrightarrow -$).

The selection rule for g can be found by examining the symmetry of the wavefunctions (*34*) with respect to the cyclic permutation (123):

$$(123)\,|J, k, \ell\rangle = e^{\frac{2\pi i}{3}(k-\ell)}\,|J, k, \ell\rangle. \qquad [1]$$

Combining this with the required invariance of the transition dipole moment matrix elements with respect to (123), we see that

$$(123)\langle J', k', \ell' | \hat{\mu} | J'', k'', \ell'' \rangle = e^{\frac{2\pi i}{3}\{(k''-\ell'')-(k'-\ell')\}} \langle J', k', \ell' | \hat{\mu} | J'', k'', \ell'' \rangle \qquad [2]$$

which is only invariant when $\Delta g = (k'' - \ell'') - (k' - \ell') = 3n$.

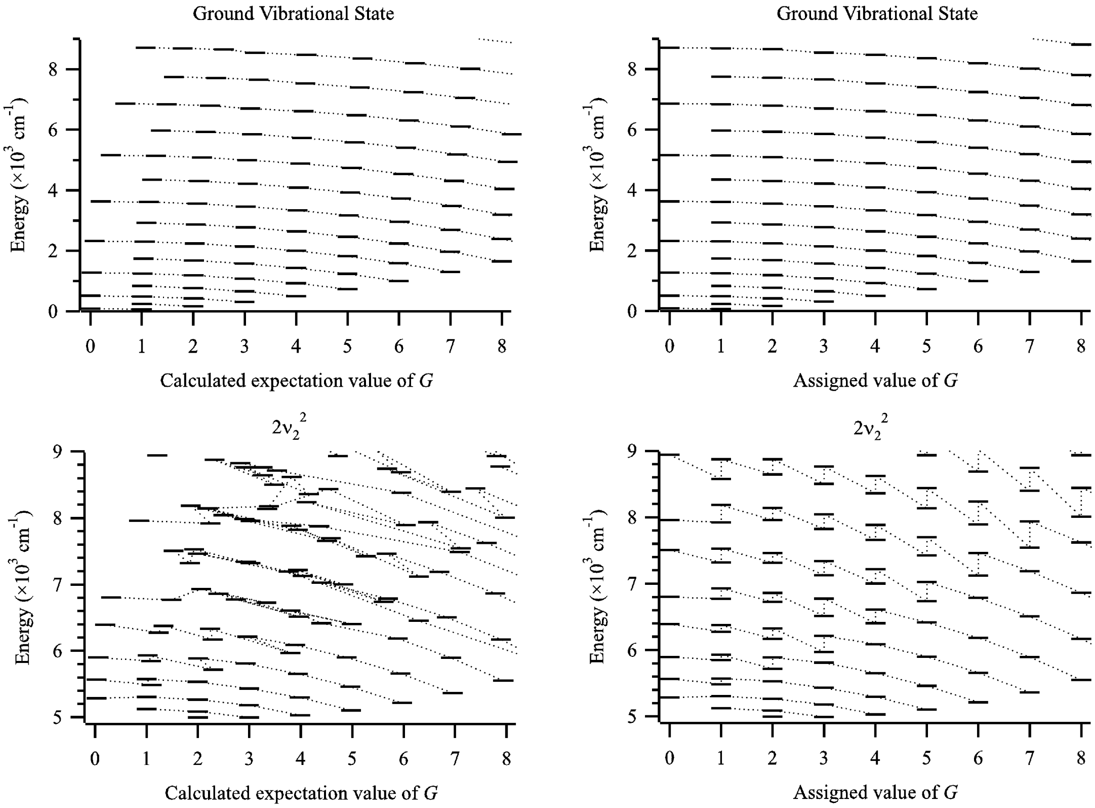

FIG. 1. Energy level diagrams of H_3^+ for the ground vibrational state (top two plots) and the $\nu_2 = 2$, $\ell = 2$ vibrational state (lower plots). (Dotted lines connect levels with the same J.) On the two left plots, Watson's calculated energy levels are plotted against the expectation values of G (see Section III.1 for comments on this calculation). On the right plots, the same energy levels are plotted versus our assigned values of G, presented in Table 3. Before being relabeled, the levels in the ground state look much like a classic oblate symmetric top with a small distortion in G at higher energy. The excited vibrational states are highly perturbed, and this mixing is the reason for many of the mislabeled transitions the literature. Once the G values are assigned, the energy level diagram looks relatively well behaved. Similar figures for every vibrational state below 9000 cm^{-1} are available online (*39*).

The possible selection rules for k (the projection of J) can be derived from the "triangle rule" to be $\Delta k = 0$ or ± 1. Because the parity is linked to k by the symmetry of the wavefunctions (*34*) with respect to the inversion (E^*) operation

$$E^*|J, k, \ell\rangle = (-1)^k |J, k, \ell\rangle \qquad [3]$$

and because the parity selection rule is $+ \leftrightarrow -$, Δk must be odd, restricting its selection rule to $\Delta k = \pm 1$.

The selection rule for ℓ depends on those of g and k:

$$\Delta g = g' - g'' = (k' - \ell') - (k'' - \ell'') = \Delta k - \Delta \ell$$
$$\Delta \ell = \Delta k - \Delta g = (\pm 1) - (\pm 3n) \qquad [4]$$
$$\Delta \ell \neq 3n.$$

For transitions with $\Delta \ell = \pm 1$ (e.g., the $\Delta \nu_2 = 1$ fundamental and hot bands), Δg must be 0, and for transitions with $\Delta \ell = \pm 2$ ($\Delta \upsilon_2 = 2$ overtone bands), Δg must be ± 3.

It should be kept in mind that the selection rules for g, k, and ℓ are not rigorous, because these quantum numbers are not rigorous. For example, the $\Delta k = \pm 1$ selection rule can break down due to mixing, but $\Delta k =$ odd is maintained because it is based on the parity, which is a rigorously good quantum number.

Finally, we consider the selection rules (which are only approximate) for the vibrational quantum numbers. The ν_1 normal mode is totally symmetric and therefore has the selection rule[2] $\Delta \upsilon_1 = 0$. For the symmetry-allowed ν_2 mode, the selection rule $\Delta \upsilon_2 = \pm 1$ holds in the approximation of using harmonic oscillator wavefunctions and only the first order term in the Taylor series expansion of $\hat{\mu}$. Because the H_3^+ potential and dipole operator are very anharmonic, this is a poor approximation, and transitions with $\Delta \upsilon_2 > 1$ have reasonable intensity.

[2] The selection rule $\Delta \upsilon_1 = 0$ requires some qualification. The band $\nu_1 \leftarrow 0$ has the vibrational symmetry $A_1 \leftarrow A_1$, which is forbidden, but can become allowed via the rotation–vibration interaction. Bands such as $\nu_1 + \nu_2 \leftarrow \nu_2$ are qualitatively different in that they have vibrational symmetry $E \leftarrow E$, which is allowed through a vibrational interaction alone (*24*). All of these bands are very weak because the change in the dipole moment is small upon excitation of totally symmetric mode, but $\nu_1 \leftarrow 0$ is by far the weakest, since it relies on an accidental degeneracy for the rotation–vibration interaction to be effective.

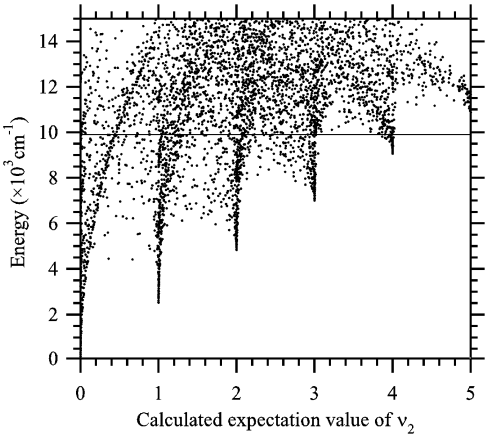

FIG. 2. Rovibrational energy of H_3^+ plotted against the expectation value of the approximate quantum number υ_2. Energies and expectation values (see Section III.1 for comments on this calcluation) are from the calculations of Watson (*27, 54*). The solid line is drawn at the barrier to linearity. This plot shows that at lower energies, υ_2 describes the system quite well, but at higher energies, the amount of mixing increases to the point where the value of this approximate quantum number has little meaning.

II.1.4. Effects of Mixing

Levels with the same good quantum numbers [J, I, and $\pm$] can mix with one another. The strength of the mixing is inversely proportional to the energy separation between the two unmixed levels, so that strong mixing is increasingly common at higher energies where the levels tend to be more closely spaced. When mixing occurs, the energy levels are shifted from the oblate symmetric top energy pattern and the approximate quantum numbers break down. The mixed states can no longer be described by single integral values of g, ν_1, ν_2, and ℓ, but can be described by their expectation values, which are linear combinations of the quantum numbers of the unmixed values. The extent of the mixing can be visualized by plotting the energy versus the expectation values of the quantum numbers (see Figs. 1 and 2). When the energy levels are not significantly mixed, the expectation values of their quantum numbers will be nearly integral.

The selection rules for mixed levels incorporate the selection rules of each of the levels involved in the mixing. A consequence of this mixing is the appearance of additional lines in the spectrum—forbidden transitions effectively borrow intensity from allowed ones. One example of these forbidden transitions is the pure rotational transitions, which obey the selection rule $\Delta\ell = 0$. These transitions are weak, but should be observable experimentally (see Section IV.1). Each transition's intensity will depend on the magnitude of mixing, and must be treated on a line by line basis. The topic of rovibrational level mixing and the breakdown of the approximate quantum numbers is discussed further in Section III.1.

II.2. Previous Laboratory Work

Many infrared absorption and emission studies of H_3^+ have been performed in the laboratory over the past two decades to characterize the rovibrational spectrum and energy levels of H_3^+ (see (*40*) for a recent review). These works were considered in our analysis and in this section we briefly summarize each of them (see Table 1). It should be noted that the predissociation spectrum of H_3^+ has also been measured in the laboratory (*41–43*) and is the subject of a recent review (*44*). This subject, however, lies outside the scope of this paper.

The infrared spectrum of H_3^+ was initially sought after by Herzberg in the mid 1960s when it became clear that H_3^+ did not possess a stable excited electronic state (*45*). In the course of this work he observed a group of emission lines near 3600 cm^{-1} in hydrogen hollow-cathode discharges. These were eventually identified by Watson as emission lines of neutral H_3, which are produced in excited states after dissociative recombination of H_5^+ with electrons. It was not until 1980 that Oka (*2*) observed in absorption the first 15 lines of the ν_2 fundamental of H_3^+ between 2450 and 2950 cm^{-1}. His success was made possible by the development of the broadly tunable difference frequency (DF) spectrometer by Pine (*46*) and the use of the long positive column discharge by Woods (*47*). In his search he scanned roughly 500 cm^{-1}, a feat only possible with the DF laser. To increase the sensitivity, he frequency modulated the radiation and achieved a signal-to-noise ratio of ~30 for the strongest H_3^+ lines. In the first studies, a liquid-nitrogen-cooled positive column discharge was used to produce H_3^+ in a pure hydrogen discharge.

In the year that followed, Oka (*16*) was able to extend his observations to higher J levels (to a total of 30 lines) by studying a warmer, ice-cooled discharge. By 1984, the frequency coverage was expanded by making adjustments to the DF laser and by using diode lasers. Two major advances in sensitivity also occured. It was found that modulating the discharge current (concentration modulation (*48*)) or applying an AC field across a positive column discharge (velocity modulation (*49*)) could substantially improve the sensitivity. The combination of these improvements enabled Watson, Oka, and co-workers (*17*) to observe an additional 16 $\nu_2 \leftarrow 0$ transitions, bringing the total up to 46.

All of the observed lines up to this point were from levels with $J \leq 5$, and it was expected that large perturbations would occur at higher J between the ν_1 and ν_2 states. With this in mind, Majewski *et al.* (*18*) in Ottawa constructed a high-pressure hollow-cathode discharge coupled to a Fourier transform infrared (FTIR) spectrometer to observe the emission of H_3^+ in a hydrogen discharge. With an ingeniously designed hollow-cathode discharge and a pressure discrimination method, this technique turned out to be very effective, nearly tripling the number of observed lines and probing levels up to $J' = 10$. Many perturbations were indeed observed, and they provided a new test for theoretical calculations. Many additional emission features were recorded around 2 μm. At the time, the authors could not rule out the possibility that the 2-μm lines were due to Rydberg H_2 or H_3 neutral transitions, and consequently the lines were not reported.

In 1987 Trafton *et al.* (*6*) and in 1988 Drossart *et al.* (*7*) stumbled upon a rich set of unidentified emission features at 2 μm while observing H_2 emission in Jupiter. This prompted

TABLE 1
Summary of the Laboratory Spectroscopic Studies of H_3^+

Label	cm^{-1}	Observed	Assignment	Technique[a]	Reference
Oka80	2450–2950†	15 lines	$\nu_2 \leftarrow 0$	*l*-N_2 cooled positive column, DF laser, FM detection	T. Oka, *Phys. Rev. Lett.* **45,** 531–534 (1980).
Oka81	2450–3030†	30 lines (15 new)	$\nu_2 \leftarrow 0$	*l*-N_2 and ice-water cooled positive column, DF laser, FM detection	T. Oka, *Phil. Trans. R. Soc. Lond. A* **303,** 543–549 (1981).
Wat84	2210–3030†	46 lines (16 new)	$\nu_2 \leftarrow 0$	*l*-N_2 cooled positive column, DF and diode lasers, VM and CM detection	J. K. G. Watson, S. C. Foster, A. R. W. McKellar, P. Bernath, T. Amano, F. S. Pan, M. W. Crofton, R. S. Altman, and T. Oka, *Can. J. Phys.* **62,** 1875–1885 (1984).
Maj87	1800–3300	113 lines (67 new)	$\nu_2 \leftrightarrow 0$	Water cooled, high-pressure hollow cathode, FTIR emission, and diode laser absorption	W. A. Majewski, M. D. Marshall, A. R. W. McKellar, J. W. C. Johns, and J. K. G. Watson, *J. Mol. Spectrosc.* **122,** 341–355 (1987).
Maj89	4500–5100	47 new lines	$2\nu_2^2 \rightarrow 0$	Water cooled, high-pressure hollow cathode, FTIR emission	W. A. Majewski, P. A. Feldman, J. K. G. Watson, S. Miller, and and J. Tennyson, *Astrophys. J.* **347,** L51–L54 (1989).
Nak90	2400–2800	12 re-measured	$\nu_2 \leftarrow 0$	Water cooled hollow cathode, FTIR absorption	T. Nakanaga, F. Ito, K. Sugawara, H. Takeo, and C. Matsumura, *Chem. Phys. Lett.* **169,** 269–273 (1990).
Baw90	2080–2950†	14 new lines	$\nu_2 \leftarrow 0$	*l*-N_2 cooled positive column, DF laser, VM detection	M. G. Bawendi, B. D. Rehfuss, and T. Oka, *J. Chem. Phys.* **93,** 6200–6209 (1990).
		70 new lines	$2\nu_2^2 \leftarrow \nu_2$		
		14 new lines	$2\nu_2^0 \leftarrow \nu_2$		
		21 new lines	$\nu_1 + \nu_2 \leftarrow \nu_1$		
		136 new lines	unassigned		
Xu90	4550–6000†	34 lines (7 new)	$2\nu_2^2 \leftarrow 0$	*l*-N_2 cooled positive column, DF laser, VM detection	L.-W. Xu, C. M. Gabrys, and T. Oka, *J. Chem. Phys.* **93,** 6210–6215 (1990).
Lee91	6860–6900†	4 new lines	$3\nu_2^1 \leftarrow 0$	*l*-N_2 cooled positive column, diode laser, VM detection	S. S. Lee, B. F. Ventrudo, D. T. Cassidy, T. Oka, S. Miller, J. Tennyson, *J. Mol. Spectrosc.* **145,** 222–224 (1991).
Xu92	2400–3300†	9 new lines	$\nu_1 \leftarrow 0$	*l*-N_2 cooled positive column, DF laser, VM detection	L.-W. Xu, M. Rösslein, C. M. Gabrys, and T. Oka, *J. Mol. Spectrosc.* **153,** 726–737 (1992).
		21 new lines	$\nu_1 + \nu_2 \leftarrow \nu_2$		
		30 new lines	$\nu_2 \leftarrow 0$		
		13 new lines	$2\nu_2^2 \leftarrow \nu_2$		
		89 new lines	unassigned		
Ven94	6800–7270†	15 lines (11 new)	$3\nu_2^1 \leftarrow 0$	*l*-N_2 cooled positive column, diode laser, VM detection	B. F. Ventrudo, D. T. Cassidy, Z. Y. Guo, S. Joo, S. S. Lee, and T. Oka, *J. Chem. Phys.* **100,** 6263–6266 (1994).
Uy94	2690–3580†	75 lines (37 new)	$\nu_2 \leftarrow 0$	Water cooled positive column, DF laser, VM detection	D. Uy, C. M. Gabrys, M.-F. Jagod, and T. Oka, *J. Chem. Phys* **100,** 6267–6274 (1994).
Maj94	1800–2550	52 new lines	$\nu_2 \rightarrow 0$	Water cooled, high-pressure hollow cathode, FTIR emission	W. A. Majewski, A. R. W. McKellar, D. Sadovskií, and J. K. G. Watson, *Can. J. Phys.* **72,** 1016–1027 (1994).
	2900–5000	9 new lines	$2\nu_2^2 \rightarrow 0$		
		12 new lines	$\nu_1 + \nu_2 \rightarrow \nu_1$		
		31 new lines	$2\nu_2^2 \rightarrow \nu_2$		
		16 new lines	$2\nu_2^0 \rightarrow \nu_2$		
		2 new lines	$3\nu_2^3 \rightarrow \nu_2$		
		1 new line	$3\nu_2^3 \rightarrow 2\nu_2^2$		
McK98	2450–2850	27 re-measured	$\nu_2 \leftarrow 0$	Refrig. methanol cooled hollow cathode, FTIR absorption	A. R. W. McKellar and J. K. G. Watson, *J. Mol. Spectrosc.* **191,** 215–217 (1998).
Joo00	~1550	1 new line	$\nu_2 \leftarrow 0$	*l*-N_2 cooled positive column, diode laser, VM detection	S. Joo, F. Kühnemann, M.-F. Jagod, and T. Oka, *The Royal Society Discussion Meeting on Astronomy, Physics and Chemistry of H_3^+*, London, February 9–10 (2000) (poster).
McC00	7850–8170	28 new lines	$\nu_1 + 2\nu_2^2 \leftarrow 0$	*l*-N_2 cooled positive column, diode laser, VM detection	B. J. McCall and T. Oka, *J. Chem. Phys.* **113,** 3104–3110 (2000).
		2 new lines	$2\nu_1 + \nu_2 \leftarrow 0$		
Lin01	3000–4200	6 lines (5 new)	$\nu_2 \leftarrow 0$	*l*-N_2 cooled positive column, CCL, VM detection	C. M. Lindsay, R. M. Rade, Jr., and T. Oka, *J. Mol. Spectrosc.* **210,** 51–59 (2001).
		22 lines (10 new)	$\nu_1 \leftarrow 0$		
		5 lines (4 new)	$2\nu_2^0 \leftarrow \nu_2$		
		76 lines (44 new)	$2\nu_2^2 \leftarrow \nu_2$		
		4 lines (3 new)	$2\nu_2^2 \leftarrow \nu_1$		
		1 new line	$2\nu_2^0 \leftarrow \nu_1$		
		25 lines (9 new)	$\nu_1 + \nu_2 \leftarrow \nu_2$		
		14 lines (7 new)	$\nu_1 + \nu_2 \leftarrow \nu_1$		
		2 new lines	$2\nu_1 \leftarrow \nu_1$		
		1 re-measured	$\nu_1 + 2\nu_2^2 \leftarrow \nu_1 + \nu_2$		
		3 lines (2 new)	$3\nu_2^3 \leftarrow 2\nu_2^2$		
		3 lines (1 new)	$3\nu_2^1 \leftarrow 2\nu_2^0$		
		6 lines (5 new)	unassigned		

[a] Abbreviations used in this column are defined as follows: FM = frequency modulation; VM = velocity modulation; DF = difference frequency; CM = concentration modulation; CCL = color center laser.

† Region was not scanned continuously.

the Ottawa group to revisit the 2 μm lines observed with the FTIR emission apparatus, and after a month, Watson assigned many of the FTIR and Jovian features to the $2\nu_2^2 \leftarrow 0$ band of H_3^+. The new-found confidence in these assignments was based upon the latest *ab initio* calculations of Miller and Tennyson (*50*) as well as the yet-to-be published work on the $2\nu_2^2 \leftarrow \nu_2$ hot band by Bawendi *et al.* in Chicago (see below). Once assigned, 47 lines of the $2\nu_2^2 \leftarrow 0$ band were reported from the FTIR studies (*19*).

Quite apart from the work in Chicago and Ottawa, Nakanaga and co-workers in 1990 successfully performed the first FTIR *absorption* spectroscopy of molecular ions, including 12 fundamental transitions of H_3^+ (*20*). While all of these lines had been observed initially 9 years earlier, this work represented the first accurate measurement of the relative absorption intensities.

After several years of refining their technique of DF laser/velocity modulation spectroscopy of carbocations (*51*) and introducing the helium-dominated positive column discharge, the Chicago group revisited H_3^+ with a tremendous increase in sensitivity. The next 5 years brought seven experiments which substantially increased the number of probed levels. Initially, Bawendi *et al.* (*21*) observed lines of the $2\nu_2^2 \leftarrow \nu_2$, $2\nu_2^0 \leftarrow \nu_2$, and $\nu_1 + \nu_2 \leftarrow \nu_1$ hot bands as well as 14 new fundamental lines and 136 lines which they could not confidently assign. Shortly after, Xu *et al.* (*22*) observed the $2\nu_2^2 \leftarrow 0$ band, though they only observed seven lines not covered in Majewski's work. Two years later, Xu *et al.* (*24*) reported the $\nu_1 \leftarrow 0$ and $\nu_1 + \nu_2 \leftarrow \nu_2$ forbidden bands, as well as more transitions from the $\nu_2 \leftarrow 0$ and $2\nu_2^2 \leftarrow \nu_2$ bands, and additional unassignable lines. Advances in external cavity near infrared diode lasers enabled the scanning to be extended to higher frequency allowing the second overtone, $3\nu_2^1 \leftarrow 0$, to be observed (*23, 25*). During this period a diode laser was also used to measure the lowest frequency line to date (the $\nu_2 \leftarrow 0$ $P(12, 12)$ at 1546.901 cm^{-1}), though this was only reported recently (*29*). Finally, Uy and co-workers (*26*) recorded an H_3^+ spectrum with a water-cooled cell and observed highly excited rotational levels of the ν_2 fundamental, up to $J' = 16$.

With the large amount of experimental data made available, Watson (*52, 27*) and, independently, Dinelli *et al.* (*53*) produced empirically fitted potentials which were used to calculate more accurate transition frequencies (see Section 4.2 for more details). All of the experimental data available at the time, as well as some newly measured FTIR emission lines (*27*), were collected and included in these calculations. These calculations proved to be essential to understanding the unassigned lines in Bawendi's and Xu's (1992) data, which were assigned in subsequent papers (*27, 33*).

Four years later, McKellar and Watson recorded a clean broadband absorption spectrum of H_3^+ with an FTIR spectrometer. Their work was similar to that of Nakanaga *et al.* 8 years earlier, but achieved about a factor of 10 improvement in signal-to-noise ratio enabling them to observe 27 lines of the ν_2 fundamental. This beautiful spectrum has been published in its entirety in a letter (*28*).

No new data were reported until the year 2000 when McCall and Oka (*30*) recorded lines from the $\nu_1 + 2\nu_2^2 \leftarrow 0$ and $2\nu_1 + \nu_2 \leftarrow 0$ combination bands using an external cavity diode laser and the velocity modulation/positive column discharge technique. Thirty lines were observed from these two bands, probing the highest vibrational states observed to date.

Most recently, Lindsay and co-workers (*31*) used a computer-controlled color center laser (CCL) spectrometer to continuously scan H_3^+ from 3000–4200 cm^{-1}. The improved sensitivity of their spectrometer and the hottest discharge to date enabled them to study very high rovibrational levels. A total of 96 new transitions were observed from a variety of hot, overtone, fundamental, and forbidden bands—some probing rovibrational levels in the vicinity of the barrier to linearity.

A total of 895 unique transitions of H_3^+ have been reported over the past 21 years, probing every vibrational state below the barrier to linearity (except $3\nu_1$ and $4\nu_2$). Many of these transitions have been recorded multiple times by multiple techniques with multiple sensitivities. This work was only possible with substantial advancements to the sensitivity of the experiments, which improved dramatically over the last 21 years. It is interesting to note that if the sensitivity of the latest studies were applied to the transitions observed by Oka in 1980, the signal-to-noise ratio would be 3000–6000—a two-orders-of-magnitude improvement over the initial spectrum!

III. ANALYSIS AND RESULTS

In this section we explain our efforts to assign approximate quantum numbers to every energy level below 9000 cm^{-1}, evaluate the assignment and quality of every reported laboratory absorption and emission transition, and determine energy levels from the experimental transitions. Most of the results of this work are tabulated here in print, but an electronic version of the complete work (tables and figures) is available online (*39*).

III.1. Labeling of Rovibrational Levels below 9000 cm^{-1}

Much of the confusion in "assigning" transitions in the literature is based upon energy level labeling and not the actual assignment of the transitions. This distinction is important—most of the assignments (that is the identification of an observed transition based on a particular calculated transition between two levels with a similar frequency and intensity) were correctly made, but there has been confusion in the naming of the transition and energy levels which were involved in the transition. Before each transition can be labeled, every energy level must be given a unique label. Below the barrier to linearity, the approximate quantum numbers G, v_1, v_2, and ℓ are reasonably good and can be used to label rovibrational energy levels. Many of these levels mix, and the resulting levels have character of two or more levels with different values of the approximate quantum numbers. In most cases this mixing is not complete, and

TABLE 2
Heavily Mixed Rovibrational Levels of H_3^+ below 9000 cm^{-1} (Each Row Corresponds to a Set of Mixed Levels)

$\nu_1 + 2\nu_2^0$ (5,4)	$\nu_1 + 2\nu_2^0$ (5,2)	$\nu_1 + 2\nu_2^2$ (5,2)*l*	$\nu_1 + 2\nu_2^2$ (5,2)*u*
$3\nu_2^3$ (6,2)*l*	$3\nu_2^1$ (6,2)*u*	$\nu_1 + 2\nu_2^2$ (6,3)	
$2\nu_2^2$ (7,0)	$\nu_1 + \nu_2$ (7,3)*l*		
$\nu_1 + \nu_2$ (7,3)*u*	ν_1 (7,6)		
$\nu_1 + \nu_2$ (7,5)*l*	$2\nu_2^2$ (7,4)*u*		
ν_1 (8,6)	$\nu_1 + \nu_2$ (8,3)*u*		
$2\nu_2^0$ (8,2)	$2\nu_2^2$ (8,2)*u*		
$\nu_1 + \nu_2$ (8,5)*l*	ν_1 (8,8)		
ν_2 (9,2)*u*	ν_1 (9,5)		
$2\nu_2^2$ (9,5)*l*	$2\nu_2^0$ (9,1)		
$2\nu_2^2$ (9,1)*u*	$\nu_1 + \nu_2$ (9,2)*l*		
$2\nu_2^0$ (9,3)	$2\nu_2^2$ (9,3)*u*		
ν_1 (10,5)	ν_2 (10,2)*u*		
$2\nu_2^0$ (10,2)	$2\nu_2^2$ (10,4)		
$\nu_1 + \nu_2$ (11,9)*l*	$2\nu_2^2$ (11,6)		
ν_2 (12,6)*l*	ν_1 (12,9)		

each mixed level can be labeled by the quantum numbers of the dominant unmixed level.

Theoretical calculations of energy levels provide only the quantum numbers J, parity, and (in most cases) I—the assignment of the approximate quantum numbers to each level must be done manually. This task would be nearly impossible without the help of the expectation values calculated by Watson (*54*). Even with the expectation values, this task is not easy. One can appreciate the difficulty in applying labels by examining the energy dependence of various expectation values. In Fig. 2 the energy is plotted versus the expectation value of v_2. At energies close to each band origin, the values of $\langle v_2 \rangle$ are very close to integers. As the energy approaches 10 000 cm^{-1} however, many levels have expectation values in between the integer values, as a result of mixing. Likewise, we can look at the expectation values of G (Fig. 1). While well behaved in the ground vibrational state (top left), G becomes extremely mixed at higher vibrational states (bottom left). By carefully considering the energy, the expectation values of G, v_1, v_2, and ℓ, and the values of J, I, and parity of all of the levels simultaneously, it is possible to assign integral values of G, v_1, v_2, and ℓ for each energy level (Fig. 1 right, top and bottom). We have produced energy level diagrams similar to those in Fig. 1 for all vibrational states below 9000 cm^{-1}, and these are available online (*39*). Please note that these calculated expectation values are only approximate and were performed with the intention of forming a qualitative picture of the nature of the energy levels (*54*).

The five quantum numbers J, G, v_1, v_2, and ℓ are not sufficient to uniquely label each level. For levels with $\ell \neq 0$ and $(J - |\ell|) \geq G \geq 1$ there are two ways to form the same G for different values of k. Take as an example a level where $\ell = 1$ and $J = 2$. Since $G \equiv |k - \ell|$, both $k = 0$ and $k = 2$ make $G = 1$. These levels always differ in energy, and we have distinguished them by assigning a "*u*" and an "*l*" to the upper and lower energy level, respectively (*30*). In the earliest papers, these levels were designated by "I" or "II" (*2, 16*) or later with "+" or "−". Also used was the U notation initially defined by Watson (*34*) as $+1$ for "*u*" levels and -1 for "*l*" levels of the ν_2 vibrational state. Later, Miller and Tennyson (*50*) extended the notation to arbitrary v_2 by redefining $U = +|\ell|$ for "*u*" and $U = -|\ell|$ for "*l*" levels. We have abandoned these other notations due to the confusion with the value of the real quantum numbers ℓ and parity. We instead use the symbol (*40*)

$$(J, G)\{u \mid l\} \qquad [5]$$

to label individual rotational levels within the vibrational state,

$$v_1\nu_1 + v_2\nu_2^{|\ell|} \quad \text{or} \quad v_1 v_2^{|\ell|}. \qquad [6]$$

A small number of levels are so badly mixed that the assignment of their approximate quantum numbers is almost arbitrary. In some cases the expectation value of one quantum number suggests an assignment to one vibrational state, while another suggests a different vibrational state. Table 2 lists all of the badly mixed levels below 9000 cm^{-1}. Above 9000 cm^{-1}, the density of states becomes quite large and severe mixing occurs for many levels with $J \gtrsim 5$. For these levels, it probably is not useful to assign approximate quantum numbers. It should still be possible, however, to label low J levels with approximate quantum numbers because their density of states is much lower and the mixing will be less complete. At very high energy, even the low J levels will mix and their approximate quantum numbers will eventually fail. When this occurs, levels will have to be labeled by the only good quantum numbers $(J, I, \pm)$ and the energy-ordering index n.

The results of our energy level labeling scheme are listed in Table 3. Every rovibrational level below 9000 cm^{-1} has been labeled with J, G, v_1, v_2, ℓ, and (where appropriate) u or l. A few levels have been labeled above 9000 cm^{-1}, corresponding to the upper states of some of the experimentally observed transitions. We have related these labels to the quantum numbers usually used in the theoretical calculations, J, I, parity, and n. Note that our assignment of n, the index ordering levels with the same J, I, and parity by energy, is not necessarily final. We based n on the ordering of the energy levels in the calculations of Watson. It is possible, though unlikely, that for very closely spaced energy levels, the ordering of these levels may change in more accurate calculations, thus changing the assigned values of n. Also included in this table are the experimentally determined energy levels, which are the subject of Section III.3.

Our work is not the first attempt at labeling the energy levels. In 1994, Majewski *et al.* (which we refer to as Maj94 for the remainder of the paper) labeled each of the experimentally determined levels available at the time. This list was later expanded by Dinelli *et al.* (Din97) (*33*) to include many of the levels below 9000 cm^{-1}. The list of Din97 is not complete, however; 273 levels were left unlabeled. Of the roughly 720 levels that our work and Din97 have in common, 79 levels differ in assignment. Ten

TABLE 3
Energy Level Labels and Experimentally Determined Energy Levels

Q. N.[a]	E_{calc}[b]	E_{exp}[c]	Label[d]		Q. N.[a]	E_{calc}[b]	E_{exp}[c]	Label[d]		Q. N.[a]	E_{calc}[b]	E_{exp}[c]	Label[d]	
J I P n	(cm^{-1})	(cm^{-1})	Rot.	Vib.	*J I P n*	(cm^{-1})	(cm^{-1})	Rot.	Vib.	*J I P n*	(cm^{-1})	(cm^{-1})	Rot.	Vib.
1 *p* − 1	64.123	64.121(00)*	(1,1)	00^0	1 *p* − 3	3240.678	3240.739(18)*	(1,1)	10^0	10 *p* − 3	4348.219	4348.435(64)	(10,1)	00^0
1 *o* + 1	86.959	86.960(00)*	(1,0)	00^0	4 *p* − 3	3260.197	3260.219(07)*	(4,2)*l*	01^1	8 *p* + 4	4371.260	4371.318(09)*	(8,7)*l*	01^1
2 *p* + 1	169.296	169.295(04)*	(2,2)	00^0	1 *o* + 2	3263.054	3263.145(16)	(1,0)	10^0	6 *p* + 7	4378.282	4378.380(10)*	(6,1)*u*	01^1
2 *p* − 1	237.350	237.356(05)*	(2,1)	00^0	6 *p* + 3	3269.582	3269.591(09)*	(6,7)	01^1	6 *p* − 7	4389.279	4389.287(09)	(6,5)	10^0
3 *o* − 1	315.342	315.349(04)*	(3,3)	00^0	5 *p* + 3	3300.113	3300.141(08)*	(5,5)	01^1	5 *p* − 8	4398.694		(5,1)	10^0
3 *p* + 1	428.009	428.018(07)*	(3,2)	00^0	4 *p* + 4	3326.091	3326.118(08)*	(4,1)*l*	01^1	6 *o* − 3	4400.982	4401.056(10)*	(6,0)	01^1
3 *p* − 1	494.753	494.775(07)*	(3,1)	00^0	9 *p* + 2	3335.438	3335.559(19)*	(9,4)	00^0	5 *o* + 4	4419.137		(5,0)	10^0
4 *p* + 1	502.023	502.032(06)*	(4,4)	00^0	2 *p* + 4	3343.086	3343.147(14)*	(2,2)	10^0	7 *p* − 5	4420.158	4420.218(14)*	(7,4)*l*	01^1
3 *o* + 1	516.867	516.873(07)*	(3,0)	00^0	4 *p* − 4	3351.353	3351.385(08)*	(4,2)*u*	01^1	7 *p* + 5	4431.609	4431.693(08)*	(7,5)*u*	01^1
4 *o* − 1	658.698	658.720(06)*	(4,3)	00^0	11 *p* + 1	3352.780		(11,10)	00^0	13 *o* + 1	4449.473		(13,12)	00^0
5 *p* − 1	728.991	729.022(07)*	(5,5)	00^0	5 *p* − 3	3396.514	3396.519(09)*	(5,4)*l*	01^1	7 *p* − 6	4456.873	4456.867(09)*	(7,7)	10^0
4 *p* + 2	768.451	768.476(09)*	(4,2)	00^0	12 *o* + 1	3402.858		(12,12)	00^0	14 *p* + 1	4494.966		(14,14)	00^0
4 *p* − 1	833.555	833.583(08)*	(4,1)	00^0	2 *p* − 3	3409.771	3409.825(15)*	(2,1)	10^0	10 *p* + 5	4539.221		(10,11)	01^1
5 *p* + 1	928.943	928.965(10)*	(5,4)	00^0	4 *p* + 5	3423.085	3423.125(08)*	(4,1)*u*	01^1	11 *o* + 1	4544.240	4544.410(22)	(11,6)	00^0
6 *o* + 1	995.842	995.884(05)*	(6,6)	00^0	4 *o* − 2	3447.011	3447.031(09)*	(4,0)	01^1	7 *o* + 3	4562.728	4562.825(10)*	(7,3)*l*	01^1
5 *o* − 1	1080.453	1080.490(08)*	(5,3)	00^0	9 *o* − 2	3460.941	3461.058(17)*	(9,3)	00^0	8 *p* + 5	4567.212	4567.277(08)*	(8,7)*u*	01^1
5 *p* + 2	1187.067	1187.115(10)*	(5,2)	00^0	10 *p* − 1	3484.646	3484.761(16)*	(10,7)	00^0	6 *p* + 8	4575.977	4575.987(14)	(6,4)	10^0
6 *p* − 1	1238.409	1238.462(11)*	(6,5)	00^0	3 *o* − 3	3485.258	3485.306(12)*	(3,3)	10^0	9 *o* + 3	4605.661	4605.735(33)*	(9,9)	01^1
5 *p* − 2	1250.267	1250.313(10)*	(5,1)	00^0	5 *p* − 4	3510.119	3510.142(07)*	(5,4)*u*	01^1	12 *o* − 1	4634.047		(12,9)	00^0
5 *o* + 1	1271.225	1271.245(10)*	(5,0)	00^0	7 *p* − 4	3530.235	3530.252(16)*	(7,8)	01^1	7 *p* − 7	4635.928	4636.020(09)*	(7,4)*u*	01^1
7 *p* − 1	1302.095	1302.141(09)*	(7,7)	00^0	5 *o* + 2	3553.304	3553.333(09)*	(5,3)*l*	01^1	8 *o* − 2	4650.861	4650.945(08)*	(8,6)*l*	01^1
6 *p* + 1	1430.667	1430.706(11)*	(6,4)	00^0	9 *p* + 3	3555.305	3555.438(35)	(9,2)	00^0	7 *p* − 8	4663.773	4663.887(14)*	(7,2)*l*	01^1
6 *o* − 1	1577.279	1577.334(09)*	(6,3)	00^0	6 *o* − 2	3569.436	3569.467(07)*	(6,6)	01^1	6 *o* − 4	4719.294	4719.259(11)	(6,3)	10^0
7 *o* + 1	1586.535	1586.594(08)*	(7,6)	00^0	3 *p* + 4	3595.694	3595.739(20)	(3,2)	10^0	7 *p* + 6	4720.296	4720.421(17)	(7,1)*l*	01^1
8 *p* + 1	1647.199	1647.267(12)	(8,8)	00^0	9 *p* − 3	3609.462	3609.643(52)	(9,1)	00^0	7 *o* + 4	4721.787	4721.794(07)	(7,6)	10^0
6 *p* + 2	1679.734	1679.805(14)*	(6,2)	00^0	9 *o* + 2	3627.453	3627.578(19)	(9,0)	00^0	11 *p* − 3	4733.919		(11,5)	00^0
6 *p* − 2	1740.834	1740.906(14)*	(6,1)	00^0	5 *p* − 5	3660.307	3660.348(10)*	(5,2)*l*	01^1	7 *o* − 4	4739.173	4739.271(18)	(7,0)	01^1
7 *p* − 2	1818.077	1818.155(13)*	(7,5)	00^0	3 *p* − 5	3661.043	3661.081(21)	(3,1)	10^0	9 *p* − 5	4767.501	4767.585(11)	(9,8)*l*	01^1
8 *p* − 1	1972.727	1972.800(11)*	(8,7)	00^0	4 *p* + 6	3667.082	3667.126(16)*	(4,4)	10^0	8 *p* + 6	4774.975	4774.998(33)	(8,8)	10^0
7 *p* + 1	2002.387	2002.456(14)*	(7,4)	00^0	5 *o* + 3	3673.918	3673.958(06)*	(5,3)*u*	01^1	7 *o* + 5	4793.598	4793.695(09)*	(7,3)*u*	01^1
9 *o* − 1	2030.535	2030.623(13)*	(9,9)	00^0	3 *o* + 3	3682.683	3682.750(16)	(3,0)	10^0	6 *p* + 9	4818.401		(6,2)	10^0
7 *o* − 1	2142.025	2142.094(11)*	(7,3)	00^0	6 *p* + 4	3685.067	3685.094(10)*	(6,5)*l*	01^1	1 *p* − 4	4842.455	4842.607(71)	(1,1)	02^0
7 *p* + 2	2241.910	2241.999(20)*	(7,2)	00^0	5 *p* + 4	3722.593	3722.636(10)*	(5,1)*l*	01^1	8 *o* − 3	4862.697	4862.793(07)*	(8,6)*u*	01^1
8 *o* + 1	2242.117	2242.206(10)*	(8,6)	00^0	11 *o* − 1	3725.471	3725.625(19)	(11,9)	00^0	1 *o* + 3	4870.187	4870.309(08)*	(1,0)	02^0
7 *p* − 3	2300.773	2300.879(19)*	(7,1)	00^0	10 *o* + 1	3726.430	3726.566(16)*	(10,6)	00^0	8 *p* + 7	4874.318	4874.407(11)*	(8,5)*l*	01^1
7 *o* + 2	2320.309	2320.372(15)	(7,0)	00^0	5 *o* − 3	3743.140	3743.168(14)*	(5,0)	01^1	6 *p* − 8	4877.837		(6,1)	10^0
9 *p* + 1	2396.323	2396.426(15)	(9,8)	00^0	5 *p* − 6	3792.977	3793.038(08)*	(5,2)*u*	01^1	13 *p* − 2	4879.901		(13,11)	00^0
10 *p* + 1	2451.425		(10,10)	00^0	4 *o* − 3	3820.769	3820.805(12)*	(4,3)	10^0	11 *p* + 3	4886.315	4886.494(31)	(11,4)	00^0
8 *p* − 2	2462.786	2462.889(15)*	(8,5)	00^0	6 *p* + 5	3825.386	3825.442(07)*	(6,5)*u*	01^1	7 *p* − 9	4891.925	4892.057(14)	(7,2)*u*	01^1
0 *p* + 1	2521.416	2521.411(05)*	(0,1)	01^1	8 *o* + 2	3828.991	3829.019(13)*	(8,9)	01^1	12 *p* + 2	4932.993		(12,8)	00^0
1 *p* − 2	2548.171	2548.164(11)*	(1,2)	01^1	5 *p* + 5	3863.351	3863.417(09)*	(5,1)*u*	01^1	2 *p* + 5	4942.656	4942.720(15)	(2,2)	02^0
1 *p* + 1	2609.542	2609.541(05)*	(1,1)	01^1	7 *p* + 3	3877.008	3877.036(10)*	(7,7)	01^1	11 *o* − 2	4949.854		(11,12)	01^1
2 *o* + 1	2614.279	2614.279(11)*	(2,3)	01^1	12 *p* − 1	3884.031		(12,11)	00^0	7 *p* + 7	4961.582	4961.729(16)	(7,1)*u*	01^1
1 *o* − 1	2616.686	2616.684(05)*	(1,0)	01^1	6 *p* − 3	3884.088	3884.117(10)*	(6,4)*l*	01^1	7 *p* − 10	4962.125	4962.118(11)	(7,5)	10^0
8 *p* + 2	2639.046	2639.135(17)*	(8,4)	00^0	5 *p* − 7	3888.654	3888.682(08)*	(5,5)	10^0	9 *p* − 6	4992.888	4992.978(13)	(9,8)*u*	01^1
9 *p* − 1	2701.980	2702.076(13)*	(9,7)	00^0	10 *p* − 2	3926.036	3926.180(23)	(10,5)	00^0	1 *o* − 2	4994.698	4994.833(08)*	(1,3)	02^2
3 *p* − 2	2719.486	2719.482(12)*	(3,4)	01^1	4 *p* + 7	3928.143		(4,2)	10^0	11 *o* − 3	4994.803		(11,3)	00^0
2 *p* − 2	2723.958	2723.962(06)*	(2,2)	01^1	13 *p* − 1	3931.766		(13,13)	00^0	0 *p* + 2	4997.920	4998.049(15)	(0,2)	02^2
2 *p* + 2	2755.565	2755.565(04)*	(2,1)*l*	01^1	4 *p* − 5	3991.803	3991.806(25)	(4,1)	10^0	2 *p* − 4	5023.366	5023.458(13)*	(2,1)	02^0
8 *o* − 1	2775.568	2775.667(13)*	(8,3)	00^0	7 *o* − 2	4010.200	4010.245(07)*	(7,6)*l*	01^1	10 *p* − 4	5026.026		(10,10)	01^1
2 *p* + 3	2790.335	2790.344(04)*	(2,1)*u*	01^1	6 *o* + 2	4029.988	4030.048(09)*	(6,3)*l*	01^1	8 *p* − 5	5028.265	5028.395(12)*	(8,4)*l*	01^1
2 *o* − 1	2812.850	2812.857(05)*	(2,0)	01^1	6 *p* − 4	4035.720	4035.770(08)*	(6,4)*u*	01^1	2 *p* + 6	5032.288	5032.393(07)*	(2,4)	02^2
10 *o* − 1	2856.600	2856.725(15)	(10,9)	00^0	11 *p* + 2	4044.000		(11,8)	00^0	14 *p* − 1	5048.185		(14,13)	00^0
4 *p* + 3	2863.938	2863.944(12)*	(4,5)	01^1	5 *p* + 6	4084.701	4084.730(14)*	(5,4)	10^0	3 *o* − 4	5078.915	5078.930(09)*	(3,3)	02^0
8 *p* + 3	2868.766	2868.892(27)	(8,2)	00^0	10 *p* + 3	4086.290	4086.425(25)	(10,4)	00^0	9 *p* + 4	5086.222	5086.331(10)*	(9,7)*l*	01^1
3 *o* + 2	2876.835	2876.847(06)*	(3,3)	01^1	6 *p* − 5	4129.260	4129.331(11)*	(6,2)*l*	01^1	11 *p* + 4	5087.285		(11,2)	00^0
11 *p* − 1	2909.130		(11,11)	00^0	6 *o* + 3	4147.034	4147.057(07)*	(6,6)	10^0	1 *p* + 2	5087.485	5087.617(08)*	(1,2)	02^2
8 *p* − 3	2925.302	2925.456(39)	(8,1)	00^0	9 *p* − 4	4165.459	4165.479(17)*	(9,10)	01^1	15 *o* − 1	5091.529		(15,15)	00^0
3 *p* − 3	2931.365	2931.366(05)*	(3,2)*l*	01^1	7 *o* − 3	4177.864	4177.920(06)*	(7,6)*u*	01^1	3 *p* − 6	5105.206	5105.292(10)*	(3,5)	02^2
9 *o* + 1	2957.195	2957.306(13)*	(9,6)	00^0	6 *p* + 6	4188.726	4188.806(11)*	(6,1)*l*	01^1	8 *p* + 8	5107.141	5107.271(11)*	(8,5)*u*	01^1
3 *p* − 4	2992.421	2992.436(05)*	(3,2)*u*	01^1	6 *o* + 4	4202.235	4202.300(07)*	(6,3)*u*	01^1	8 *p* − 6	5109.777	5109.740(19)	(8,7)	10^0
3 *p* + 2	3002.888	3002.905(05)*	(3,1)*l*	01^1	10 *o* − 2	4215.094	4215.251(20)	(10,3)	00^0	1 *p* − 5	5125.166	5125.292(06)*	(1,1)	02^2
3 *o* − 2	3025.943	3025.951(08)*	(3,0)	01^1	8 *p* − 4	4222.533	4222.583(11)*	(8,8)	01^1	11 *p* − 4	5136.560		(11,1)	00^0
5 *o* − 2	3047.383	3047.394(11)*	(5,6)	01^1	5 *o* − 4	4232.684	4232.694(14)*	(5,3)	10^0	7 *p* + 8	5136.682	5136.658(15)	(7,4)	10^0
3 *p* + 3	3063.453	3063.478(05)*	(3,1)*u*	01^1	7 *p* + 4	4249.902	4249.973(10)*	(7,5)*l*	01^1	9 *o* − 3	5149.109		(9,9)	10^0
4 *p* − 2	3069.310	3069.317(07)*	(4,4)	01^1	12 *p* + 1	4286.946		(12,10)	00^0	11 *o* + 2	5152.963	5153.139(22)	(11,0)	00^0
4 *o* + 1	3145.267	3145.276(05)*	(4,3)*l*	01^1	10 *p* + 4	4296.478		(10,2)	00^0	8 *o* + 3	5171.026	5171.168(11)*	(8,3)*l*	01^1
9 *p* − 2	3167.221	3167.341(17)*	(9,5)	00^0	6 *p* − 6	4309.271	4309.368(11)*	(6,2)*u*	01^1	2 *o* − 2	5181.056	5181.184(07)*	(2,3)	02^2
10 *p* + 2	3196.769	3196.907(19)	(10,8)	00^0	11 *p* − 2	4315.413		(11,7)	00^0	12 *p* − 2	5189.071		(12,7)	00^0
4 *o* + 2	3233.351	3233.377(06)*	(4,3)*u*	01^1	5 *p* + 7	4337.019		(5,2)	10^0	10 *o* + 2	5198.110	5198.221(11)	(10,9)*l*	01^1

TABLE 3—*Continued*

Q. N.[a]	E_{calc}[b]	E_{exp}[c]	Label[d]		Q. N.[a]	E_{calc}[b]	E_{exp}[c]	Label[d]		Q. N.[a]	E_{calc}[b]	E_{exp}[c]	Label[d]	
J I P n	(cm^{-1})	(cm^{-1})	Rot.	Vib.	J I P n	(cm^{-1})	(cm^{-1})	Rot.	Vib.	J I P n	(cm^{-1})	(cm^{-1})	Rot.	Vib.
3 p + 5	5210.738	5210.797(12)*	(3,2)	02^0	4 o − 5	5810.924	5811.003(06)*	(4,3)	02^2	6 o − 5	6301.641	6301.446(09)*	(6,3)	02^0
4 o + 3	5215.696	5215.742(08)*	(4,6)	02^2	2 p + 9	5815.659	5815.854(12)*	(2,1)u	11^1	13 o + 2	6304.993		(13,6)	00^0
4 p + 8	5251.799	5251.736(16)	(4,4)	02^0	9 p − 8	5819.792		(9,7)	10^0	9 p + 10	6306.607	6306.854(34)	(9,1)u	01^1
13 p + 1	5253.446		(13,10)	00^0	10 p − 6	5827.581	5827.721(13)	(10,8)u	01^1	9 p − 12	6310.290	6310.308(27)	(9,5)	10^0
8 p − 7	5257.167	5257.344(29)	(8,2)l	01^1	5 o − 5	5830.536	5830.435(07)*	(5,3)	02^0	7 o + 7	6312.444	6312.163(08)*	(7,6)	02^0
2 p + 7	5266.301	5266.427(08)*	(2,2)	02^2	2 o − 3	5835.140	5835.365(12)*	(2,0)	11^1	1 p − 7	6323.167		(1,1)	20^0
7 o − 5	5269.950		(7,3)	10^0	10 p + 7	5842.601	5842.715(11)*	(10,7)l	01^1	10 p + 10	6326.372		(10,8)	10^0
3 p − 7	5282.255	5282.318(11)*	(3,1)	02^0	9 p + 8	5842.747	5842.897(14)	(9,5)u	01^1	5 p + 12	6327.871	6327.954(06)*	(5,2)u	02^2
2 o + 2	5286.801	5286.913(06)*	(2,0)	02^2	4 p − 8	5846.716	5846.800(08)*	(4,1)l	02^2	9 p − 13	6333.126	6332.831(16)	(9,11)	02^2
3 p + 6	5299.131	5299.227(09)*	(3,4)	02^2	12 o − 2	5856.687		(12,3)	00^0	16 o − 1	6341.543		(16,15)	00^0
8 p − 8	5304.760	5304.879(13)*	(8,4)u	01^1	13 p + 2	5858.836		(13,8)	00^0	4 p + 14	6342.605	6342.581(23)	(4,1)l	11^1
2 p − 5	5304.836	5304.960(07)*	(2,1)	02^2	13 p − 3	5880.157		(13,14)	01^1	1 o + 4	6345.170		(1,0)	20^0
3 o + 4	5305.521	5305.584(09)*	(3,0)	02^0	4 p + 12	5888.230	5888.310(08)*	(4,2)u	02^2	5 p + 13	6346.262	6346.291(06)*	(5,5)	11^1
8 p + 9	5312.854	5313.058(40)	(8,1)l	01^1	8 o − 5	5895.174	5895.122(21)	(8,3)	10^0	11 o + 4	6359.874	6360.031(18)	(11,9)u	01^1
9 p + 5	5328.204	5328.318(10)*	(9,7)u	01^1	6 p − 9	5895.861	5895.803(08)*	(6,7)	02^2	4 p − 12	6363.351	6363.417(22)	(4,2)u	11^1
9 o − 4	5341.999	5342.110(09)*	(9,6)l	01^1	4 o + 4	5896.787	5896.838(08)*	(4,0)	02^2	11 p − 8	6373.929	6374.075(19)	(11,8)l	01^1
8 o + 4	5361.226	5361.203(12)	(8,6)	10^0	5 p − 11	5899.394	5899.405(07)*	(5,5)	02^2	5 p − 14	6376.427	6376.531(13)*	(5,1)u	02^2
5 p − 9	5363.833	5363.825(09)*	(5,7)	02^2	14 p − 2	5900.751		(14,11)	00^0	17 p − 1	6380.839		(17,17)	00^0
7 p + 9	5368.025		(7,2)	10^0	9 p − 9	5908.498	5908.688(37)	(9,2)l	01^1	5 o + 7	6391.743	6391.860(08)*	(5,0)	02^2
12 p + 3	5396.949		(12,13)	01^1	3 o + 6	5909.950	5910.110(06)*	(3,3)	11^1	6 p + 13	6395.046	6394.877(10)	(6,2)	02^0
12 o + 2	5406.041		(12,6)	00^0	4 p + 13	5920.770	5920.863(09)*	(4,5)	11^1	14 o + 2	6399.234		(14,15)	01^1
7 p − 11	5424.988		(7,1)	10^0	12 p + 5	5922.883		(12,2)	00^0	10 p − 7	6400.921	6401.106(27)	(10,4)l	01^1
3 o − 5	5431.017	5431.122(06)*	(3,3)	02^2	4 p − 9	5931.782	5931.881(06)*	(4,1)u	02^2	6 p + 14	6403.624	6403.513(08)*	(6,4)l	02^2
4 o − 4	5434.341	5434.331(12)	(4,3)	02^0	5 p + 9	5939.804	5939.707(12)	(5,2)	02^0	5 p − 15	6410.567	6410.544(19)	(5,4)l	11^1
7 o + 6	5443.899		(7,0)	10^0	10 o − 3	5944.621		(10,9)	10^0	10 o − 5	6412.156	6412.314(12)	(10,6)u	01^1
10 o + 3	5454.327	5454.430(11)	(10,9)u	01^1	3 p − 11	5949.328	5949.443(17)	(3,2)l	11^1	6 p − 11	6415.774	6415.757(07)*	(6,5)	02^2
4 p − 6	5460.400	5460.463(10)*	(4,5)	02^2	11 p − 6	5950.826		(11,10)u	01^1	2 p + 10	6422.880		(2,2)	20^0
5 p − 10	5460.611	5460.464(24)	(5,5)	02^0	9 p + 9	5962.005		(9,1)l	01^1	11 p + 6	6429.599		(11,10)	10^0
8 o + 5	5463.022	5463.104(10)*	(8,3)u	01^1	12 p − 4	5969.587		(12,1)	00^0	4 p + 15	6430.890	6430.944(23)	(4,1)u	11^1
11 p + 5	5483.252		(11,11)	01^1	5 o − 6	5971.155	5971.228(08)*	(5,3)l	02^2	9 p + 11	6449.215	6449.198(39)	(9,4)	10^0
3 p − 8	5486.357	5486.457(06)*	(3,1)l	02^2	12 o − 3	5976.967		(12,12)	01^1	7 p − 13	6451.317	6451.126(14)*	(7,8)	11^1
9 p + 6	5487.233	5487.329(18)	(9,8)	10^0	9 o − 6	5979.029	5979.217(21)	(9,0)	01^1	4 o − 6	6453.613	6453.690(19)	(4,0)	11^1
14 o + 1	5502.846		(14,12)	00^0	8 p + 12	5981.430		(8,2)	10^0	6 p − 12	6461.276		(6,1)	02^0
8 p − 9	5532.618	5532.751(20)	(8,2)u	01^1	6 p − 10	5984.075	5983.896(13)	(6,5)	02^0	13 p − 5	6476.011		(13,5)	00^0
3 p + 7	5533.626	5533.730(06)*	(3,2)	02^2	7 p − 12	5985.536	5985.149(13)	(7,7)	02^0	12 p + 7	6481.539		(12,11)u	01^1
4 p + 9	5544.226	5544.213(08)*	(4,2)	02^0	5 p − 12	6003.275	6003.183(14)	(5,1)	02^0	8 o − 6	6482.308	6482.118(19)*	(8,9)	02^2
6 p + 10	5549.695	5549.624(11)*	(6,8)	02^2	11 p − 7	6003.418		(11,11)	10^0	12 o + 3	6483.120		(12,12)	10^0
0 p + 3	5554.029		(0,1)	11^1	3 p − 12	6015.800	6015.946(17)	(3,2)u	11^1	2 p − 7	6488.458		(2,1)	20^0
10 p − 5	5555.295	5555.440(16)	(10,8)l	01^1	5 o + 6	6023.187	6023.081(17)	(5,0)	02^0	7 p − 14	6505.291	6505.157(08)*	(7,7)	02^2
10 p + 6	5558.547		(10,10)	10^0	3 p + 8	6023.657	6023.757(18)	(3,1)l	11^1	13 p + 3	6506.815		(13,13)	01^1
9 p + 7	5565.214	5565.255(12)*	(9,5)l	01^1	9 p − 10	6031.544	6031.681(15)	(9,4)u	01^1	6 o − 6	6516.118	6516.152(09)*	(6,3)l	02^2
3 o + 5	5567.276	5567.389(07)*	(3,0)	02^2	8 p + 13	6034.410	6034.182(13)*	(8,10)	02^2	5 p − 16	6529.268	6529.276(11)*	(5,4)u	11^1
3 p − 9	5573.651	5573.764(05)*	(3,1)u	02^2	8 p − 11	6035.672		(8,1)	10^0	10 o + 4	6539.707	6539.950(14)	(10,3)l	01^1
13 o − 1	5577.736		(13,9)	00^0	3 o − 6	6047.437	6047.564(19)	(3,0)	11^1	14 o − 1	6552.138		(14,9)	00^0
1 p − 6	5584.000	5584.224(10)*	(1,2)	11^1	9 o + 5	6053.084	6053.096(14)*	(9,6)	10^0	9 o − 7	6559.077		(9,3)	10^0
12 p − 3	5585.628		(12,5)	00^0	11 o + 3	6057.273	6057.448(13)	(11,9)l	01^1	3 o − 7	6561.242		(3,3)	20^0
8 p − 10	5604.263	5604.254(22)	(8,5)	10^0	3 p + 9	6080.829	6080.967(18)	(3,1)u	11^1	5 o + 8	6568.335	6568.247(10)*	(5,3)l	11^1
8 p + 10	5606.619	5606.814(20)	(8,1)u	01^1	10 o − 4	6087.435	6087.522(11)*	(10,6)l	01^1	7 p − 15	6571.908		(7,5)	02^0
9 o − 5	5610.185	5610.323(10)*	(9,6)u	01^1	5 p + 10	6089.800	6089.815(06)*	(5,4)	02^2	15 o + 1	6574.418		(15,12)	00^0
4 p − 7	5610.453	5610.451(13)	(4,1)	02^0	13 p − 4	6100.528		(13,7)	00^0	10 p − 8	6579.738		(10,7)	10^0
8 o − 4	5628.911	5629.057(13)	(8,0)	01^1	4 p − 10	6105.534	6105.639(06)*	(4,4)	11^1	12 p − 5	6591.347		(12,10)l	01^1
1 p + 3	5640.267	5640.488(15)*	(1,1)	11^1	5 o − 7	6129.541	6129.539(07)*	(5,6)	11^1	6 p + 15	6608.128	6608.127(07)*	(6,4)u	02^2
1 o − 3	5644.521	5644.739(15)	(1,0)	11^1	6 p + 11	6141.434	6141.238(13)	(6,4)	02^0	10 p − 9	6612.267		(10,2)l	01^1
4 p + 10	5652.415	5652.479(07)*	(4,4)	02^2	10 p + 8	6145.084	6145.224(14)	(10,7)u	01^1	13 p + 4	6612.793		(13,4)	00^0
2 o + 3	5653.801	5654.004(06)*	(2,3)	11^1	15 p − 1	6154.036		(15,13)	00^0	10 p + 11	6628.474	6628.649(18)	(10,5)u	01^1
5 o + 5	5659.211	5659.227(07)*	(5,6)	02^2	4 o + 5	6158.228	6158.271(15)*	(4,3)l	11^1	6 o − 7	6639.008	6638.903(05)*	(6,6)	11^1
11 p − 5	5662.198		(11,10)l	01^1	12 p + 6	6158.807		(12,11)l	01^1	11 p + 7	6644.910	6644.997(17)	(11,7)l	01^1
15 p + 1	5679.206		(15,14)	00^0	5 p + 11	6169.392	6169.455(08)*	(5,2)l	02^2	6 p + 16	6650.995	6650.933(10)*	(6,5)l	11^1
9 p − 7	5689.513	5689.686(14)*	(9,4)l	01^1	7 p + 10	6170.176	6170.055(11)*	(7,8)	02^2	9 o − 8	6651.211	6650.536(16)*†	(9,9)	02^0
5 p + 8	5690.933	5690.831(12)	(5,4)	02^0	9 o + 6	6175.031	6175.176(14)	(9,3)u	01^1	9 p + 12	6654.121		(9,2)	10^0
6 o + 5	5705.301	5705.046(15)	(6,6)	02^0	6 o + 6	6184.588	6184.537(07)*	(6,6)	02^2	10 p + 12	6665.886	6666.104(18)	(10,1)l	01^1
4 p + 11	5716.408	5716.491(08)*	(4,2)l	02^2	5 o − 8	6213.676	6213.703(06)*	(5,3)u	02^2	10 o + 5	6669.331	6668.954(16)	(10,12)	02^2
16 p + 1	5720.486		(16,16)	00^0	9 p − 11	6225.491	6225.639(27)	(9,2)u	01^1	3 p + 10	6669.884		(3,2)	20^0
12 p + 4	5730.235		(12,4)	00^0	10 p + 9	6226.551	6226.722(20)	(10,5)l	01^1	5 p − 17	6672.901		(5,2)l	11^1
2 p − 6	5755.800	5756.002(11)*	(2,2)	11^1	14 p + 2	6248.125		(14,10)	00^0	7 p + 11	6674.151	6673.853(14)	(7,4)	02^0
8 p + 11	5762.544	5762.522(20)	(8,4)	10^0	6 p + 12	6250.711	6250.710(09)*	(6,7)	11^1	8 p − 12	6676.055	6675.655(14)	(8,7)	02^0
3 p − 10	5764.716	5764.879(07)*	(3,4)	11^1	4 o + 6	6254.620	6254.705(10)*	(4,3)u	11^1	5 o + 9	6679.239		(5,3)u	11^1
7 o − 6	5773.241	5773.110(11)*	(7,9)	02^2	4 p − 11	6276.360	6276.370(22)	(4,2)l	11^1	13 o − 2	6686.925		(13,12)l	01^1
2 p + 8	5778.823	5778.995(16)	(2,1)l	11^1	5 p − 13	6276.694	6276.726(07)*	(5,1)l	02^2	13 o − 3	6700.977		(13,3)	00^0
9 o + 4	5809.240	5809.413(12)*	(9,3)l	01^1	8 p + 14	6300.971	6300.448(19)†	(8,8)	02^0	9 p − 14	6705.311		(9,1)	10^0

TABLE 3—*Continued*

Q. N.[a] J I P n	E_{calc}[b] (cm^{-1})	E_{exp}[c] (cm^{-1})	Label[d] Rot.	Vib.
11 p − 9	6710.274	6710.449(19)	(11,8)u	01^1
9 o + 7	6722.382		(9,0)	10^0
6 p + 17	6724.776	6724.704(11)*	(6,2)l	02^2
5 p + 14	6733.406		(5,1)l	11^1
3 p − 13	6734.090		(3,1)	20^0
7 p − 16	6736.644	6736.501(11)	(7,5)l	02^2
4 p + 16	6738.201		(4,4)	20^0
5 o − 9	6753.295		(5,0)	11^1
3 o + 7	6755.339		(3,0)	20^0
11 o − 4	6765.378	6765.479(18)	(11,9)	10^0
8 o + 6	6766.598	6766.387(12)	(8,9)	11^1
6 p − 13	6768.699	6768.675(14)*	(6,1)l	02^2
6 o − 8	6775.243	6775.358(05)*	(6,3)u	02^2
7 o + 8	6784.144	6784.078(06)*	(7,6)	02^2
5 p − 18	6792.527		(5,2)u	11^1
13 p + 5	6798.691		(13,2)	00^0
7 o − 7	6801.893	6801.634(14)	(7,3)	02^0
6 o + 7	6803.721	6803.674(08)*	(6,0)	02^2
10 o + 6	6804.407	6804.385(17)	(10,6)	10^0
10 p − 10	6811.587	6811.748(17)	(10,4)u	01^1
14 p + 3	6816.687		(14,8)	00^0
16 p + 2	6831.384		(16,14)	00^0
9 p + 13	6832.272	6832.012(23)*	(9,10)	02^2
13 p − 6	6842.607		(13,1)	00^0
6 p + 18	6842.645	6842.628(11)*	(6,5)u	11^1
13 o + 3	6857.353		(13,0)	00^0
6 p + 19	6858.525	6858.614(10)*	(6,2)u	02^2
5 p + 15	6859.884	6859.846(27)	(5,1)u	11^1
8 p + 15	6862.974	6862.763(11)*	(8,8)	02^2
7 p + 12	6863.533	6863.442(14)	(7,7)	11^1
6 p − 14	6885.871	6885.838(07)*	(6,4)l	11^1
11 o − 5	6889.006	6888.997(16)	(11,6)l	01^1
4 o − 7	6889.507		(4,3)	20^0
7 p + 13	6910.479		(7,2)	02^0
12 p − 6	6924.053		(12,10)u	01^1
6 p − 15	6929.171	6929.194(10)*	(6,1)u	02^2
12 o + 4	6934.573	6934.696(19)	(12,9)l	01^1
15 p − 2	6942.487		(15,11)	00^0
8 o + 7	6942.604	6942.162(31)	(8,6)	02^0
12 p − 7	6946.958		(12,11)	10^0
5 p − 19	6953.844		(5,5)	20^0
15 p − 3	6954.114		(15,16)	01^1
10 o + 7	6958.960	6959.029(17)	(10,3)u	01^1
7 p − 17	6961.325		(7,1)	02^0
10 p − 11	6967.179	6967.296(36)	(10,5)	10^0
7 o − 8	6985.302	6985.098(12)	(7,6)l	11^1
7 o + 9	6990.002	6989.796(20)	(7,0)	02^0
4 p + 17	6994.960		(4,2)	20^0
13 p − 7	6996.883		(13,13)	10^0
11 p + 8	6999.062		(11,5)l	01^1
7 p + 14	7002.735	7002.630(09)	(7,4)l	02^2
0 p + 4	7005.822		(0,1)	03^1
11 p + 9	7008.607	7008.759(17)	(11,7)u	01^1
7 p − 18	7027.151	7027.114(09)	(7,5)u	02^2
17 p + 1	7034.173		(17,16)	00^0
6 p − 16	7034.347		(6,4)u	11^1
10 p + 13	7035.883	7035.014(19)	(10,10)	02^0
11 p − 10	7043.023		(11,13)	02^2
6 o + 8	7043.586	7043.279(17)*	(6,3)l	11^1
14 p − 3	7044.849		(14,7)	00^0
13 o − 4	7045.395		(13,12)u	01^1
1 p − 8	7046.574	7046.841(70)*	(1,2)	03^1
10 p + 14	7055.069	7055.344(53)	(10,1)u	01^1
4 p − 13	7057.420		(4,1)	20^0
18 o + 1	7071.560		(18,18)	00^0
10 p − 12	7072.371	7072.389(36)	(10,2)u	01^1
14 p − 4	7072.465		(14,14)	01^1
8 p − 13	7073.046	7072.703(22)	(8,5)	02^0
9 p + 14	7074.515	7074.017(15)	(9,8)	02^0
10 o − 6	7080.191	7080.429(15)	(10,0)	01^1

Q. N.[a] J I P n	E_{calc}[b] (cm^{-1})	E_{exp}[c] (cm^{-1})	Label[d] Rot.	Vib.
1 o − 4	7082.860		(1,0)	03^1
1 p + 4	7102.718	7103.087(70)*	(1,1)	03^1
9 p − 15	7105.227	7104.956(13)*	(9,10)	11^1
8 o + 8	7119.292	7119.112(07)*	(8,6)l	02^2
2 o + 4	7122.615	7122.646(70)*	(2,3)	03^1
7 o − 9	7126.799	7126.714(08)*	(7,3)l	02^2
6 p − 17	7137.200		(6,2)l	11^1
11 p + 10	7143.390		(11,8)	10^0
5 p + 16	7147.109		(5,4)	20^0
13 p + 6	7156.697		(13,11)l	01^1
11 p − 11	7157.738		(11,4)l	01^1
6 o + 9	7184.268	7184.132(24)	(6,3)u	11^1
8 p − 14	7187.096	7186.960(11)	(8,7)	02^2
10 p + 15	7191.871		(10,4)	10^0
6 p + 20	7192.784		(6,1)l	11^1
7 p + 15	7193.350	7193.266(12)	(7,5)l	11^1
2 p + 11	7208.359	7208.334(70)*	(2,1)l	03^1
7 o − 10	7209.275	7209.165(07)*	(7,6)u	11^1
6 o + 10	7214.088		(6,6)	20^0
7 p + 16	7215.802	7215.768(09)*	(7,4)u	02^2
10 p − 13	7220.112		(10,11)	02^2
3 p − 14	7230.283		(3,4)	03^1
12 p − 8	7231.551		(12,8)l	01^1
2 p − 8	7235.508	7235.742(70)*	(2,2)	03^1
8 p − 15	7237.698		(8,8)	11^1
14 o + 3	7240.093		(14,6)	00^0
8 p + 16	7245.339	7244.972(17)	(8,4)	02^0
14 p + 4	7245.506		(14,13)l	01^1
11 o + 5	7255.270		(11,3)l	01^1
9 o − 9	7256.963	7256.689(34)*	(9,9)	02^2
11 o − 6	7257.663	7257.845(16)	(11,6)u	01^1
15 p + 2	7267.339		(15,10)	00^0
16 p − 1	7272.831		(16,13)	00^0
5 o − 10	7292.388		(5,3)	20^0
6 p − 18	7295.826		(6,2)u	11^1
2 p + 12	7301.181	7301.423(50)*	(2,1)u	03^1
12 o + 5	7304.749	7304.925(24)	(12,9)u	01^1
10 o − 7	7316.361		(10,3)	10^0
7 p + 17	7317.914	7317.753(12)	(7,2)l	02^2
7 p − 19	7318.407	7318.322(15)	(7,1)l	02^2
12 p + 8	7319.294		(12,10)	10^0
1 p − 9	7325.092		(1,4)	03^3
2 o − 4	7327.984	7328.209(18)*	(2,0)	03^1
7 o − 11	7340.062	7340.114(08)*	(7,3)u	02^2
9 p − 16	7349.528	7348.806(13)†	(9,7)	02^0
8 p + 17	7352.822	7352.467(13)	(8,7)l	11^1
11 p − 12	7357.593		(11,2)l	01^1
6 p + 21	7361.961		(6,1)u	11^1
3 p − 15	7362.607	7362.203(70)*	(3,2)l	03^1
2 p + 13	7368.759		(2,5)	03^3
4 p + 18	7374.555		(4,5)	03^1
1 o + 5	7380.868		(1,3)	03^3
10 p + 16	7381.747		(10,2)	10^0
6 o − 9	7383.902		(6,0)	11^1
11 p − 13	7391.054		(11,7)	10^0
3 o + 8	7394.164		(3,3)	03^1
5 p + 17	7394.743		(5,2)	20^0
14 p − 5	7400.014		(14,5)	00^0
8 o − 7	7401.351		(8,3)	02^0
11 p + 11	7405.502		(11,1)l	01^1
3 o − 8	7418.573	7418.432(13)	(3,6)	03^3
7 p + 18	7422.683	7422.591(14)	(7,5)u	11^1
8 p − 16	7425.250	7425.161(08)*	(8,5)l	02^2
11 o − 7	7427.159	7427.400(24)	(11,0)	01^1
10 p − 14	7429.353		(10,1)	10^0
7 p − 20	7436.896	7436.606(12)	(7,4)l	11^1
6 p − 19	7444.159		(6,5)	20^0
12 p + 9	7454.321		(12,14)	02^2
11 p − 14	7454.676		(11,11)	02^0
5 p − 20	7455.136		(5,1)	20^0

Q. N.[a] J I P n	E_{calc}[b] (cm^{-1})	E_{exp}[c] (cm^{-1})	Label[d] Rot.	Vib.
3 p + 11	7460.169		(3,1)l	03^1
7 p + 19	7462.158	7462.319(12)	(7,2)u	02^2
8 o + 9	7463.737	7463.686(08)*	(8,6)u	02^2
11 p + 12	7472.560	7472.755(24)	(11,5)u	01^1
10 p + 17	7474.940		(10,11)	11^1
5 o + 10	7475.145		(5,0)	20^0
8 p + 18	7478.072		(8,2)	02^0
9 o + 8	7487.746		(9,6)	02^0
0 o + 1	7492.558	7492.912(13)†	(0,3)	03^3
12 p + 10	7494.243		(12,7)l	01^1
13 o + 4	7496.871		(13,12)	10^0
3 o − 9	7498.146		(3,0)	03^1
7 p − 21	7499.704		(7,7)	20^0
7 o + 10	7504.956	7504.928(11)*	(7,0)	02^2
10 o − 8	7507.678	7507.250(34)	(10,9)	02^0
2 p − 9	7514.456		(2,4)	03^3
4 p + 19	7514.707		(4,7)	03^3
13 p + 7	7518.884		(13,11)u	01^1
13 p − 8	7522.856		(13,10)l	01^1
3 p − 16	7525.632		(3,2)u	03^1
14 p + 5	7528.745		(14,4)	00^0
7 p − 22	7529.091	7529.104(12)*	(7,1)u	02^2
17 o − 1	7532.405		(17,15)	00^0
8 p − 17	7533.994		(8,1)	02^0
9 p − 17	7543.585	7543.360(08)	(9,7)l	02^2
14 p + 6	7543.859		(14,14)	10^0
16 p + 3	7544.997		(16,17)	01^1
8 p + 19	7550.745	7550.536(10)	(8,7)u	11^1
4 o + 7	7551.194	7550.316(17)*	(4,3)l	03^1
15 o − 2	7552.649		(15,9)	00^0
5 o − 11	7554.025		(5,6)	03^1
1 p − 10	7571.716		(1,2)	03^3
11 o + 6	7592.288	7592.299(21)	(11,6)	10^0
7 o + 11	7596.047	7595.852(11)*	(7,3)l	11^1
3 p + 12	7597.008		(3,1)u	03^1
4 p − 14	7598.521		(4,4)	03^1
12 o − 4	7607.102	7607.488(24)	(12,6)l	11^1
7 p − 23	7618.630	7618.564(17)	(7,4)u	11^1
8 o − 8	7620.729	7620.408(12)	(8,6)l	11^1
9 p + 15	7622.656	7622.455(12)	(9,8)	02^2
6 p + 22	7628.078		(6,4)	20^0
12 p − 9	7632.355		(12,8)u	01^1
11 p − 15	7638.575	7638.738(29)	(11,4)u	01^1
5 p − 21	7639.368		(5,8)	03^3
14 p + 7	7641.001		(14,13)u	01^1
11 o + 7	7645.892		(11,12)	02^2
9 o + 9	7651.520	7651.050(13)	(9,9)	11^1
8 p + 20	7656.631	7656.488(15)*	(8,4)l	02^2
16 o + 1	7658.990		(16,12)	00^0
3 p + 13	7659.448		(3,5)	03^3
14 o − 2	7662.640		(14,3)	00^0
7 p − 24	7667.810		(7,2)l	11^1
15 o + 2	7673.607		(15,15)	01^1
9 p − 18	7676.894	7676.650(34)	(9,8)u	11^1
10 p + 18	7686.921	7686.522(17)	(10,10)	02^2
8 p − 18	7697.713	7697.709(10)	(8,5)u	02^2
4 p − 15	7701.393		(4,2)l	03^1
2 p + 14	7702.893	7702.986(12)*	(2,1)	03^3
14 p + 8	7710.495		(14,2)	00^0
7 p + 20	7717.101		(7,1)l	11^1
7 o − 12	7734.043		(7,0)	11^1
7 o + 12	7743.316	7742.932(15)	(7,3)u	11^1
12 o − 5	7749.110		(12,9)	10^0
14 p − 6	7751.221		(14,1)	00^0
2 p − 10	7751.596	7751.830(09)*†	(2,2)	03^3
14 o − 3	7752.530		(14,12)l	01^1
11 p − 16	7754.315		(11,5)	10^0
18 p − 1	7756.049		(18,17)	00^0
2 o + 5	7758.547	7758.675(12)†	(2,3)	03^3
11 o + 8	7766.629	7766.831(25)	(11,3)u	01^1

TABLE 3—*Continued*

Q. N.[a]	E_{calc}[b]	E_{exp}[c]	Label[d]	
J I P n	(cm^{-1})	(cm^{-1})	Rot.	Vib.
6 o − 10	7768.674		(6,3)	20^0
6 p + 23	7769.017		(6,7)	03^1
5 p − 22	7769.343	7767.914(70)*	(5,4)l	03^1
4 p + 20	7773.696		(4,1)l	03^1
9 p − 19	7778.214	7777.748(34)	(9,5)	02^0
8 p + 21	7785.048		(8,5)l	11^1
4 o − 8	7786.995	7786.722(09)*	(4,6)	03^3
10 p + 19	7787.226	7786.171(12)	(10,8)	02^0
19 p − 1	7791.596		(19,19)	00^0
4 o + 8	7795.070	7794.757(13)	(4,3)u	03^1
3 p − 17	7796.561		(3,4)	03^3
7 o + 13	7797.199	7796.716(15)†	(7,6)	20^0
6 o + 11	7798.639		(6,9)	03^3
15 p + 3	7801.887		(15,8)	00^0
12 p + 11	7808.089		(12,5)l	01^1
8 o − 9	7822.890	7822.667(08)*	(8,3)l	02^2
5 p + 18	7831.448		(5,5)	03^1
15 p − 4	7833.506		(15,14)l	01^1
8 p + 22	7837.460		(8,8)	20^0
1 p − 11	7839.758		(1,1)	12^0
13 o + 5	7844.719		(13,9)l	01^1
11 p + 13	7846.486		(11,1)u	01^1
8 o − 10	7851.386	7851.267(11)	(8,6)u	11^1
3 o + 9	7854.403		(3,3)	03^3
1 o + 6	7857.588		(1,0)	12^0
6 p + 24	7865.379		(6,2)	20^0
7 p − 25	7866.075		(7,2)u	11^1
3 o − 10	7866.482	7866.300(07)*	(3,0)	03^3
0 p + 5	7869.974	7870.015(10)†	(0,2)	12^2
1 o − 5	7872.300	7872.661(10)	(1,3)	12^2
9 p + 16	7875.817		(9,4)	02^0
11 o − 8	7878.132		(11,12)	11^1
11 p − 17	7882.766		(11,2)u	01^1
8 p + 23	7883.920	7883.910(10)	(8,4)u	02^2
9 o + 10	7891.450	7891.333(07)*	(9,6)l	02^2
13 p − 9	7897.671		(13,11)	10^0
13 o − 5	7903.526		(13,15)	02^2
12 o + 6	7907.409		(12,12)	02^0
12 p + 12	7911.595		(12,7)u	01^1
2 p + 15	7914.800	7915.081(10)	(2,4)	12^2
4 p − 16	7915.419	7915.179(16)	(4,2)u	03^1
10 p − 15	7921.531		(10,10)	11^1
8 p − 19	7921.988	7921.807(17)	(8,1)l	02^2
6 p − 20	7923.430		(6,1)	20^0
13 p − 10	7927.073		(13,10)u	01^1
7 p + 21	7931.270		(7,1)u	11^1
9 p − 20	7935.986	7935.837(09)*	(9,7)u	02^2
12 p − 10	7954.901		(12,4)l	01^1
8 p + 24	7956.627	7956.409(15)	(8,2)l	02^2
1 p + 5	7958.502	7958.833(10)	(1,2)	12^2
8 o + 10	7959.597	7959.452(19)	(8,0)	02^2
2 p + 16	7963.525		(2,2)	12^0
5 p + 19	7964.453		(5,7)	03^3
5 o + 11	7964.573	7963.581(70)*	(5,3)l	03^1
4 p + 21	7966.380		(4,1)u	03^1
11 p + 14	7975.338		(11,10)	02^0
3 p + 14	7977.777		(3,1)	03^3
9 p − 21	7980.439		(9,8)l	11^1
9 o − 10	7984.334		(9,3)	02^0
11 p + 15	7984.584		(11,4)	10^0
1 p − 12	7989.277	7989.534(11)	(1,1)	12^2
3 p − 18	7991.546	7991.670(11)	(3,5)	12^2
7 p − 26	7993.597		(7,10)	03^3
17 p + 2	7994.364		(17,14)	00^0
16 p − 2	8002.762		(16,11)	00^0
12 p + 13	8003.329		(12,8)	10^0
7 p − 27	8003.851		(7,5)	20^0
10 p + 20	8006.507	8006.247(12)	(10,8)l	02^2
2 p − 11	8013.644		(2,1)	12^0
15 p − 5	8017.246		(15,7)	00^0
3 p − 19	8017.654		(3,2)	03^3
7 p − 28	8019.418		(7,8)	03^1
6 p + 25	8020.895		(6,5)l	03^1
4 o − 9	8031.115	8030.925(13)*	(4,0)	03^1
4 p + 22	8036.056		(4,5)	03^3
8 o − 11	8043.282	8043.489(10)	(8,3)u	02^2
8 p − 20	8045.233		(8,4)l	11^1
5 p − 23	8054.048		(5,4)u	03^1
9 p + 17	8055.975		(9,7)l	11^1
2 o − 5	8057.083	8057.354(21)*	(2,3)	12^2
11 o − 9	8058.834		(11,3)	10^0
8 p + 25	8071.099		(8,5)u	11^1
4 p + 23	8074.027		(4,1)l	03^3
14 p − 7	8078.755		(14,13)	10^0
5 p − 24	8090.997		(5,2)l	03^1
10 o − 9	8092.072	8091.784(33)	(10,9)	02^2
6 o − 11	8099.519		(6,6)	03^1
12 o + 7	8100.211		(12,3)l	01^1
9 p + 18	8104.543		(9,2)	02^0
4 o + 9	8105.366	8105.227(11)	(4,6)	12^2
10 o + 8	8108.521		(10,9)l	11^1
10 p − 16	8109.690		(10,7)	02^0
12 p − 11	8109.750		(12,13)	02^2
15 o − 3	8123.151		(15,15)	10^0
13 p − 11	8128.161		(13,8)l	01^1
2 p + 17	8135.537	8135.727(11)*	(2,2)	12^2
9 p − 22	8135.925	8135.743(12)	(9,5)l	02^2
14 p + 9	8136.791		(14,11)l	01^1
5 o − 12	8138.695	8137.585(71)*	(5,0)	03^1
3 o − 11	8139.528	8139.068(12)	(3,3)	12^0
8 p + 26	8139.636	8139.751(15)	(8,2)u	02^2
2 o + 6	8142.021	8142.088(11)	(2,0)	12^2
14 o − 4	8142.969		(14,12)u	01^1
8 p − 21	8143.854		(8,7)	20^0
9 o + 11	8145.964	8145.790(09)	(9,0)	02^0
12 o − 6	8149.413		(12,6)u	01^1
12 p − 12	8151.257		(12,2)l	01^1
11 p − 18	8152.184		(11,11)	02^2
5 p + 20	8153.168		(5,1)l	03^1
11 p + 16	8160.296		(11,2)	10^0
4 p − 17	8167.805		(4,4)	03^3
2 p − 12	8168.050	8168.185(11)	(2,1)	12^2
9 o − 11	8169.582		(9,9)	20^0
17 o − 2	8172.423		(17,18)	01^1
9 p − 23	8176.283	8176.101(12)	(9,1)	02^0
3 p + 15	8176.849	8176.975(11)	(3,4)	12^2
7 p + 22	8176.919		(7,4)	20^0
6 p − 21	8181.377		(6,8)	03^3
8 p − 22	8182.966	8182.943(16)	(8,1)u	02^2
8 o + 11	8183.324	8182.737(20)	(8,3)l	11^1
12 p + 14	8197.456		(12,1)l	01^1
15 o + 3	8197.917		(15,6)	00^0
11 p − 19	8203.419		(11,1)	10^0
11 o + 9	8218.112		(11,0)	10^0
3 p + 16	8221.093		(3,2)	12^0
13 p + 8	8224.778		(13,10)	10^0
8 p + 27	8225.035		(8,11)	03^3
5 o + 12	8230.298	8229.545(15)	(5,3)u	03^1
12 p − 13	8237.880		(12,7)	10^0
9 o + 12	8237.934	8237.796(09)	(9,6)u	02^2
4 o − 10	8247.865		(4,0)	03^3
11 o − 10	8253.293	8251.782(12)	(11,9)	02^0
8 p − 23	8253.742		(8,2)l	11^1
18 p + 1	8254.233		(18,16)	00^0
5 p − 25	8256.823		(5,7)	12^2
10 o + 9	8260.234		(10,6)	02^0
3 p − 20	8260.436		(3,1)	12^0
15 p − 6	8266.460		(15,14)u	01^1
5 p − 26	8269.548		(5,2)l	03^3
3 o + 10	8275.007		(3,0)	12^0
6 p − 22	8275.953		(6,4)l	03^1
5 o − 13	8277.627	8277.033(09)*	(5,6)	03^3
13 o + 6	8281.674		(13,9)u	01^1
8 p − 24	8288.656	8288.481(16)	(8,4)u	11^1
9 o − 12	8294.533		(9,6)l	11^1
9 p + 19	8296.092		(9,7)u	11^1
3 o − 12	8302.131	8302.108(12)*	(3,3)	12^2
8 p + 28	8303.162		(8,1)l	11^1
7 o − 13	8303.281	8300.927(18)†	(7,6)l	03^1
8 o + 12	8305.143		(8,9)	03^1
7 o − 14	8306.730		(7,3)	20^0
16 p + 4	8306.809		(16,10)	00^0
16 p − 3	8309.933		(16,16)	01^1
12 p + 15	8315.622		(12,13)	11^1
4 p + 24	8332.152		(4,1)u	03^3
3 p − 21	8335.467	8335.280(21)	(3,1)l	12^2
4 p − 18	8340.205	8340.064(12)	(4,5)	12^2
12 p + 16	8348.569		(12,5)u	01^1
15 p − 7	8352.686		(15,5)	00^0
9 p + 20	8359.938	8359.769(13)	(9,4)l	02^2
4 p + 25	8365.683		(4,4)	12^0
4 o + 10	8365.752	8365.478(08)*†	(4,3)	03^3
4 p − 19	8366.382	8366.107(13)†	(4,2)	03^3
8 o + 13	8370.655		(8,6)	20^0
6 p + 26	8377.251		(6,5)u	03^1
15 p + 4	8378.098		(15,13)l	01^1
11 p + 17	8380.507		(11,11)	11^1
10 p − 17	8380.721		(10,5)	02^0
14 p + 10	8391.253		(14,16)	02^2
13 p + 9	8391.710		(13,7)l	01^1
13 p − 12	8394.156		(13,13)	02^0
10 p − 18	8395.134	8394.981(14)	(10,7)l	02^2
17 p − 2	8395.571		(17,13)	00^0
5 p − 27	8397.251		(5,2)u	03^1
3 p + 17	8400.644	8400.492(12)*	(3,2)	12^2
7 p + 23	8401.355		(7,7)	03^1
7 p + 24	8402.733		(7,2)	20^0
5 p + 21	8405.601		(5,1)l	03^3
6 o + 12	8413.795		(6,3)l	03^1
3 o + 11	8425.544	8425.436(16)*	(3,0)	12^2
7 o + 14	8432.257		(7,9)	03^3
12 o + 8	8435.511		(12,6)	10^0
3 p − 22	8435.637	8435.428(12)	(3,1)u	12^2
9 p − 24	8438.879	8438.843(12)	(9,5)u	02^2
10 p + 21	8443.972	8443.688(14)	(10,8)u	02^2
9 p + 21	8444.698		(9,5)l	11^1
10 o + 10	8445.678		(10,9)u	11^1
6 p + 27	8447.143		(6,8)	12^2
8 o + 14	8447.999		(8,3)u	11^1
16 o + 2	8449.967		(16,15)l	01^1
7 p − 29	8458.186		(7,1)	20^0
13 o − 6	8468.234		(13,6)l	01^1
15 p + 5	8472.890		(15,4)	00^0
7 o + 15	8476.591		(7,0)	20^0
12 p − 14	8477.374		(12,11)	02^0
6 p + 28	8482.606		(6,7)	03^3
14 p − 8	8482.722		(14,10)l	01^1
4 o − 11	8484.009		(4,3)	12^0
5 p + 22	8485.982		(5,5)	03^3
0 p + 6	8488.013		(0,1)	21^1
9 o − 13	8492.697		(9,12)	03^3
8 p − 25	8496.564		(8,2)u	11^1
9 o − 14	8500.207	8499.940(12)	(9,3)l	02^2
14 o + 4	8502.347		(14,12)	10^0
11 o − 11	8505.700	8505.370(12)	(11,9)l	02^2
19 o + 1	8506.101		(19,18)	00^0
12 p − 15	8506.621		(12,4)u	01^1
6 p − 23	8517.159		(6,2)l	03^1
1 p − 13	8519.809		(1,2)	21^1
4 p + 26	8523.090	8522.615(21)	(4,4)	12^2

TABLE 3—*Continued*

Q. N.[a]	E_{calc}[b]	E_{exp}[c]	Label[d]		Q. N.[a]	E_{calc}[b]	E_{exp}[c]	Label[d]		Q. N.[a]	E_{calc}[b]	E_{exp}[c]	Label[d]	
$J\ I\ P\ n$	(cm^{-1})	(cm^{-1})	Rot.	Vib.	$J\ I\ P\ n$	(cm^{-1})	(cm^{-1})	Rot.	Vib.	$J\ I\ P\ n$	(cm^{-1})	(cm^{-1})	Rot.	Vib.
4 $p+27$	8532.944	8532.448(12)	(4,2)*l*	12^2	8 $p-27$	8719.623		(8,10)	03^3	13 $p+13$	8898.676		(13,8)	10^0
15 $o-4$	8538.865		(15,3)	00^0	7 $p-30$	8723.372		(7,4)*l*	03^1	14 $p+12$	8915.420		(14,14)	02^0
20 $p+1$	8539.875		(20,20)	00^0	7 $o-16$	8729.497		(7,6)*u*	03^1	15 $p-9$	8918.591		(15,17)	02^2
5 $o+13$	8540.141	8539.642(12)	(5,6)	12^2	16 $p+5$	8733.833		(16,16)	10^0	16 $o+3$	8919.168		(16,15)*u*	01^1
10 $p+22$	8543.308		(10,4)	02^0	12 $p-17$	8734.530		(12,2)*u*	01^1	8 $o-13$	8919.473		(8,3)	20^0
10 $p-19$	8545.624		(10,8)*l*	11^1	18 $o-1$	8737.452		(18,15)	00^0	9 $p-30$	8924.988	8924.601(21)	(9,2)*l*	11^1
9 $p+22$	8548.456		(9,8)	20^0	8 $p-28$	8738.991		(8,8)	03^1	11 $p+20$	8930.701		(11,8)*l*	02^2
6 $o+13$	8550.179		(6,3)*l*	03^3	10 $p-20$	8740.025	8739.733(12)	(10,7)*u*	02^2	10 $o-11$	8931.540		(10,9)	20^0
5 $p+23$	8557.172		(5,1)*u*	03^1	2 $p+19$	8744.402		(2,1)*u*	21^1	10 $p-23$	8935.174	8934.919(13)	(10,5)*l*	02^2
11 $p-20$	8561.525		(11,10)*l*	11^1	12 $p+18$	8746.539		(12,10)*l*	02^2	5 $p+26$	8938.948		(5,2)	12^0
8 $p+29$	8561.972		(8,1)*u*	11^1	4 $o+11$	8748.979	8748.137(21)	(4,0)	12^2	8 $p+32$	8939.808		(8,10)	12^2
9 $o-15$	8565.006	8564.715(15)	(9,6)*u*	11^1	4 $p+29$	8752.192	8751.462(20)	(4,2)*u*	12^2	9 $o+14$	8940.205	8940.065(14)	(9,0)	02^2
1 $p+6$	8572.720		(1,1)	21^1	17 $o+1$	8756.619		(17,12)	00^0	3 $p-25$	8942.914		(3,2)*u*	21^1
4 $p+28$	8573.375		(4,2)	12^0	6 $o-12$	8757.929		(6,6)	03^3	11 $p-22$	8945.891		(11,10)*u*	11^1
1 $o-6$	8574.403		(1,0)	21^1	5 $p+24$	8759.484		(5,1)*u*	03^3	3 $p+18$	8946.610		(3,1)*l*	21^1
16 $o-2$	8575.190		(16,9)	00^0	2 $o-6$	8761.535		(2,0)	21^1	6 $p-27$	8946.897		(6,2)*u*	03^1
14 $p+11$	8575.666		(14,11)*u*	01^1	9 $o-16$	8762.271	8762.094(11)	(9,3)*u*	02^2	6 $o+15$	8948.553	8946.888(12)*	(6,6)	12^0
9 $p-25$	8575.676		(9,1)*l*	02^2	10 $p+24$	8763.050		(10,2)	02^0	12 $o-9$	8949.021		(12,3)	10^0
10 $p+23$	8578.169		(10,10)	20^0	9 $o+13$	8765.826		(9,3)*l*	11^1	9 $p+27$	8952.113		(9,1)*l*	11^1
4 $p-20$	8579.827		(4,1)	12^0	11 $p-21$	8772.922		(11,7)	02^0	14 $p-10$	8955.250		(14,10)*u*	01^1
12 $p-16$	8582.886		(12,5)	10^0	15 $o-5$	8773.852		(15,12)*l*	01^1	9 $p-31$	8957.405		(9,8)*l*	03^1
8 $o-12$	8583.064		(8,0)	11^1	5 $p-30$	8774.892	8774.058(31)	(5,5)	12^2	9 $o-17$	8959.407		(9,0)	11^1
13 $p-13$	8587.078		(13,8)*u*	01^1	6 $p-25$	8777.967		(6,7)	12^2	5 $p+27$	8962.886	8961.863(13)	(5,4)	12^2
2 $o+7$	8590.380		(2,3)	21^1	9 $p+25$	8780.294	8780.023(20)	(9,5)*u*	11^1	3 $o-13$	8971.474		(3,0)	21^1
11 $p+18$	8594.359		(11,10)	02^2	10 $p-21$	8786.124		(10,8)*u*	11^1	5 $p-32$	8971.972		(5,1)	12^0
11 $p+19$	8605.314		(11,8)	02^0	14 $o+5$	8786.369		(14,9)*l*	01^1	6 $o-13$	8973.388		(6,0)	03^1
6 $p+29$	8605.757		(6,1)*l*	03^1	13 $p-14$	8787.329		(13,4)*l*	01^1	5 $o+15$	8979.321		(5,0)	12^0
13 $p+10$	8611.877		(13,14)	02^2	13 $p-15$	8787.748		(13,14)	11^1	8 $o-14$	8980.344	8978.305(13)†	(8,6)*l*	03^1
7 $p+25$	8611.959		(7,5)*l*	03^1	8 $p+31$	8789.389		(8,4)	20^0	17 $p+3$	8981.093		(17,17)	01^1
8 $p+30$	8615.863		(8,7)*l*	03^1	4 $p-22$	8791.144	8790.446(21)	(4,1)*u*	12^2	11 $o-12$	8982.013	8981.477(12)	(11,9)*u*	02^2
9 $p+23$	8618.836		(9,4)*u*	02^2	7 $p-31$	8792.745		(7,8)	03^3	13 $p-16$	8983.051		(13,2)*l*	01^1
5 $p-28$	8620.874		(5,4)	03^3	5 $p-31$	8793.409		(5,2)*u*	03^3	10 $p+27$	8983.186		(10,11)	03^1
6 $p-24$	8624.270		(6,4)*u*	03^1	15 $p+8$	8794.725		(15,13)*u*	01^1	6 $p+31$	8985.268		(6,1)*l*	03^3
9 $p-26$	8626.456		(9,10)	03^1	5 $p+25$	8794.729		(5,4)	12^0	12 $p+20$	8986.242		(12,2)	10^0
8 $p-26$	8629.365		(8,5)	20^0	10 $p+25$	8795.279		(10,13)	03^3	7 $p+26$	8987.697		(7,1)*l*	03^1
5 $p-29$	8636.047	8634.652(14)	(5,5)	12^0	6 $p-26$	8795.648		(6,2)*l*	03^3	19 $p-2$	8993.902		(19,17)	00^0
12 $o+9$	8641.551		(12,3)*u*	01^1	5 $o-15$	8808.177	8807.586(18)	(5,3)*l*	12^2	11 $p-23$	8997.677		(11,11)	20^0
9 $p+24$	8645.701	8645.499(29)	(9,2)*l*	02^2	16 $p+6$	8809.895		(16,8)	00^0	10 $o+12$	9017.962	9017.824(11)	(10,6)*u*	02^2
13 $o-7$	8650.911		(13,9)	10^0	10 $p+26$	8819.788		(10,7)*l*	11^1	5 $o-17$	9050.652	9049.264(18)*	(5,6)	21^1
13 $p+11$	8651.186		(13,5)*l*	01^1	12 $p+19$	8820.198		(12,4)	10^0	5 $o-18$	9078.301	9077.153(32)	(5,3)*u*	12^2
12 $o+10$	8651.889		(12,12)	02^2	10 $p-22$	8828.587		(10,1)	02^0	9 $o+17$	9165.074	9164.618(22)	(9,3)*u*	11^1
5 $o-14$	8652.117		(5,0)	03^3	6 $o+14$	8834.528	8833.688(09)	(6,3)*u*	03^1	5 $p+29$	9186.991	9185.774(37)	(5,2)*u*	12^2
15 $p+6$	8654.498		(15,2)	00^0	9 $p-28$	8835.646		(9,7)	20^0	5 $o+16$	9241.971	9241.090(21)	(5,0)	12^2
7 $o-15$	8671.382		(7,9)	12^2	18 $p+2$	8837.258		(18,19)	01^1	11 $p-26$	9252.173	9251.699(15)	(11,7)*u*	02^2
12 $p+17$	8676.488		(12,1)*u*	01^1	3 $o+12$	8841.826		(3,3)	21^1	10 $o-13$	9268.164	9267.795(13)	(10,3)*l*	02^2
4 $o-12$	8680.186	8679.526(12)	(4,3)	12^2	13 $p+12$	8847.726		(13,7)*u*	01^1	6 $o+17$	9290.552	9289.879(12)	(6,3)*u*	03^3
5 $o+14$	8683.673	8682.938(12)	(5,3)	03^3	4 $p+30$	8852.976	8852.149(12)	(4,5)	21^1	6 $p+36$	9314.461	9313.066(21)	(6,4)*u*	12^2
2 $p-13$	8688.456		(2,2)	21^1	14 $p-9$	8859.933		(14,11)	10^0	10 $o-14$	9347.534	9346.886(15)	(10,6)*u*	11^1
10 $o+11$	8691.214	8690.955(11)	(10,6)*l*	02^2	13 $o+7$	8861.412		(13,3)*l*	01^1	7 $o+18$	9366.462	9364.720(14)	(7,3)*u*	03^1
15 $p-8$	8691.410		(15,1)	00^0	7 $p-32$	8868.239		(7,4)*l*	03^3	6 $o-16$	9410.563	9409.489(09)	(6,0)	03^3
15 $p+7$	8691.807		(15,14)	10^0	3 $p-24$	8869.083		(3,2)*l*	21^1	6 $p+37$	9429.922	9428.608(13)	(6,1)*u*	03^3
4 $p-21$	8696.975		(4,1)*l*	12^2	12 $o-8$	8869.733		(12,12)	11^1	8 $o-16$	9448.280	9446.240(10)*	(8,6)*u*	03^1
3 $p-23$	8700.697		(3,4)	21^1	9 $p-29$	8872.506	8872.119(21)	(9,1)*u*	02^2	12 $o-11$	9497.654	9497.272(14)	(12,9)*u*	02^2
2 $p+18$	8704.167		(2,1)*l*	21^1	9 $p+26$	8873.489	8873.350(23)	(9,2)*u*	02^2	10 $o-16$	9564.168	9564.295(15)	(10,3)*u*	02^2
15 $o+4$	8704.195		(15,0)	00^0	7 $o+16$	8885.813		(7,3)*l*	03^1	12 $p-21$	9644.523	9643.344(22)	(12,7)*l*	02^2
12 $o-7$	8706.587	8706.844(26)	(12,0)	01^1	5 $o-16$	8887.790	8886.456(13)	(5,3)	12^0	11 $o+15$	9886.631	9886.079(13)	(11,6)*u*	02^2
9 $p-27$	8707.442		(9,4)*l*	11^1	11 $o+10$	8894.796		(11,9)*l*	11^1					
10 $o-10$	8712.267		(10,3)	02^0	6 $p+30$	8898.674		(6,1)*u*	03^1					

[a] Quantum numbers J, I (o for $I = 3/2$ and p for $I = 1/2$), and parity (P). The column labeled n is an index for levels with the same J, I, and P ordering them by energy.

[b] Calculated energy value from Watson (*52*).

[c] Experimentally determined energy with its uncertainty in the last digits (2σ) in parentheses.

[d] Rotational and vibrational labels assigned as described in Section III.1.

† Unusually large deviation from *ab initio* calculations.

* Level constructed using only transitions verified by combination differences.

of these discrepancies can be blamed on the arbitrary assignment of the highly mixed levels in Table 2. Most of the remaining disagreements appear to be errors in the assignments of Din97. During our analysis, we found that some of their labels violated parity and symmetry requirements, some levels were labeled as a being part of a pair of G levels when there was only one way to form G, and one label was assigned to two separate levels. Probably most of these misassignments were caused by not considering all of the levels simultaneously, which was essential to our analysis.

III.2. Compilation and Assignment of Laboratory Data

Once the energy levels were given unique labels, the next step was to compile and analyze the frequency, uncertainty, and assignment for every transition reported. Every study in Table 1 was included in our analysis. (Please note that reference to each of these works for the remainder of the paper will be made using the labels assigned in Table 1.)

Instead of reviewing every assignment made (many transitions have been assigned and reassigned more than three times), we decided to consider all of the data simultaneously and make our own assignments independently. To make the assignments, we compared the transition frequencies to the variational calculations of Watson (*55*) and Neale, Miller, and Tennyson (NMT) (*56*), which are both based on spectroscopically fitted potential energy surfaces. We found that a combination of both calculations was necessary in our analysis. The NMT calculations were very good, generally differing from experiment by $\sim$0.05 cm^{-1}. There is a serious problem with these predictions, however, for levels with $J > 9$, and the error can be as high as several cm^{-1} (see Section IV.2). Watson's calculations, though not as precise, are very reliable and were used to assign levels of high J.

The intensity predictions[3] of both calculations were very similar, with NMT's, on average, lower than Watson's by $\sim$1% (with a standard deviation of 8%). H_3^+ is known to exhibit nonthermal population distributions in laboratory discharges, but can be described effectively as having thermal distributions among vibrational states and rotational levels, individually (*31*). We adjusted the theoretical intensities accordingly, assuming a vibrational temperature of 1200 K and a rotational temperature of 500 K. While the discharges used in each of the experiments had different temperatures, the values that we chose are roughly the average, and served to predict the order of magnitude of each transition's intensity.

Transition intensities were only reported in the literature for a few of the studies. Fortunately, we had access to all of the previous laser scans performed in Chicago (Baw90, Xu90, Lee91, Xu92, Ven94, Uy94, Joo00, McC00, and Lin01), and it was very important to our assignments to look at the transition intensities. By comparing the experimental intensities to the theoretically calculated intensities, we were able to determine roughly the sensitivity cutoff, limiting the number of possible lines available for each assignment. For lines that were very close together, it was useful to look at the original scans to see if some features were hidden on the shoulder of other transitions. In several cases we concluded that two calculated transitions were completely overlapped and were observed as a single feature. Studying these scans also enabled us to judge the quality of each line and make an estimate of the uncertainty on a line by line basis. We did not have access to the raw data from the FTIR emission studies and were not able to make such judgements on those lines.

During our analysis, we found that the uncertainties reported in the literature did not account for the discrepancies between different measurements of transition frequencies. This prompted us to re-examine the uncertainty for every experiment, and in most circumstances to increase them. We were rather conservative in our assignment of uncertainties, preferring to overestimate rather than underestimate the error. It is probably safe to consider our values as roughly two times the standard deviation.

A few systematic errors were identified which also have led to an increase in the uncertainty. As recently reported in McC00, it was found that the rate at which a scan needs to be performed is much slower than had previously been thought. In this work, the authors observed small shifts in the transition frequency due to the scan rate and the lock-in detection time constant. We have studied this phenomenon carefully and have concluded that one needs to spend at least 30 time constants on a velocity-modulated transition to avoid a frequency shift in the absorption feature. This requirement was not met in previous laser scans (in Chicago) and must be taken into account by increasing the uncertainty in every transition to 0.01 cm^{-1}. This error will not apply to the FTIR emission and absorption data (Maj87, Maj89, Nak90, Maj94, McK98). Another frequency error was noticed in the work of Uy94, in which several of the reported transitions disagreed with other reported values by 0.02–0.03 cm^{-1}.

Finally, there seemed to be a larger than expected difference in some of the reported FTIR emission transition frequencies (Maj89, Maj94) when compared to the theory and laser absorption experiments. Some of the lines that we were unable to assign (Table 4) from Maj89 and Maj94 were within 0.2 cm^{-1} of theoretically predicted lines that should be very strong. One difficulty with the FTIR emission experiments is the ubiquitous Rydberg H_2 emission. While these background features were identified by their strong pressure dependence (the Rydbergs are quenched at higher pressure), the apparent H_3^+ line position could be displaced if it were on the side of a strong H_2 signal. It is also possible that some of the lines attributed to H_3^+ are in fact H_2 lines which happen to increase in intensity with pressure.

It became apparent during our work that many of the assignments in Din97 were based on frequency alone. While the differences between the calculated and observed transition

[3] Note that in the paper of Neale, Miller, and Tennyson (*56*), the upper and lower values of J are switched in the equations relating transition probabilities to the Einstein A-coefficients. In their equations (2) and (3), each J' should be changed to J'', and vice versa.

TABLE 4
Remaining Unassigned Transitions

Frequency (cm^{-1})	Ref [a]	Frequency (cm^{-1})	Ref [a]	Frequency (cm^{-1})	Ref [a]
1980.367	Maj94	2702.321*	Baw90	3124.264*	Lin01
2028.198	Maj94	2708.432	Baw90	3128.912*	Xu92
2134.607	Maj94	2708.778	Baw90	3137.325	Xu92
2174.478	Maj94	2716.843*	Baw90	3161.895*	Xu92
2405.031	Baw90	2754.319	Baw90	3175.891	Maj94
2483.977	Baw90	2807.248*	Baw90	3177.467*	Maj94
2579.828	Baw90	2882.795*	Baw90	3180.420*	Xu92
2611.471*	Baw90	2915.872	Xu92	3182.593	Xu92
2612.538	Baw90	2918.157	Xu92	3182.605*	Lin01
2614.022*	Baw90	2932.711	Baw90	3188.562*	Maj94
2622.894*	Baw90	2942.920*	Maj94	3205.732*	Maj94
2623.274*	Baw90	2950.516	Maj94	3206.893*	Xu92
2626.289	Baw90	2958.735	Xu92	3235.521*	Lin01
2630.492	Baw90	2958.899	Xu92	3241.009	Maj94
2630.603*	Baw90	2965.791*	Xu92	3249.591*	Lin01
2653.290*	Baw90	2987.381	Maj94	3357.525*	Lin01
2653.559*	Baw90	2990.280*	Maj94	4394.944	Maj94
2653.692*	Baw90	2995.601*	Xu92	4587.373	Maj89
2672.862	Baw90	3005.898	Xu92	4756.345	Maj89
2673.229	Baw90	3022.332	Xu92	4788.544	Maj89
2674.344*	Baw90	3023.904*	Maj94	4823.315	Xu90
2680.330	Baw90	3104.125*	Lin01	4823.348	Maj89
2680.485	Baw90	3120.826	Xu92	4823.892	Maj94
2699.334*	Baw90	3121.475*	Xu92	4942.862	Maj89

Note. Some of these lines were previously assigned but have been 'unassigned' during our analysis. Transitions marked with asterisks do not have any reasonable assignment and are likely not due to H_3^+. Lines without an asterisk had one or more candidate assignments whose frequency and/or intensity difference from theory was too large to make a confident assignment.

[a] Reference from which the transition frequency was taken. Labels used in this column are defined in Table 1.

frequencies were usually small, sometimes assignments were made to transitions predicted to have intensities orders of magnitude weaker than the experimental sensitivity. This may partly be due to the fact that observed intensities are rarely published in the literature, and we urge experimenters to publish this information in the future. Frequently our reassignment of such lines increased the frequency difference from theory but ultimately made a much more reasonable assignment.

Once all of the assignments were made, we verified many of them by checking for combinations of other transitions that led to the same energy differences (combination differences). A program was written to search for all possible combinations of transitions that created closed "loops" of up to 6 transitions. The frequency of every verified transition agreed within 1.5 times the uncertainty in the frequency calculated by a combination of other transitions.

To label the transitions, we have extended the energy level notation from Section III.1 using the band symbol

$$v_1'\nu_1 + v_2'\nu_2^{|\ell'|} \leftarrow v_1''\nu_1 + v_2''\nu_2^{|\ell''|} \qquad [7]$$

or more compactly

$$v_1'v_2'^{|\ell'|} \leftarrow v_1''v_2''^{|\ell''|} \qquad [8]$$

and the branch symbol

$$^{\{n|t|\pm6|\pm9|\ldots\}}\{P|Q|R\}(J'', G'')^{\{u\,|\,l\}}_{\{u\,|\,l\}}, \qquad [9]$$

where P, Q, and R correspond to the usual $\Delta J = -1, 0, +1$. As was done for the level labels, u and l are appended to the end of the symbol, when appropriate, as a superscript and/or subscript referring to the upper and lower states in the transition, respectively. The preceding superscript specifies ΔG when it is not 0. For overtone and forbidden bands ΔG can equal ±3 (or ±1),[4] signified by t and n for the + and −, respectively. For highly mixed levels $|\Delta G| > 3$ are possible and these are labeled by ±6, ±9, etc.

A total of 895 unique transition frequencies have been reported in the literature, and we were able to assign 823 of them to transitions of H_3^+. Table 5 lists the adopted frequency, estimated uncertainty, assignment, and literature reference for each assigned transition. The assignments of 486 of these transitions were verified by their combination differences and are denoted by asterisks. For transitions that have been reported multiple times, we used the least uncertain measurement for the frequency. In cases where more than one equally accurate measurement was available, we chose the earliest measurement to include in this table. Many of the previous assignments have been changed due to both the new labeling scheme of energy levels and the reassignment of lines to different transitions. Surprisingly, we found that fewer than 4% of the lines were assigned incorrectly upon their initial observation. Most of the assignment conflicts were in the lines that were not initially assigned in Baw00 and Xu92. An expanded version of this table is available in electronic form online and includes the calculated lower state energies and Einstein A coefficients. This version also credits the first reported observation and first correct assignment of each line. An online intensity calculator is also available at the authors' Web site (http://h3plus.uchicago.edu).

The remaining 72 unassigned transitions are listed in Table 4 and should be considered carefully before being assigned in the future. Some of these that had been previously assigned are no longer assigned. Many of them (marked with an asterisk) had no reasonable theoretically predicted lines of sufficient intensity within $\sim$1 cm^{-1} of the reported transition, and are likely

[4] This "rule" is somewhat misleading and deserves more explanation. The signed G, denoted $g \equiv k - \ell$, carries the selection rule of $\Delta g = 0, \pm3, \pm6, \ldots$ due to the parity and nuclear spin selection rules. The confusion begins when g goes from a positive to a negative value or vice versa. Take for example an overtone transition where $k'' = \pm1$, $\ell'' = 0$ and $k' = 0$, $\ell' = \pm2$. In this case $g'' = \pm1$, $g' = \mp2$, $G'' = 1$, and $G' = 2$. The transition $\Delta g = \mp3$ is clearly allowed but ΔG appears to be a misleading +1. Both transitions are properly labeled with an n; a label of t would denote the transition $g'' = \pm1$ to $g' = \pm4$ where $\Delta g = \pm3$ and $\Delta G = +3$.

TABLE 5
Observed and Assigned Laboratory Transitions of H_3^+

Frequency[a] (cm^{-1})	Assignment[b] Label	Band	Ref[c]
1546.901 (10)	$P(12, 12)$	$01^1 \leftarrow 00^0$	Joo00
1798.396 (02)*	$P(9, 9)$	$01^1 \leftarrow 00^0$	Maj87
1826.160 (02)	$P(9, 8)$	$01^1 \leftarrow 00^0$	Maj87
1843.560 (10)*	$P(10, 7)^u$	$01^1 \leftarrow 00^0$	Maj94
1865.199 (10)*	$P(9, 7)^u$	$01^1 \leftarrow 00^0$	Maj94
1867.905 (10)	$P(11, 6)^u$	$01^1 \leftarrow 00^0$	Maj94
1868.703 (10)*	$P(9, 10)$	$02^2 \leftarrow 01^1$	Maj94
1876.392 (10)*	$P(9, 9)$	$02^2 \leftarrow 01^1$	Maj94
1882.985 (10)	$P(8, 8)$	$01^1 \leftarrow 00^0$	Maj94
1883.755 (10)*	$P(10, 6)^u$	$01^1 \leftarrow 00^0$	Maj94
1904.235 (10)*	$P(8, 7)$	$01^1 \leftarrow 00^0$	Maj94
1905.488 (10)*	$P(9, 6)^u$	$01^1 \leftarrow 00^0$	Maj94
1916.714 (10)	$P(10, 5)^u$	$01^1 \leftarrow 00^0$	Maj94
1921.286 (10)*	$P(8, 6)_u$	$02^2 \leftarrow 01^1$	Maj94
1925.254 (10)	$P(11, 4)^u$	$01^1 \leftarrow 00^0$	Maj94
1927.291 (10)	$P(11, 0)$	$01^1 \leftarrow 00^0$	Maj94
1927.792 (10)	$P(7, 2)^u$	$11^1 \leftarrow 10^0$	Maj94
1933.653 (10)*	$P(4, 3)_l$	$02^0 \leftarrow 01^1$	Maj94
1935.714 (10)*	$P(8, 6)^u$	$01^1 \leftarrow 00^0$	Maj94
1937.873 (10)*	$P(8, 7)_u$	$02^2 \leftarrow 01^1$	Maj94
1939.934 (10)*	$P(9, 5)^u$	$01^1 \leftarrow 00^0$	Maj94
1944.087 (10)*	$P(8, 9)$	$02^2 \leftarrow 01^1$	Maj94
1945.254 (10)	$P(10, 4)^u$	$01^1 \leftarrow 00^0$	Maj94
1947.467 (10)*	$P(8, 8)$	$02^2 \leftarrow 01^1$	Maj94
1958.420 (10)	$P(10, 1)^u$	$01^1 \leftarrow 00^0$	Maj94
1959.957 (50)*	$P(3, 1)_u$	$02^0 \leftarrow 01^1$	Maj94
1967.450 (02)*	$P(7, 7)$	$01^1 \leftarrow 00^0$	Maj87
1968.800 (02)*	$P(8, 5)^u$	$01^1 \leftarrow 00^0$	Maj87
1969.319 (10)*	$P(9, 4)^u$	$01^1 \leftarrow 00^0$	Maj94
1977.313 (10)	$P(9, 2)^u$	$01^1 \leftarrow 00^0$	Maj94
1981.672 (10)*	$P(7, 3)^u_u$	$02^2 \leftarrow 01^1$	Maj94
1982.486 (10)*	$P(6, 6)$	$11^1 \leftarrow 10^0$	Maj94
1982.874 (02)*	$P(7, 6)$	$01^1 \leftarrow 00^0$	Maj87
1984.067 (10)*	$P(7, 5)_u$	$02^2 \leftarrow 01^1$	Maj94
1990.807 (10)*	$P(6, 0)$	$02^2 \leftarrow 01^1$	Maj94
1996.884 (10)*	$P(8, 4)^u$	$01^1 \leftarrow 00^0$	Maj94
1997.172 (10)	$P(9, 1)^u$	$01^1 \leftarrow 00^0$	Maj94
2001.479 (10)	$P(9, 0)$	$01^1 \leftarrow 00^0$	Maj94
2002.045 (10)*	$P(9, 3)^u$	$01^1 \leftarrow 00^0$	Maj94
2006.615 (10)*	$P(7, 6)_u$	$02^2 \leftarrow 01^1$	Maj94
2007.290 (10)*	$P(7, 5)^u$	$01^1 \leftarrow 00^0$	Maj87
2011.400 (10)*	$P(6, 3)^u_u$	$02^2 \leftarrow 01^1$	Maj94
2018.029 (10)*	$P(8, 3)^u$	$01^1 \leftarrow 00^0$	Maj94
2018.760 (10)*	$P(7, 7)$	$02^2 \leftarrow 01^1$	Maj94
2019.376 (10)*	$P(7, 8)$	$02^2 \leftarrow 01^1$	Maj94
2020.914 (10)*	$P(5, 4)$	$11^1 \leftarrow 10^0$	Maj94
2022.011 (10)*	$P(5, 3)^u$	$11^1 \leftarrow 10^0$	Maj94
2023.165 (10)	$P(8, 2)^u$	$01^1 \leftarrow 00^0$	Maj94
2032.182 (10)*	$P(5, 5)$	$11^1 \leftarrow 10^0$	Maj94
2033.318 (10)*	$P(7, 4)^u$	$01^1 \leftarrow 00^0$	Maj87
2036.291 (10)	$P(8, 1)^u$	$01^1 \leftarrow 00^0$	Maj94
2051.510 (10)*	$P(6, 6)$	$01^1 \leftarrow 00^0$	Maj87
2054.047 (10)*	$P(6, 4)_u$	$02^2 \leftarrow 01^1$	Maj94
2057.444 (10)*	$P(2, 0)$	$02^0 \leftarrow 01^1$	Maj94
2060.200 (10)*	$P(7, 3)^u$	$01^1 \leftarrow 00^0$	Maj87
2061.680 (10)*	$P(6, 5)$	$01^1 \leftarrow 00^0$	Maj87
2067.366 (10)*	$P(7, 2)^u$	$01^1 \leftarrow 00^0$	Maj87
2073.951 (10)*	$P(6, 5)_u$	$02^2 \leftarrow 01^1$	Maj94
2077.500 (10)*	$P(7, 1)^u$	$01^1 \leftarrow 00^0$	Maj87
2079.433 (10)*	$P(6, 4)^u$	$01^1 \leftarrow 00^0$	Maj87
2080.683 (10)	$P(7, 0)$	$01^1 \leftarrow 00^0$	Maj94
2089.305 (10)*	$P(4, 3)$	$11^1 \leftarrow 10^0$	Baw90
2089.764 (10)*	$P(6, 6)$	$02^2 \leftarrow 01^1$	Baw90
2094.236 (10)*	$P(6, 7)$	$02^2 \leftarrow 01^1$	Maj94
2095.263 (10)*	$P(5, 2)^u_u$	$02^2 \leftarrow 01^1$	Maj94
2096.629 (10)*	$P(6, 3)^u$	$01^1 \leftarrow 00^0$	Maj87
2097.745 (10)*	$P(4, 4)$	$11^1 \leftarrow 10^0$	Baw90
2113.241 (10)*	$P(6, 2)^u$	$01^1 \leftarrow 00^0$	Maj87
2120.357 (10)*	$P(4, 0)$	$02^2 \leftarrow 01^1$	Maj94
2122.513 (10)*	$P(6, 1)^u$	$01^1 \leftarrow 00^0$	Maj87
2134.241 (10)*	$Q(7, 6)_u$	$02^0 \leftarrow 01^1$	Maj94
2134.922 (10)*	$P(5, 5)$	$01^1 \leftarrow 00^0$	Maj87
2137.039 (10)*	$P(5, 3)_u$	$02^2 \leftarrow 01^1$	Maj94
2140.348 (10)*	$P(5, 4)$	$01^1 \leftarrow 00^0$	Maj87
2142.328 (10)*	$P(5, 4)_u$	$02^2 \leftarrow 01^1$	Maj94
2152.615 (10)	$P(3, 0)$	$11^1 \leftarrow 10^0$	Maj94
2152.887 (10)*	$P(5, 3)^u$	$01^1 \leftarrow 00^0$	Maj87
2160.320 (10)*	$P(5, 5)$	$02^2 \leftarrow 01^1$	Maj94
2164.278 (10)*	$P(5, 2)^u$	$01^1 \leftarrow 00^0$	Maj87
2168.349 (10)*	$P(5, 6)$	$02^2 \leftarrow 01^1$	Baw90
2168.698 (10)*	$P(3, 3)$	$11^1 \leftarrow 10^0$	Baw90
2172.815 (10)*	$P(5, 1)^u$	$01^1 \leftarrow 00^0$	Maj87
2175.780 (10)*	$P(5, 0)$	$01^1 \leftarrow 00^0$	Maj87
2182.348 (10)*	$P(4, 2)_u$	$02^2 \leftarrow 01^1$	Maj94
2197.743 (10)*	$P(4, 3)_u$	$02^2 \leftarrow 01^1$	Maj94
2202.691 (10)	$P(4, 6)$	$03^3 \leftarrow 02^2$	Maj94
2217.451 (10)*	$P(4, 4)$	$01^1 \leftarrow 00^0$	Wat84
2218.129 (10)*	$P(4, 3)$	$01^1 \leftarrow 00^0$	Wat84
2223.965 (10)*	$P(4, 2)^u$	$01^1 \leftarrow 00^0$	Wat84
2229.895 (10)*	$P(4, 1)^u$	$01^1 \leftarrow 00^0$	Wat84
2229.912 (10)*	$P(4, 4)$	$02^2 \leftarrow 01^1$	Maj94
2241.077 (10)*	$P(2, 2)$	$11^1 \leftarrow 10^0$	Baw90
2241.347 (10)*	$P(4, 5)$	$02^2 \leftarrow 01^1$	Baw90
2250.525 (10)	$Q(7, 0)$	$02^0 \leftarrow 01^1$	Maj94
2253.633 (10)*	$Q(1, 0)$	$02^0 \leftarrow 01^1$	Maj94
2260.480 (10)	$Q(11, 3)^l$	$01^1 \leftarrow 00^0$	Maj94
2260.480 (10)	$Q(1, 1)$	$03^1 \leftarrow 02^0$	Maj94
2265.551 (10)	$Q(6, 2)_l$	$02^0 \leftarrow 01^1$	Maj94
2271.405 (10)*	$Q(6, 3)_l$	$02^0 \leftarrow 01^1$	Maj94
2274.262 (10)	$Q(11, 0)$	$01^1 \leftarrow 00^0$	Maj94
2277.104 (10)*	$Q(5, 3)_l$	$02^0 \leftarrow 01^1$	Maj94
2279.406 (30)*	$Q(3, 1)_l$	$02^0 \leftarrow 01^1$	Maj94
2279.406 (30)*	$Q(3, 2)_l$	$02^0 \leftarrow 01^1$	Maj94
2279.632 (10)*	$Q(3, 0)$	$02^0 \leftarrow 01^1$	Maj94
2279.913 (10)	$Q(5, 0)$	$02^0 \leftarrow 01^1$	Maj94
2280.547 (10)	$Q(5, 1)_l$	$02^0 \leftarrow 01^1$	Maj94
2284.000 (10)*	$Q(4, 2)_l$	$02^0 \leftarrow 01^1$	Maj94
2284.333 (10)	$Q(4, 1)_l$	$02^0 \leftarrow 01^1$	Maj94
2295.577 (10)*	$P(3, 1)^u$	$01^1 \leftarrow 00^0$	Wat84
2295.947 (10)*	$P(3, 2)$	$01^1 \leftarrow 00^0$	Wat84
2295.980 (10)*	$P(3, 0)$	$01^1 \leftarrow 00^0$	Wat84
2298.930 (10)*	$P(3, 3)$	$01^1 \leftarrow 00^0$	Wat84
2304.343 (10)*	$P(3, 3)$	$02^2 \leftarrow 01^1$	Maj94
2312.918 (10)*	$P(3, 4)$	$02^2 \leftarrow 01^1$	Maj94
2314.681 (10)	$Q(10, 4)^l$	$01^1 \leftarrow 00^0$	Maj94
2324.698 (10)	$Q(10, 3)^l$	$01^1 \leftarrow 00^0$	Maj94
2331.823 (10)	$Q(11, 9)^l$	$01^1 \leftarrow 00^0$	Maj94
2333.983 (10)	$Q(5, 0)$	$11^1 \leftarrow 10^0$	Maj94
2334.544 (10)	$Q(5, 1)^l$	$11^1 \leftarrow 10^0$	Maj94
2335.567 (10)*	$Q(5, 3)^l$	$11^1 \leftarrow 10^0$	Maj94
2341.498 (10)	$Q(10, 9)^l$	$01^1 \leftarrow 00^0$	Maj94
2348.355 (10)*	$Q(9, 3)^l$	$01^1 \leftarrow 00^0$	Maj94
2350.775 (10)	$Q(4, 1)^l$	$11^1 \leftarrow 10^0$	Maj94
2351.639 (10)	$Q(9, 0)$	$01^1 \leftarrow 00^0$	Maj94
2353.250 (10)	$Q(9, 2)^l$	$01^1 \leftarrow 00^0$	Maj94
2354.125 (10)*	$Q(9, 4)^l$	$01^1 \leftarrow 00^0$	Maj94
2357.951 (10)*	$Q(10, 7)^l$	$01^1 \leftarrow 00^0$	Maj94
2360.957 (10)*	$Q(10, 6)^l$	$01^1 \leftarrow 00^0$	Maj94
2362.676 (10)	$Q(3, 1)^l$	$11^1 \leftarrow 10^0$	Maj94
2364.814 (10)	$Q(3, 0)$	$11^1 \leftarrow 10^0$	Maj94
2371.155 (10)	$Q(9, 8)^l$	$01^1 \leftarrow 00^0$	Maj94
2372.185 (10)*	$P(2, 1)$	$01^1 \leftarrow 00^0$	Wat84
2378.869 (10)*	$P(2, 2)$	$01^1 \leftarrow 00^0$	Wat84
2380.555 (10)*	$P(2, 3)$	$02^2 \leftarrow 01^1$	Maj94
2384.252 (10)*	$Q(9, 7)^l$	$01^1 \leftarrow 00^0$	Maj94
2384.802 (10)*	$Q(9, 6)^l$	$01^1 \leftarrow 00^0$	Maj94
2387.602 (10)	$Q(8, 1)^l$	$01^1 \leftarrow 00^0$	Maj94
2388.452 (10)	$Q(8, 2)^l$	$01^1 \leftarrow 00^0$	Maj94
2389.257 (10)*	$Q(8, 4)^l$	$01^1 \leftarrow 00^0$	Maj94
2394.556 (10)	$R(1, 2)$	$02^0 \leftarrow 01^1$	Baw90
2395.500 (10)*	$Q(8, 3)^l$	$01^1 \leftarrow 00^0$	Baw90
2397.911 (10)*	$Q(9, 5)^l$	$01^1 \leftarrow 00^0$	Maj94
2398.519 (10)*	$Q(8, 7)^l$	$01^1 \leftarrow 00^0$	Maj87
2399.749 (10)*	$Q(1, 1)$	$11^1 \leftarrow 10^0$	Baw90
2402.621 (10)*	$Q(6, 0)$	$02^2 \leftarrow 01^1$	Baw90
2403.350 (20)*	$Q(2, 3)$	$12^2 \leftarrow 11^1$	Baw90
2406.029 (10)*	$Q(2, 1)^u$	$11^1 \leftarrow 10^0$	Baw90
2408.730 (10)*	$Q(8, 6)^l$	$01^1 \leftarrow 00^0$	Maj87
2411.518 (10)*	$Q(8, 5)^l$	$01^1 \leftarrow 00^0$	Maj87
2412.859 (10)*	$Q(2, 2)$	$11^1 \leftarrow 10^0$	Baw90
2413.314 (10)*	$Q(5, 1)^l_u$	$02^2 \leftarrow 01^1$	Baw90
2413.922 (10)*	$R(1, 1)$	$02^0 \leftarrow 01^1$	Baw90
2416.289 (10)*	$R(1, 0)$	$21^1 \leftarrow 20^0$	Baw90
2417.764 (10)*	$Q(7, 4)^l$	$01^1 \leftarrow 00^0$	Maj87
2418.899 (10)	$Q(7, 0)$	$01^1 \leftarrow 00^0$	Baw90
2419.558 (30)	$Q(7, 1)^l$	$01^1 \leftarrow 00^0$	Baw90
2420.207 (10)	$Q(3, 2)^u$	$11^1 \leftarrow 10^0$	Baw90
2420.728 (10)	$Q(7, 3)^l$	$01^1 \leftarrow 00^0$	Baw90
2421.888 (10)*	$Q(7, 2)^l$	$01^1 \leftarrow 00^0$	Baw90
2422.983 (10)*	$Q(3, 1)^l_u$	$02^2 \leftarrow 01^1$	Baw90
2423.646 (10)*	$Q(7, 6)^l$	$01^1 \leftarrow 00^0$	Maj87
2423.675 (20)*	$Q(4, 1)^l_u$	$02^2 \leftarrow 01^1$	Baw90
2424.797 (10)*	$Q(3, 3)$	$11^1 \leftarrow 10^0$	Baw90
2431.821 (10)*	$Q(7, 5)^l$	$01^1 \leftarrow 00^0$	Maj87
2433.901 (10)*	$Q(4, 3)^u$	$11^1 \leftarrow 10^0$	Baw90
2436.653 (10)*	${}^tQ(6, 3)_u$	$11^1 \leftarrow 01^1$	Baw90
2438.509 (10)*	$Q(4, 4)$	$11^1 \leftarrow 10^0$	Baw90
2446.632 (10)*	$Q(6, 5)^l$	$01^1 \leftarrow 00^0$	Maj87
2447.903 (10)*	$Q(6, 1)^l$	$01^1 \leftarrow 00^0$	Maj87
2449.533 (10)*	$Q(6, 2)^l$	$01^1 \leftarrow 00^0$	Maj87
2449.800 (10)*	$Q(4, 0)$	$02^2 \leftarrow 01^1$	Baw90
2449.885 (10)	$P(1, 2)$	$02^2 \leftarrow 01^1$	Baw90
2452.718 (10)*	$Q(6, 3)^l$	$01^1 \leftarrow 00^0$	Maj87
2453.408 (10)*	$Q(6, 4)^l$	$01^1 \leftarrow 00^0$	Maj87
2454.417 (10)*	${}^tQ(7, 4)$	$10^0 \leftarrow 00^0$	Baw90
2456.273 (20)*	$Q(4, 2)^l_l$	$02^2 \leftarrow 01^1$	Baw90
2457.290 (05)	$P(1, 1)$	$01^1 \leftarrow 00^0$	McK98
2457.613 (10)*	$Q(5, 5)$	$11^1 \leftarrow 10^0$	Baw90
2457.912 (10)*	$R(1, 0)$	$03^1 \leftarrow 02^0$	Baw90
2458.850 (10)	$R(1, 1)^u$	$03^1 \leftarrow 02^0$	Baw90
2464.652 (10)*	$R(2, 3)$	$02^0 \leftarrow 01^1$	Baw90
2467.553 (10)*	$Q(5, 4)^l$	$01^1 \leftarrow 00^0$	Baw90
2469.235 (10)	$Q(5, 3)_u$	$03^3 \leftarrow 02^2$	Baw90
2470.605 (10)	${}^tQ(8, 4)$	$10^0 \leftarrow 00^0$	Baw90
2471.384 (10)	$R(3, 3)^l$	$03^1 \leftarrow 02^0$	Baw90
2471.923 (10)	$Q(5, 0)$	$01^1 \leftarrow 00^0$	Baw90
2472.325 (10)*	$Q(5, 1)^l$	$01^1 \leftarrow 00^0$	Maj87
2472.846 (10)*	$Q(5, 3)^l$	$01^1 \leftarrow 00^0$	Maj87
2473.238 (10)*	$Q(5, 2)^l$	$01^1 \leftarrow 00^0$	Maj87
2474.054 (10)*	$Q(2, 0)$	$02^2 \leftarrow 01^1$	Baw90
2477.797 (10)†	$Q(4, 2)_u$	$03^3 \leftarrow 02^2$	Baw90
2483.553 (10)*	$Q(3, 1)^l_l$	$02^2 \leftarrow 01^1$	Baw90
2486.559 (05)*	$Q(4, 3)^l$	$01^1 \leftarrow 00^0$	McK98
2486.844 (10)*	$R(2, 2)$	$02^0 \leftarrow 01^1$	Baw90
2491.745 (05)*	$Q(4, 2)^l$	$01^1 \leftarrow 00^0$	McK98
2491.906 (10)*	$Q(6, 6)$	$11^1 \leftarrow 10^0$	Baw90
2491.976 (10)*	$R(2, 1)_u$	$02^0 \leftarrow 01^1$	Baw90
2492.537 (05)*	$Q(4, 1)^l$	$01^1 \leftarrow 00^0$	McK98
2492.728 (10)*	$R(2, 0)$	$02^0 \leftarrow 01^1$	Baw90
2497.349 (10)	$R(1, 0)$	$12^2 \leftarrow 11^1$	Baw90
2498.080 (10)†	$P(1, 3)$	$03^3 \leftarrow 02^2$	Baw90
2503.350 (05)*	$Q(3, 2)^l$	$01^1 \leftarrow 00^0$	McK98
2508.134 (05)*	$Q(3, 1)^l$	$01^1 \leftarrow 00^0$	McK98
2508.757 (10)*	$Q(4, 1)^u_u$	$02^2 \leftarrow 01^1$	Baw90
2509.078 (05)	$Q(3, 0)$	$01^1 \leftarrow 00^0$	McK98
2509.726 (10)	$R(3, 3)^l$	$21^1 \leftarrow 20^0$	Baw90
2510.291 (10)*	$Q(3, 1)^u_u$	$02^2 \leftarrow 01^1$	Baw90
2514.619 (10)*	$Q(2, 1)_u$	$02^2 \leftarrow 01^1$	Baw90
2515.755 (10)*	$Q(1, 1)$	$02^2 \leftarrow 01^1$	Baw90
2518.211 (05)*	$Q(2, 1)^l$	$01^1 \leftarrow 00^0$	McK98

TABLE 5—*Continued*

Frequency[a] (cm^{-1})	Assignment[b] Label	Band	Ref[c]
2520.677 (10)*	$Q(4,1)^l_l$	$02^2 \leftarrow 01^1$	Baw90
2529.724 (05)	$Q(1,0)$	$01^1 \leftarrow 00^0$	McK98
2532.253 (10)	$R(3,4)$	$02^0 \leftarrow 01^1$	Baw90
2534.922 (10)*	$Q(5,2)^u_u$	$02^2 \leftarrow 01^1$	Baw90
2536.931 (10)*	$Q(4,2)^u_u$	$02^2 \leftarrow 01^1$	Baw90
2538.253 (10)	$R(1,1)^l$	$11^1 \leftarrow 10^0$	Baw90
2539.451 (10)*	$Q(1,2)$	$02^2 \leftarrow 01^1$	Baw90
2539.744 (10)*	$Q(5,3)^u_u$	$02^2 \leftarrow 01^1$	Baw90
2541.293 (10)*	$Q(3,2)_u$	$02^2 \leftarrow 01^1$	Baw90
2541.433 (10)*	$Q(3,0)$	$02^2 \leftarrow 01^1$	Baw90
2542.467 (10)*	$Q(2,2)$	$02^2 \leftarrow 01^1$	Baw90
2545.420 (05)*	$Q(1,1)$	$01^1 \leftarrow 00^0$	McK98
2552.988 (05)*	$Q(2,1)^u$	$01^1 \leftarrow 00^0$	McK98
2554.276 (10)*	$Q(3,3)$	$02^2 \leftarrow 01^1$	Baw90
2554.475 (10)*	$Q(4,3)$	$03^3 \leftarrow 02^2$	Baw90
2554.666 (05)*	$Q(2,2)$	$01^1 \leftarrow 00^0$	McK98
2557.484 (10)	$R(3,3)$	$02^0 \leftarrow 01^1$	Baw90
2561.497 (05)*	$Q(3,3)$	$01^1 \leftarrow 00^0$	McK98
2564.418 (05)*	$Q(3,2)^u$	$01^1 \leftarrow 00^0$	McK98
2566.904 (10)*	$Q(2,3)$	$02^2 \leftarrow 01^1$	Baw90
2567.288 (05)*	$Q(4,4)$	$01^1 \leftarrow 00^0$	McK98
2568.708 (05)*	$Q(3,1)^u$	$01^1 \leftarrow 00^0$	McK98
2569.726 (10)*	$^tQ(6,3)$	$10^0 \leftarrow 00^0$	Xu92
2570.858 (10)*	$Q(3,1)^u_l$	$02^2 \leftarrow 01^1$	Baw90
2570.987 (10)*	$Q(4,6)$	$03^3 \leftarrow 02^2$	Baw90
2571.118 (05)*	$Q(5,5)$	$01^1 \leftarrow 00^0$	McK98
2572.220 (10)	$R(1,0)$	$11^1 \leftarrow 10^0$	Baw90
2572.357 (10)*	$Q(6,4)^u_u$	$02^2 \leftarrow 01^1$	Baw90
2573.057 (10)*	$Q(6,3)^u_u$	$02^2 \leftarrow 01^1$	Baw90
2573.582 (10)*	$Q(6,6)$	$01^1 \leftarrow 00^0$	Maj87
2574.659 (05)*	$Q(4,3)^u$	$01^1 \leftarrow 00^0$	McK98
2574.893 (10)*	$Q(7,7)$	$01^1 \leftarrow 00^0$	Baw90
2575.112 (30)*	$Q(9,9)$	$01^1 \leftarrow 00^0$	Baw90
2575.112 (10)*	$R(1,1)^u$	$11^1 \leftarrow 10^0$	Baw90
2575.312 (10)	$Q(8,8)$	$01^1 \leftarrow 00^0$	Baw90
2577.492 (10)†	$Q(2,3)$	$03^3 \leftarrow 02^2$	Baw90
2577.629 (10)*	$Q(4,3)_u$	$02^2 \leftarrow 01^1$	Baw90
2577.694 (10)*	$R(1,1)$	$03^3 \leftarrow 02^2$	Baw90
2579.390 (10)	$R(2,0)$	$03^3 \leftarrow 02^2$	Baw90
2579.672 (10)*	$Q(5,4)_u$	$02^2 \leftarrow 01^1$	Baw90
2579.748 (10)*	$Q(3,4)$	$02^2 \leftarrow 01^1$	Baw90
2581.184 (10)*	$Q(5,4)^u$	$01^1 \leftarrow 00^0$	Maj87
2582.909 (10)*	$Q(4,2)^u$	$01^1 \leftarrow 00^0$	Baw90
2583.155 (10)*	$Q(4,4)$	$02^2 \leftarrow 01^1$	Baw90
2586.985 (10)*	$Q(6,5)^u$	$01^1 \leftarrow 00^0$	Maj87
2589.541 (10)*	$Q(4,1)^u$	$01^1 \leftarrow 00^0$	Baw90
2590.071 (10)*	$R(2,0)$	$12^2 \leftarrow 11^1$	Baw90
2590.315 (10)*	$Q(6,5)_u$	$02^2 \leftarrow 01^1$	Baw90
2591.323 (10)*	$Q(7,6)^u$	$01^1 \leftarrow 00^0$	Baw90
2593.460 (10)*	$Q(5,3)^u$	$01^1 \leftarrow 00^0$	Maj87
2594.477 (10)*	$Q(8,7)^u$	$01^1 \leftarrow 00^0$	Baw90
2595.880 (10)†	$R(6,6)^l$	$03^1 \leftarrow 02^0$	Baw90
2596.520 (20)	$R(4,5)$	$02^0 \leftarrow 01^1$	Baw90
2596.520 (20)	$Q(4,5)$	$02^2 \leftarrow 01^1$	Baw90
2597.058 (10)*	$R(4,3)_u$	$02^0 \leftarrow 01^1$	Baw90
2597.702 (10)	$Q(10,9)^u$	$01^1 \leftarrow 00^0$	Baw90
2599.268 (10)*	$Q(5,5)$	$02^2 \leftarrow 01^1$	Baw90
2600.886 (20)*	$Q(8,6)^u_u$	$02^2 \leftarrow 01^1$	Baw90‖
2602.367 (10)*	$Q(3,2)_l$	$02^2 \leftarrow 01^1$	Baw90
2603.883 (10)*	$R(0,1)$	$02^2 \leftarrow 01^1$	Baw90
2605.063 (10)*	$Q(6,4)^u$	$01^1 \leftarrow 00^0$	Baw90
2605.763 (10)*	$Q(4,1)^u_l$	$02^2 \leftarrow 01^1$	Baw90
2605.921 (10)*	$Q(5,2)^u$	$01^1 \leftarrow 00^0$	Baw90
2606.154 (10)*	$Q(7,6)_u$	$02^2 \leftarrow 01^1$	Baw90
2606.296 (10)	$R(2,2)^l$	$11^1 \leftarrow 10^0$	Baw90
2611.838 (10)*	$Q(5,6)$	$02^2 \leftarrow 01^1$	Baw90
2612.842 (10)*	$R(3,2)_l$	$02^0 \leftarrow 01^1$	Baw90
2613.540 (10)*	$Q(7,5)^u$	$01^1 \leftarrow 00^0$	Baw90
2613.932 (10)	$R(2,1)^l$	$11^1 \leftarrow 10^0$	Baw90
2615.068 (10)*	$Q(6,6)$	$02^2 \leftarrow 01^1$	Baw90
2617.809 (10)*	$Q(5,6)$	$03^3 \leftarrow 02^2$	Baw90
2620.589 (10)*	$Q(8,6)^u$	$01^1 \leftarrow 00^0$	Baw90
2621.514 (10)	$R(4,4)$	$02^0 \leftarrow 01^1$	Baw90
2624.967 (10)*	$Q(6,3)^u$	$01^1 \leftarrow 00^0$	Baw90
2626.220 (10)*	$Q(6,7)$	$02^2 \leftarrow 01^1$	Baw90
2628.097 (30)*	$Q(4,2)^u_l$	$02^2 \leftarrow 01^1$	Baw90
2628.119 (20)*	$Q(7,7)$	$02^2 \leftarrow 01^1$	Baw90
2630.814 (10)	$Q(10,8)^u$	$01^1 \leftarrow 00^0$	Baw90
2639.806 (10)*	$Q(7,8)$	$02^2 \leftarrow 01^1$	Baw90
2640.172 (10)*	$Q(8,8)$	$02^2 \leftarrow 01^1$	Baw90
2648.105 (10)*	$R(2,3)$	$12^2 \leftarrow 11^1$	Baw90
2648.692 (10)*	$Q(5,0)$	$02^2 \leftarrow 01^1$	Baw90
2649.315 (10)	$R(4,3)^l_l$	$12^2 \leftarrow 11^1$	Baw90
2650.561 (10)	$^{-6}P(4,6)$	$03^3 \leftarrow 02^2$	Baw90
2650.954 (10)*	$Q(9,9)$	$02^2 \leftarrow 01^1$	Baw90
2653.095 (10)*	$Q(8,9)$	$02^2 \leftarrow 01^1$	Baw90
2653.885 (10)*	$R(5,5)^l$	$21^1 \leftarrow 20^0$	Baw90
2657.652 (10)	$R(5,6)$	$02^0 \leftarrow 01^1$	Baw90
2660.373 (10)*	$Q(5,3)^u_l$	$02^2 \leftarrow 01^1$	Baw90
2660.638 (10)*	$^tQ(4,2)_l$	$11^1 \leftarrow 01^1$	Baw90
2664.213 (10)*†	$R(1,2)$	$03^3 \leftarrow 02^2$	Baw90
2665.729 (10)*	$Q(4,3)_l$	$02^2 \leftarrow 01^1$	Baw90
2666.142 (10)†	$R(7,6)^l$	$03^1 \leftarrow 02^0$	Baw90
2666.500 (10)	$Q(9,10)$	$02^2 \leftarrow 01^1$	Baw90
2670.234 (10)*	$R(1,0)$	$02^2 \leftarrow 01^1$	Baw90
2671.142 (10)	$R(2,1)^u$	$11^1 \leftarrow 10^0$	Baw90
2672.799 (10)	$R(2,2)^u$	$11^1 \leftarrow 10^0$	Baw90
2672.958 (10)	$R(3,3)^l$	$11^1 \leftarrow 10^0$	Baw90
2679.487 (10)	$R(4,2)_l$	$02^0 \leftarrow 01^1$	Baw90
2680.631 (10)	$R(3,2)^l$	$11^1 \leftarrow 10^0$	Baw90
2681.500 (10)	$R(3,1)^l$	$11^1 \leftarrow 10^0$	Baw90
2683.755 (10)	$R(5,5)$	$02^0 \leftarrow 01^1$	Baw90
2685.157 (10)*	$R(4,3)_l$	$02^0 \leftarrow 01^1$	Baw90
2685.942 (10)*	$^tQ(5,2)_l$	$11^1 \leftarrow 01^1$	Xu92
2691.443 (05)*	$R(1,1)^l$	$01^1 \leftarrow 00^0$	McK98
2695.420 (10)*	$R(1,1)$	$02^2 \leftarrow 01^1$	Baw90
2696.110 (10)*	$R(2,1)^l_u$	$02^2 \leftarrow 01^1$	Baw90
2700.573 (10)*	$R(3,0)$	$12^2 \leftarrow 11^1$	Baw90
2704.382 (10)	$R(3,2)^u$	$03^1 \leftarrow 02^0$	Baw90
2709.405 (10)*	$^nR(4,4)^u$	$02^2 \leftarrow 10^0$	Baw90
2709.479 (10)	$R(3,1)^u_u$	$12^2 \leftarrow 11^1$	Baw90
2713.789 (10)	$R(4,5)$	$12^0 \leftarrow 11^1$	Baw90
2715.559 (10)	$R(6,7)$	$02^0 \leftarrow 01^1$	Baw90
2715.827 (10)	$R(3,3)^u$	$03^1 \leftarrow 02^0$	Baw90†
2718.262 (10)*	$R(1,2)$	$02^2 \leftarrow 01^1$	Baw90
2719.437 (10)*†	$^{-6}Q(2,4)$	$03^3 \leftarrow 02^2$	Baw90
2724.058 (10)*	$R(3,2)^l_u$	$02^2 \leftarrow 01^1$	Baw90
2725.342 (10)*	$R(3,0)$	$03^1 \leftarrow 02^0$	Baw90
2725.898 (05)*	$R(1,0)$	$01^1 \leftarrow 00^0$	McK98
2726.220 (05)*	$R(1,1)^u$	$01^1 \leftarrow 00^0$	McK98
2730.887 (10)*	$R(2,1)^l_l$	$02^2 \leftarrow 01^1$	Baw90
2733.639 (10)*	$^tR(8,7)_l$	$11^1 \leftarrow 01^1$	Baw90
2734.526 (10)	$R(5,2)_l$	$02^0 \leftarrow 01^1$	Baw90
2735.515 (10)	$R(3,2)^u_u$	$12^2 \leftarrow 11^1$	Baw90
2737.851 (10)*	$R(4,3)^l_u$	$02^2 \leftarrow 01^1$	Baw90
2740.568 (10)*	$^tR(5,4)_u$	$11^1 \leftarrow 01^1$	Baw90
2742.697 (10)*	$R(6,6)$	$02^0 \leftarrow 01^1$	Baw90
2743.418 (10)	$R(4,4)^l$	$11^1 \leftarrow 10^0$	Baw90
2744.586 (10)	$R(4,2)^l$	$11^1 \leftarrow 10^0$	Baw90
2744.719 (10)	$R(5,4)_l$	$02^0 \leftarrow 01^1$	Baw90
2745.307 (10)	$Q(6,3)^u_l$	$02^2 \leftarrow 01^1$	Baw90
2747.457 (10)*	$R(4,3)^l$	$11^1 \leftarrow 10^0$	Baw90
2748.106 (10)*	$R(5,3)_l$	$02^0 \leftarrow 01^1$	Baw90
2754.535 (10)*	$R(2,0)$	$02^2 \leftarrow 01^1$	Baw90
2756.142 (10)	$^tR(7,6)_l$	$11^1 \leftarrow 01^1$	Baw90
2762.070 (05)*	$R(2,2)^l$	$01^1 \leftarrow 00^0$	McK98
2762.250 (10)*†	$R(5,5)^l$	$11^1 \leftarrow 10^0$	Baw90
2765.545 (05)*	$R(2,1)^l$	$01^1 \leftarrow 00^0$	McK98
2766.032 (10)*	$^tR(6,5)_l$	$11^1 \leftarrow 01^1$	Baw90
2767.678 (10)	$R(3,2)^u$	$11^1 \leftarrow 10^0$	Baw90
2769.393 (10)*	$R(3,3)^u$	$11^1 \leftarrow 10^0$	Baw90
2769.863 (10)	$R(3,1)^u$	$11^1 \leftarrow 10^0$	Baw90
2770.196 (10)†	$R(7,8)$	$02^0 \leftarrow 01^1$	Baw90
2770.940 (10)	$R(3,0)$	$11^1 \leftarrow 10^0$	Baw90
2771.586 (10)	$R(6,3)_l$	$02^0 \leftarrow 01^1$	Baw90
2783.325 (10)*	$R(3,1)^l_u$	$02^2 \leftarrow 01^1$	Baw90
2783.417 (10)*	$R(2,1)^u_u$	$02^2 \leftarrow 01^1$	Baw90
2785.121 (10)*	$R(3,2)^l_l$	$02^2 \leftarrow 01^1$	Baw90
2787.400 (10)	$R(4,0)$	$12^2 \leftarrow 11^1$	Baw90
2789.736 (10)	$R(6,4)_l$	$02^0 \leftarrow 01^1$	Baw90
2795.213 (10)	$R(4,3)^u$	$03^1 \leftarrow 02^0$	Baw90
2798.620 (10)	$R(7,7)$	$02^0 \leftarrow 01^1$	Baw90
2801.108 (10)	$R(5,4)^l$	$11^1 \leftarrow 10^0$	Baw90
2809.767 (10)*	$R(2,2)$	$02^2 \leftarrow 01^1$	Baw90
2810.597 (10)*	$R(5,3)^l$	$11^1 \leftarrow 10^0$	Baw90
2816.843 (10)*	$R(2,3)$	$02^2 \leftarrow 01^1$	Baw90
2817.349 (10)*	$R(5,6)$	$12^0 \leftarrow 11^1$	Baw90
2818.072 (10)*	$R(4,2)^l_u$	$02^2 \leftarrow 01^1$	Baw90
2818.196 (10)*	$R(2,1)^u_l$	$02^2 \leftarrow 01^1$	Baw90
2821.518 (10)*	$R(8,9)$	$02^0 \leftarrow 01^1$	Baw90
2822.357 (30)	$R(4,2)^u_u$	$12^2 \leftarrow 11^1$	Baw90
2822.448 (30)	$R(4,3)^u_u$	$12^2 \leftarrow 11^1$	Baw90
2822.730 (20)	$R(7,5)_l$	$02^0 \leftarrow 01^1$	Baw90
2823.138 (05)*	$R(2,2)^u$	$01^1 \leftarrow 00^0$	McK98
2824.754 (10)	$R(7,4)_l$	$02^0 \leftarrow 01^1$	Baw90
2825.956 (10)*	$R(4,3)^l_l$	$02^2 \leftarrow 01^1$	Baw90
2826.117 (05)*	$R(2,1)^u$	$01^1 \leftarrow 00^0$	McK98
2829.925 (05)*	$R(3,3)^l$	$01^1 \leftarrow 00^0$	McK98
2831.340 (10)*	$R(3,1)^l$	$01^1 \leftarrow 00^0$	Wat84
2832.198 (05)*	$R(3,2)^l$	$01^1 \leftarrow 00^0$	McK98
2836.028 (10)*	$^nR(5,5)^l$	$02^2 \leftarrow 10^0$	Baw90
2838.041 (10)	$R(6,6)^l$	$11^1 \leftarrow 10^0$	Baw90
2841.148 (10)	$^tQ(2,0)$	$11^1 \leftarrow 01^1$	Baw90
2842.191 (10)*	$R(5,3)^l_u$	$02^2 \leftarrow 01^1$	Baw90
2843.898 (20)*	$R(3,1)^l_l$	$02^2 \leftarrow 01^1$	Baw90‖
2844.464 (10)*	$^nR(5,4)^u$	$02^2 \leftarrow 10^0$	Baw90‡
2851.433 (10)	$R(8,8)$	$02^0 \leftarrow 01^1$	Baw90
2852.156 (10)	$^tR(2,0)$	$12^0 \leftarrow 02^2$	Baw90
2853.598 (10)*	$R(4,1)^l_u$	$02^2 \leftarrow 01^1$	Baw90
2854.191 (10)*	$^tR(5,4)_l$	$11^1 \leftarrow 01^1$	Baw90
2862.151 (10)*	$R(4,4)^u$	$11^1 \leftarrow 10^0$	Baw90
2864.369 (10)	$R(4,2)^u$	$11^1 \leftarrow 10^0$	Baw90
2868.040 (10)	$R(4,1)^u$	$11^1 \leftarrow 10^0$	Baw90
2868.404 (10)*	$R(3,1)^u_u$	$02^2 \leftarrow 01^1$	Baw90
2869.535 (10)	$R(9,10)$	$02^0 \leftarrow 01^1$	Baw90
2870.890 (10)*	$R(3,0)$	$02^2 \leftarrow 01^1$	Baw90
2884.148 (10)*	$^tQ(3,0)$	$11^1 \leftarrow 01^1$	Xu92
2889.052 (10)*	$R(4,1)^l$	$01^1 \leftarrow 00^0$	Baw90
2890.993 (10)*	$^tR(4,3)_l$	$21^1 \leftarrow 11^1$	Baw90
2891.867 (10)*	$R(4,2)^l$	$01^1 \leftarrow 00^0$	Wat84
2893.103 (10)	$R(5,0)$	$12^2 \leftarrow 11^1$	Baw90
2893.369 (10)*	$R(5,4)^l_u$	$02^2 \leftarrow 01^1$	Baw90
2894.488 (10)*	$R(4,4)^l$	$01^1 \leftarrow 00^0$	Oka81
2894.610 (10)*	$R(4,3)^l$	$01^1 \leftarrow 00^0$	Oka81
2895.600 (10)	$R(7,7)^l$	$11^1 \leftarrow 10^0$	Baw90
2895.874 (10)*	$R(3,2)^u_u$	$02^2 \leftarrow 01^1$	Baw90
2896.161 (10)*	$^tR(4,3)_u$	$11^1 \leftarrow 01^1$	Baw90
2898.614 (10)*	$R(7,6)^l$	$11^1 \leftarrow 10^0$	Baw90
2901.516 (10)	$R(9,9)$	$02^0 \leftarrow 01^1$	Baw90
2901.653 (10)	$R(8,8)^u$	$11^1 \leftarrow 10^0$	Baw90
2902.523 (10)	$R(5,4)^u_u$	$12^2 \leftarrow 11^1$	Baw90
2909.239 (10)*	$R(4,2)^l_l$	$02^2 \leftarrow 01^1$	Xu92
2918.026 (10)*	$R(3,3)^u$	$01^1 \leftarrow 00^0$	Oka81
2923.361 (10)*	$R(3,2)^u$	$01^1 \leftarrow 00^0$	Oka81
2924.414 (10)*	$R(6,3)^l_u$	$02^2 \leftarrow 01^1$	Xu92
2928.351 (10)*	$R(3,1)^u$	$01^1 \leftarrow 00^0$	Oka81
2928.470 (10)	$^nR(6,5)^l$	$02^2 \leftarrow 10^0$	Xu92
2930.163 (10)*	$R(3,0)$	$01^1 \leftarrow 00^0$	Oka81
2931.917 (30)	$R(7,6)_l$	$02^0 \leftarrow 01^1$	Carbo‖
2932.988 (10)*	$R(3,4)$	$02^2 \leftarrow 01^1$	Baw90

TABLE 5—*Continued*

Frequency[a] (cm^{-1})	Assignment[b] Label	Band	Ref[c]	Frequency[a] (cm^{-1})	Assignment[b] Label	Band	Ref[c]	Frequency[a] (cm^{-1})	Assignment[b] Label	Band	Ref[c]
2934.155 (10)*	$R(3,3)$	$02^2 \leftarrow 01^1$	Baw90	3042.578 (10)	$R(6,4)^u$	$11^1 \leftarrow 10^0$	Xu92	3152.951 (05)	$R(6,2)^u_u$	$02^2 \leftarrow 01^1$	Lin01
2934.355 (10)*†	$R(3,3)$	$03^3 \leftarrow 02^2$	Baw90	3046.045 (05)	$R(5,1)^l_l$	$02^2 \leftarrow 01^1$	Lin01	3159.015 (05)	$R(9,8)^l$	$01^1 \leftarrow 00^0$	Lin01
2938.491 (10)*	$R(5,1)^l$	$01^1 \leftarrow 00^0$	Xu92	3050.552 (05)*	$R(8,4)^l$	$01^1 \leftarrow 00^0$	Lin01	3160.236 (05)	$R(10,7)^l$	$01^1 \leftarrow 00^0$	Lin01
2941.187 (10)*	$R(7,6)^l_u$	$02^2 \leftarrow 01^1$	Xu92	3051.407 (05)	$R(6,5)^l_l$	$02^2 \leftarrow 01^1$	Lin01	3162.430 (05)	$R(10,6)^l$	$01^1 \leftarrow 00^0$	Lin01
2942.209 (10)*	$R(5,2)^l$	$01^1 \leftarrow 00^0$	Maj87	3052.077 (05)	$R(5,1)^u_u$	$03^3 \leftarrow 02^2$	Lin01	3163.198 (05)	$^tR(5,1)^l_l$	$11^1 \leftarrow 01^1$	Lin01
2944.828 (10)*	$R(4,0)$	$02^2 \leftarrow 01^1$	Baw90	3053.355 (05)	$R(6,1)^u$	$11^1 \leftarrow 10^0$	Lin01	3167.596 (05)	$R(9,9)^l$	$01^1 \leftarrow 00^0$	Lin01
2949.555 (10)*	$R(5,3)^l$	$01^1 \leftarrow 00^0$	Maj87	3053.562 (05)	$R(10,9)_l$	$02^0 \leftarrow 01^1$	Lin01	3172.045 (05)	$R(8,7)^l_l$	$02^2 \leftarrow 01^1$	Lin01
2950.605 (10)*	$R(4,1)^l_l$	$02^2 \leftarrow 01^1$	Xu92	3056.252 (05)*	$R(7,5)^l$	$01^1 \leftarrow 00^0$	Lin01	3175.189 (05)	$R(7,5)^l_l$	$02^2 \leftarrow 01^1$	Lin01
2951.438 (20)	$R(5,3)^u$	$11^1 \leftarrow 10^0$	Carbo‖	3059.381 (10)	$R(9,5)^l$	$01^1 \leftarrow 00^0$	Xu92	3177.167 (05)*	$R(10,8)^l$	$01^1 \leftarrow 00^0$	Lin01
2953.405 (10)*	$R(4,1)^u_u$	$02^2 \leftarrow 01^1$	Xu92	3059.512 (10)	$^nP(3,4)^l$	$11^1 \leftarrow 01^1$	Xu92	3177.167 (05)*	$R(7,3)^u$	$11^1 \leftarrow 10^0$	Lin01
2955.154 (10)*	$R(5,4)^l$	$01^1 \leftarrow 00^0$	Uy94	3060.507 (05)*	$R(5,0)$	$02^2 \leftarrow 01^1$	Lin01	3177.628 (05)	$^nR(7,5)^u$	$02^2 \leftarrow 10^0$	Lin01
2956.072 (10)*	$R(5,5)^l$	$01^1 \leftarrow 00^0$	Oka81	3061.287 (10)*	$R(4,6)$	$03^3 \leftarrow 02^2$	Xu92	3179.115 (05)*	$^tR(6,3)^u_l$	$11^1 \leftarrow 01^1$	Lin01
2956.222 (10)	$^{-6}R(6,2)^u$	$01^1 \leftarrow 00^0$	Uy94‖	3062.110 (05)*	$R(6,6)^u$	$11^1 \leftarrow 10^0$	Lin01	3179.998 (05)*	$R(6,4)^u_u$	$02^2 \leftarrow 01^1$	Lin01
2956.843 (30)	$^tR(7,5)$	$10^0 \leftarrow 00^0$	Xu92‖	3062.813 (10)*	$^nR(0,1)$	$11^1 \leftarrow 01^1$	Xu92	3182.038 (05)	$R(6,6)^u$	$01^1 \leftarrow 00^0$	Lin01
2956.947 (30)*	$R(3,2)^u_l$	$02^2 \leftarrow 01^1$	Xu92	3063.078 (10)	$R(11,6)^l$	$11^1 \leftarrow 00^0$	Xu92	3182.281 (05)*	$^tR(5,2)^u_l$	$11^1 \leftarrow 01^1$	Lin01
2962.822 (10)*	$R(5,3)^l_l$	$02^2 \leftarrow 01^1$	Xu92	3063.273 (10)	$R(6,3)^u$	$03^1 \leftarrow 02^0$	Xu92	3187.488 (05)	$R(11,8)^l$	$01^1 \leftarrow 00^0$	Lin01
2964.705 (10)	$R(5,0)$	$11^1 \leftarrow 10^0$	Xu92‖	3063.935 (05)	$^tR(6,2)^l_l$	$11^1 \leftarrow 01^1$	Lin01	3188.423 (05)	$R(6,2)^l_l$	$02^2 \leftarrow 01^1$	Lin01
2964.987 (10)*	$^tR(5,3)_u$	$11^1 \leftarrow 01^1$	Xu92	3064.356 (05)*	$R(7,6)^l$	$01^1 \leftarrow 00^0$	Lin01	3193.232 (05)*	$R(6,5)^u$	$01^1 \leftarrow 00^0$	Lin01
2966.864 (10)	$R(6,4)^l_u$	$02^2 \leftarrow 01^1$	Xu92	3064.356 (05)*	$R(5,2)^l_l$	$02^2 \leftarrow 01^1$	Lin01	3194.796 (05)*	$^tR(6,0)^l$	$11^1 \leftarrow 01^1$	Lin01
2974.534 (20)*	$^tR(2,1)_u$	$11^1 \leftarrow 01^1$	Xu92	3065.578 (05)*	$R(5,2)^u_u$	$02^2 \leftarrow 01^1$	Lin01	3199.631 (05)*	$^nR(7,7)^l$	$02^2 \leftarrow 10^0$	Lin01
2974.682 (20)*	$^nQ(1,1)$	$11^1 \leftarrow 01^1$	Xu92	3065.777 (05)*	$R(5,1)^u_u$	$02^2 \leftarrow 01^1$	Lin01	3200.723 (05)	$R(10,9)^l$	$01^1 \leftarrow 00^0$	Lin01
2975.656 (10)*	$^tR(5,3)_l$	$12^0 \leftarrow 02^2$	Xu92	3066.565 (05)*	$^tR(5,3)$	$10^0 \leftarrow 00^0$	Lin01	3201.386 (05)	$R(7,1)^l_l$	$02^2 \leftarrow 01^1$	Lin01
2976.080 (10)	$R(8,7)^l_u$	$02^2 \leftarrow 01^1$	Xu92	3067.733 (05)*	$R(4,2)^u_l$	$02^2 \leftarrow 01^1$	Lin01	3201.672 (05)	$R(6,5)^u_u$	$02^2 \leftarrow 01^1$	Lin01
2976.566 (10)*	$R(4,2)^u_u$	$02^2 \leftarrow 01^1$	Xu92‡	3069.176 (05)*	$R(7,7)^l$	$01^1 \leftarrow 00^0$	Lin01	3202.174 (05)	$^tR(5,2)$	$10^0 \leftarrow 00^0$	Lin01
2977.488 (10)†	$R(8,7)_l$	$02^0 \leftarrow 01^1$	Xu92	3076.175 (10)	$R(5,3)^u_u$	$03^3 \leftarrow 02^2$	Lin01	3203.158 (10)*	$^tR(4,1)^u_l$	$11^1 \leftarrow 01^1$	Xu92‡
2979.325 (10)	$^tR(6,4)_l$	$11^1 \leftarrow 01^1$	Xu92	3077.457 (10)†	$^tR(6,3)$	$20^0 \leftarrow 10^0$	Lin01	3203.513 (10)	$R(8,6)^u$	$11^1 \leftarrow 10^0$	Xu92
2979.507 (10)	$R(6,1)^l$	$01^1 \leftarrow 00^0$	Xu92	3078.892 (05)	$R(9,3)^l$	$01^1 \leftarrow 00^0$	Lin01	3205.308 (05)	$R(6,4)^u$	$01^1 \leftarrow 00^0$	Lin01
2979.658 (10)*	$^nR(6,6)^l$	$02^2 \leftarrow 10^0$	Xu92	3085.617 (05)*	$^tR(5,3)_l$	$11^1 \leftarrow 01^1$	Lin01	3209.072 (05)*	$R(11,9)^l$	$01^1 \leftarrow 00^0$	Lin01
2980.327 (10)*	$R(4,3)^u_u$	$02^2 \leftarrow 01^1$	Carbo‖	3086.072 (05)*	$^tR(4,2)_l$	$11^1 \leftarrow 01^1$	Lin01	3210.543 (05)	$R(12,9)^l$	$01^1 \leftarrow 00^0$	Lin01
2984.082 (10)*	$R(6,2)^l$	$01^1 \leftarrow 00^0$	Xu92	3091.891 (10)*	$^nQ(2,2)^u$	$11^1 \leftarrow 01^1$	Xu92	3210.801 (05)	$R(10,10)^l$	$01^1 \leftarrow 00^0$	Lin01
2984.259 (10)*	$^tR(4,3)_l$	$11^1 \leftarrow 01^1$	Xu92	3092.324 (10)*	$^nQ(1,2)$	$11^1 \leftarrow 01^1$	Xu92‡	3212.252 (05)	$R(6,2)^u$	$01^1 \leftarrow 00^0$	Lin01
2985.494 (10)*	$R(6,3)^l$	$01^1 \leftarrow 00^0$	Xu92	3093.669 (05)	$R(7,7)^u$	$11^1 \leftarrow 10^0$	Lin01	3214.612 (05)	$R(6,6)$	$02^2 \leftarrow 01^1$	Lin01
2989.507 (20)*	$R(6,4)^l$	$01^1 \leftarrow 00^0$	Xu92	3096.416 (05)*	$R(5,5)^u$	$01^1 \leftarrow 00^0$	Lin01	3216.361 (05)*	$R(6,3)^u$	$01^1 \leftarrow 00^0$	Lin01
2989.507 (30)*	$^tR(3,2)_l$	$11^1 \leftarrow 01^1$	Xu92	3096.665 (05)*	$R(6,3)^l_l$	$02^2 \leftarrow 01^1$	Lin01	3219.108 (05)	$^tR(7,3)$	$10^0 \leftarrow 00^0$	Lin01
2989.618 (10)	$^tR(4,0)$	$12^0 \leftarrow 02^2$	Xu92	3097.259 (05)*	$^tR(2,0)$	$11^1 \leftarrow 01^1$	Lin01	3220.181 (05)	$R(7,0)$	$02^2 \leftarrow 01^1$	Lin01
2990.585 (10)*†	$^tR(5,2)^l_l$	$11^1 \leftarrow 01^1$	Xu92	3097.985 (05)*	$R(5,4)^u_u$	$02^2 \leftarrow 01^1$	Lin01	3220.816 (05)	$R(6,1)^u$	$01^1 \leftarrow 00^0$	Lin01
2993.467 (10)*	$R(7,5)^l_u$	$02^2 \leftarrow 01^1$	Xu92	3099.905 (05)*	$R(8,6)^l$	$01^1 \leftarrow 00^0$	Lin01	3221.086 (05)	$^nQ(2,3)$	$11^1 \leftarrow 01^1$	Lin01
2994.903 (10)*	$^tR(4,2)_u$	$11^1 \leftarrow 01^1$	Xu92	3100.131 (05)*	$^tR(7,3)$	$20^0 \leftarrow 10^0$	Lin01	3221.214 (05)*	$R(7,1)^u_u$	$02^2 \leftarrow 01^1$	Lin01
2998.347 (15)*	$R(11,7)^l_l$	$02^2 \leftarrow 01^1$	Lin01	3100.871 (05)	$^nR(7,6)^l$	$02^2 \leftarrow 10^0$	Lin01	3222.022 (05)	$R(5,3)^u_l$	$02^2 \leftarrow 01^1$	Lin01
3000.105 (10)	$^tR(8,6)_l$	$11^1 \leftarrow 01^1$	Xu92	3101.397 (05)	$R(5,3)^u_u$	$02^2 \leftarrow 01^1$	Lin01	3228.754 (05)*	$^tR(3,0)^u$	$11^1 \leftarrow 01^1$	Lin01
3002.355 (10)	$R(10,10)^l$	$11^1 \leftarrow 10^0$	Xu92	3102.368 (05)*	$R(8,5)^l$	$01^1 \leftarrow 00^0$	Lin01	3235.574 (05)*	$R(6,7)$	$02^2 \leftarrow 01^1$	Lin01
3002.750 (10)	$^nR(8,8)$	$02^0 \leftarrow 10^0$	Xu92	3102.736 (05)*	$^tR(3,1)_l$	$11^1 \leftarrow 01^1$	Lin01	3235.813 (05)	$R(12,10)^l$	$01^1 \leftarrow 00^0$	Lin01
3003.253 (05)	$R(5,3)^u$	$03^1 \leftarrow 02^0$	Lin01	3103.873 (05)*	$R(6,0)$	$02^2 \leftarrow 01^1$	Lin01	3236.270 (05)	$R(7,4)^l_l$	$02^2 \leftarrow 01^1$	Lin01
3006.996 (05)	$R(5,4)^l_l$	$02^2 \leftarrow 01^1$	Lin01	3106.804 (05)	$R(5,4)^u$	$01^1 \leftarrow 00^0$	Lin01	3238.614 (05)*	$R(11,10)^l$	$01^1 \leftarrow 00^0$	Lin01
3008.108 (05)*	$R(4,4)^u$	$01^1 \leftarrow 00^0$	Lin01	3108.871 (05)*	$R(7,6)^l_l$	$02^2 \leftarrow 01^1$	Lin01	3238.662 (05)	$R(9,8)^l_l$	$02^2 \leftarrow 01^1$	Lin01
3009.317 (05)*	$^tR(2,1)_l$	$11^1 \leftarrow 01^1$	Lin01	3110.877 (10)*	$^nP(5,6)^l$	$11^1 \leftarrow 01^1$	Lin01	3240.385 (05)*	$R(8,6)^l_l$	$02^2 \leftarrow 01^1$	Lin01
3011.509 (05)*	$R(6,5)^l$	$01^1 \leftarrow 00^0$	Lin01	3111.038 (10)	$^nR(9,9)$	$02^0 \leftarrow 10^0$	Lin01	3247.272 (05)	$^tR(8,2)^u_u$	$11^1 \leftarrow 01^1$	Lin01
3014.364 (05)*	$R(6,6)^l$	$01^1 \leftarrow 00^0$	Lin01	3113.532 (05)*	$R(8,7)^l$	$01^1 \leftarrow 00^0$	Lin01	3247.694 (05)	$R(7,2)^u_u$	$02^2 \leftarrow 01^1$	Lin01
3015.241 (05)*	$R(4,3)^u$	$01^1 \leftarrow 00^0$	Lin01	3115.615 (05)*	$R(5,5)$	$02^2 \leftarrow 01^1$	Lin01	3247.800 (05)	$^tR(6,1)^l_l$	$11^1 \leftarrow 01^1$	Lin01
3017.629 (05)	$R(5,0)$	$03^3 \leftarrow 02^2$	Lin01	3118.511 (05)	$R(6,4)^l_l$	$02^2 \leftarrow 01^1$	Lin01	3247.891 (05)	$R(7,4)^u_u$	$02^2 \leftarrow 01^1$	Lin01
3018.586 (05)	$R(9,8)_l$	$02^0 \leftarrow 01^1$	Lin01	3120.210 (05)	$^tR(4,2)$	$10^0 \leftarrow 00^0$	Lin01	3249.704 (05)	$R(11,11)^l$	$01^1 \leftarrow 00^0$	Lin01
3020.495 (05)	$R(4,4)$	$02^2 \leftarrow 01^1$	Lin01	3120.321 (05)*	$R(8,8)^l$	$01^1 \leftarrow 00^0$	Lin01	3249.794 (05)	$R(7,3)^u_u$	$02^2 \leftarrow 01^1$	Lin01
3021.862 (05)*	$R(6,4)^u_u$	$12^2 \leftarrow 11^1$	Lin01	3121.216 (05)	$^tR(4,0)^l$	$11^1 \leftarrow 01^1$	Lin01	3259.835 (05)*	$R(7,3)^l_l$	$02^2 \leftarrow 01^1$	Lin01
3022.424 (05)*	$^tR(5,1)^l_u$	$11^1 \leftarrow 01^1$	Lin01	3121.814 (05)*	$R(5,3)^u$	$01^1 \leftarrow 00^0$	Lin01	3261.336 (05)	$R(8,5)^l_l$	$02^2 \leftarrow 01^1$	Lin01
3023.674 (10)	$R(6,3)^u$	$11^1 \leftarrow 10^0$	Xu92	3122.252 (05)*	$R(5,2)^u$	$01^1 \leftarrow 00^0$	Lin01	3265.138 (05)	$R(7,7)^u$	$01^1 \leftarrow 00^0$	Lin01
3024.439 (10)	$^tR(8,5)$	$10^0 \leftarrow 00^0$	Lin01	3128.068 (05)*	$R(5,1)^u$	$01^1 \leftarrow 00^0$	Lin01	3265.304 (05)	$R(8,1)^u_u$	$02^2 \leftarrow 01^1$	Lin01
3024.558 (10)*	$R(4,2)^u$	$01^1 \leftarrow 00^0$	Lin01	3128.296 (05)	$R(7,2)^u$	$11^1 \leftarrow 10^0$	Lin01	3266.017 (05)	$R(7,5)^u_u$	$02^2 \leftarrow 01^1$	Lin01
3025.941 (05)*	$R(7,4)^l$	$01^1 \leftarrow 00^0$	Lin01	3129.516 (10)	$^nR(6,1)^l_l$	$02^2 \leftarrow 01^1$	Lin01	3269.095 (05)	$^nR(8,5)^u$	$02^2 \leftarrow 10^0$	Lin01
3026.162 (05)*	$^tR(6,4)$	$10^0 \leftarrow 00^0$	Lin01	3129.811 (05)	$R(5,0)$	$01^1 \leftarrow 00^0$	Lin01	3269.496 (05)	$R(8,3)^u$	$11^1 \leftarrow 10^0$	Lin01
3028.543 (05)*	$R(8,6)^l_u$	$02^2 \leftarrow 01^1$	Lin01	3130.216 (05)*	$R(9,6)^l$	$01^1 \leftarrow 00^0$	Lin01	3270.571 (05)	$R(14,12)^l$	$01^1 \leftarrow 00^0$	Lin01
3028.977 (05)*	$R(7,3)^l_u$	$02^2 \leftarrow 01^1$	Lin01	3134.077 (05)*	$R(7,6)^u$	$03^1 \leftarrow 02^0$	Lin01	3272.713 (05)	$R(12,11)^l$	$01^1 \leftarrow 00^0$	Lin01
3029.075 (10)*	$R(7,3)^l$	$01^1 \leftarrow 00^0$	Lin01	3136.793 (05)	$R(7,1)^u$	$11^1 \leftarrow 10^0$	Lin01	3276.197 (05)*	$R(7,6)^u$	$01^1 \leftarrow 00^0$	Lin01
3029.832 (05)*	$R(4,1)^u$	$01^1 \leftarrow 00^0$	Lin01	3137.145 (05)	$R(5,6)$	$02^2 \leftarrow 01^1$	Lin01	3277.429 (05)*	$^tR(8,3)$	$10^0 \leftarrow 00^0$	Lin01
3033.304 (10)	$R(6,5)^u$	$11^1 \leftarrow 10^0$	Xu92	3137.814 (05)*	$R(6,3)^u_u$	$02^2 \leftarrow 01^1$	Lin01	3282.308 (05)	$^tR(6,2)$	$10^0 \leftarrow 00^0$	Lin01
3033.746 (05)*	$R(8,3)^l$	$01^1 \leftarrow 00^0$	Lin01	3138.979 (05)	$R(7,0)$	$11^1 \leftarrow 10^0$	Lin01	3282.997 (05)	$^{-6}R(8,6)_u$	$02^0 \leftarrow 01^1$	Lin01
3035.475 (05)*	$R(4,5)$	$02^2 \leftarrow 01^1$	Lin01	3140.641 (05)	$R(9,7)^l$	$01^1 \leftarrow 00^0$	Lin01	3284.093 (05)	$R(12,12)^l$	$01^1 \leftarrow 00^0$	Lin01
3036.720 (10)	$R(12,12)$	$02^0 \leftarrow 01^1$	Lin01	3144.458 (05)	$^tR(6,3)$	$10^0 \leftarrow 00^0$	Lin01	3285.768 (05)*	$R(7,6)^u_u$	$02^2 \leftarrow 01^1$	Lin01
3037.319 (05)*	$^tR(1,0)$	$11^1 \leftarrow 01^1$	Lin01	3146.461 (10)*	$^nR(1,1)$	$11^1 \leftarrow 01^1$	Xu92	3288.443 (05)	$^tR(7,3)^u_l$	$11^1 \leftarrow 01^1$	Lin01
3038.913 (10)	$^tR(10,6)$	$10^0 \leftarrow 00^0$	Xu92	3150.724 (05)*	$R(6,1)^u_u$	$02^2 \leftarrow 01^1$	Lin01	3289.115 (05)	$R(7,5)^u$	$01^1 \leftarrow 00^0$	Lin01
3042.157 (10)*	$^tR(3,1)_u$	$11^1 \leftarrow 01^1$	Xu92	3151.824 (05)	$R(7,4)^u$	$11^1 \leftarrow 10^0$	Lin01	3290.752 (10)	$R(7,2)^u$	$01^1 \leftarrow 00^0$	Xu92

TABLE 5—*Continued*

Frequency[a] (cm^{-1})	Assignment[b] Label	Band	Ref[c]	Frequency[a] (cm^{-1})	Assignment[b] Label	Band	Ref[c]	Frequency[a] (cm^{-1})	Assignment[b] Label	Band	Ref[c]
3292.521 (05)	$R(7,2)^l_l$	$02^2 \leftarrow 01^1$	Lin01	3473.764 (05)	$R(10,6)^u_u$	$02^2 \leftarrow 01^1$	Lin01	4900.393 (10)*	${}^tR(3,3)$	$02^2 \leftarrow 00^0$	Xu90
3293.790 (05)	$R(9,6)^u$	$11^1 \leftarrow 10^0$	Lin01	3476.189 (05)	$R(9,4)^u$	$01^1 \leftarrow 00^0$	Lin01	4907.871 (10)*	${}^tQ(1,0)$	$02^2 \leftarrow 00^0$	Xu90
3296.014 (05)	$R(9,9)^u$	$11^1 \leftarrow 10^0$	Lin01	3486.049 (05)	$R(9,9)$	$02^2 \leftarrow 01^1$	Lin01	4908.672 (20)*	${}^nP(4,3)$	$02^2 \leftarrow 00^0$	Xu90
3298.990 (05)	$R(8,3)^u_u$	$02^2 \leftarrow 01^1$	Lin01	3497.971 (05)	$R(9,3)^u$	$01^1 \leftarrow 00^0$	Lin01	4914.248 (10)*	${}^tQ(3,0)$	$02^2 \leftarrow 00^0$	Xu90
3300.111 (10)*	${}^tR(5,0)^l$	$11^1 \leftarrow 01^1$	Lin01	3498.764 (05)	${}^{-6}R(9,5)^l$	$01^1 \leftarrow 00^0$	Lin01	4930.981 (20)	${}^nP(6,5)^l$	$02^2 \leftarrow 00^0$	Maj89
3301.694 (05)	${}^{-6}R(8,5)_l$	$02^0 \leftarrow 01^1$	Lin01	3499.417 (05)	$R(10,10)^u$	$01^1 \leftarrow 00^0$	Lin01	4931.596 (20)*	${}^tR(6,5)$	$02^2 \leftarrow 00^0$	Xu90
3302.423 (05)*	$R(7,4)^u$	$01^1 \leftarrow 00^0$	Lin01	3503.306 (10)	$R(10,9)^u$	$01^1 \leftarrow 00^0$	Lin01	4936.000 (20)*	${}^tR(2,2)$	$02^2 \leftarrow 00^0$	Xu90
3303.093 (05)*	$R(13,12)^l$	$01^1 \leftarrow 00^0$	Lin01	3513.541 (05)	$R(10,8)^u$	$01^1 \leftarrow 00^0$	Lin01	4955.991 (10)*	${}^nP(2,2)$	$02^2 \leftarrow 00^0$	Xu90
3305.935 (05)	$R(7,1)^u$	$01^1 \leftarrow 00^0$	Lin01	3516.951 (05)	$R(9,2)^u$	$01^1 \leftarrow 00^0$	Lin01	4966.838 (20)*	${}^tR(5,4)$	$02^2 \leftarrow 00^0$	Xu90
3307.150 (05)	$R(10,9)^l_l$	$02^2 \leftarrow 01^1$	Lin01	3521.044 (05)	$R(9,10)$	$02^2 \leftarrow 01^1$	Lin01	4968.272 (10)*	${}^tR(1,1)$	$02^2 \leftarrow 00^0$	Xu90
3308.650 (10)	$R(9,7)^l_l$	$02^2 \leftarrow 01^1$	Lin01	3523.742 (05)	${}^tR(8,1)$	$10^0 \leftarrow 00^0$	Lin01	4971.561 (10)*	${}^nP(3,3)$	$02^2 \leftarrow 00^0$	Xu90
3308.685 (05)	$R(7,0)$	$01^1 \leftarrow 00^0$	Lin01	3523.998 (05)	$R(10,7)^u$	$01^1 \leftarrow 00^0$	Lin01	4975.338 (20)*	${}^nP(6,6)^l$	$02^2 \leftarrow 00^0$	Xu90
3309.924 (05)	$R(7,7)$	$02^2 \leftarrow 01^1$	Lin01	3527.047 (05)	$R(10,9)^u_u$	$02^2 \leftarrow 01^1$	Lin01	5000.499 (10)*	${}^tR(4,3)$	$02^2 \leftarrow 00^0$	Xu90
3311.009 (05)	$R(8,0)$	$02^2 \leftarrow 01^1$	Lin01	3531.279 (05)	$R(10,6)^u$	$01^1 \leftarrow 00^0$	Lin01	5023.496 (10)*	${}^nQ(1,1)$	$02^2 \leftarrow 00^0$	Xu90
3313.752 (05)	$R(13,13)^l$	$01^1 \leftarrow 00^0$	Lin01	3546.576 (05)	$R(10,5)^u$	$01^1 \leftarrow 00^0$	Lin01	5029.071 (10)*	${}^nQ(2,1)$	$02^2 \leftarrow 00^0$	Xu90
3317.786 (05)	${}^nR(8,1)^l_u$	$11^1 \leftarrow 01^1$	Lin01	3551.579 (15)	$R(10,3)^u$	$01^1 \leftarrow 00^0$	Lin01	5032.447 (10)*	${}^tR(3,2)$	$02^2 \leftarrow 00^0$	Xu90
3321.010 (05)	$R(7,3)^u$	$01^1 \leftarrow 00^0$	Lin01	3552.313 (15)	$R(10,4)^u$	$01^1 \leftarrow 00^0$	Lin01	5054.742 (100)*	${}^nQ(4,1)^u$	$02^2 \leftarrow 00^0$	Maj89
3325.674 (10)	${}^tR(5,1)$	$10^0 \leftarrow 00^0$	Lin01	3553.705 (15)	$R(11,0)$	$01^1 \leftarrow 00^0$	Lin01	5061.882 (20)*	${}^tR(2,1)$	$02^2 \leftarrow 00^0$	Xu90
3328.773 (05)	$R(8,3)^l_l$	$02^2 \leftarrow 01^1$	Lin01	3571.295 (15)	$R(11,10)^u$	$01^1 \leftarrow 00^0$	Lin01	5094.218 (20)*	${}^tR(1,0)$	$02^2 \leftarrow 00^0$	Xu90
3329.924 (05)	$R(14,13)^l$	$01^1 \leftarrow 00^0$	Lin01	3572.419 (15)	$R(11,11)^u$	$01^1 \leftarrow 00^0$	Lin01	6806.665 (70)*	$P(3,1)^u$	$03^1 \leftarrow 00^0$	Ven94
3331.374 (05)	$R(8,4)^l_l$	$02^2 \leftarrow 01^1$	Lin01	3574.750 (15)	${}^tR(7,0)$	$10^0 \leftarrow 00^0$	Lin01	6807.297 (70)*	$P(3,3)$	$03^1 \leftarrow 00^0$	Ven94
3331.571 (05)	$R(8,5)^u_u$	$02^2 \leftarrow 01^1$	Lin01	3579.301 (15)	$R(11,9)^u$	$01^1 \leftarrow 00^0$	Lin01	6807.724 (70)*	$P(3,2)$	$03^1 \leftarrow 00^0$	Ven94
3332.520 (05)	$R(7,8)$	$02^2 \leftarrow 01^1$	Lin01	3586.139 (15)	$R(10,2)^u$	$01^1 \leftarrow 00^0$	Lin01	6811.218 (200)*	$P(3,0)$	$03^1 \leftarrow 00^0$	Ven94
3338.534 (05)	$R(14,14)^l$	$01^1 \leftarrow 00^0$	Lin01	3588.381 (15)	$R(11,8)^u$	$01^1 \leftarrow 00^0$	Lin01	6865.731 (70)*	$P(2,1)$	$03^1 \leftarrow 00^0$	Ven94
3343.327 (05)	${}^tR(9,3)$	$10^0 \leftarrow 00^0$	Lin01	3596.217 (15)	$R(11,7)^u$	$01^1 \leftarrow 00^0$	Lin01	6866.340 (70)*	$Q(5,0)$	$03^1 \leftarrow 00^0$	Ven94
3345.710 (05)	$R(8,8)^u$	$01^1 \leftarrow 00^0$	Lin01	3642.547 (10)	$R(12,12)^u$	$01^1 \leftarrow 00^0$	Maj94	6877.546 (70)*	$P(2,2)$	$03^1 \leftarrow 00^0$	Ven94
3348.845 (05)	$R(9,6)^l_l$	$02^2 \leftarrow 01^1$	Lin01	4434.861 (10)*	${}^tQ(5,4)$	$02^2 \leftarrow 00^0$	Maj94	6883.091 (70)*	$Q(5,3)^l$	$03^1 \leftarrow 00^0$	Ven94
3355.517 (05)*	$R(8,7)^u$	$01^1 \leftarrow 00^0$	Lin01	4465.095 (10)*	${}^tQ(6,4)$	$02^2 \leftarrow 00^0$	Maj94	6891.619 (70)*	$Q(4,3)^l$	$03^1 \leftarrow 00^0$	Ven94
3356.747 (05)*	$R(8,2)^u$	$01^1 \leftarrow 00^0$	Lin01	4539.759 (20)*	${}^tP(5,0)$	$02^2 \leftarrow 00^0$	Maj89	7144.212 (70)*	$R(1,1)^l$	$03^1 \leftarrow 00^0$	Ven94
3358.400 (05)	$R(15,15)^l$	$01^1 \leftarrow 00^0$	Lin01	4553.340 (10)*	${}^tQ(4,3)_u$	$03^3 \leftarrow 01^1$	Maj94	7192.908 (70)*	$R(2,2)^l$	$03^1 \leftarrow 00^0$	Ven94
3362.256 (10)	${}^tR(7,2)$	$10^0 \leftarrow 00^0$	Lin01	4557.020 (20)*	${}^tQ(4,3)$	$02^2 \leftarrow 00^0$	Xu90	7234.957 (70)*	$R(3,3)^l$	$03^1 \leftarrow 00^0$	Ven94
3368.118 (05)*	$R(8,6)^u$	$01^1 \leftarrow 00^0$	Lin01	4557.731 (10)*	${}^nP(7,1)^u$	$02^2 \leftarrow 00^0$	Maj94	7237.285 (70)*	$R(1,1)^u$	$03^1 \leftarrow 00^0$	Ven94
3368.560 (05)*	$R(8,7)^u_u$	$02^2 \leftarrow 01^1$	Lin01	4578.735 (20)*	${}^tQ(5,3)$	$02^2 \leftarrow 00^0$	Xu90	7241.245 (70)*	$R(1,0)$	$03^1 \leftarrow 00^0$	Ven94
3369.664 (05)	$R(9,5)^l_l$	$02^2 \leftarrow 01^1$	Lin01	4607.205 (20)*	${}^tQ(6,3)$	$02^2 \leftarrow 00^0$	Maj89	7265.882 (70)*	$R(4,4)^l$	$03^1 \leftarrow 00^0$	Ven94
3375.003 (05)	$R(8,6)^u_u$	$02^2 \leftarrow 01^1$	Lin01	4637.992 (50)*	${}^nP(5,1)^u$	$02^2 \leftarrow 00^0$	Maj89	7785.233 (10)*	${}^tQ(3,0)$	$12^2 \leftarrow 00^0$	McC00
3376.775 (05)	$R(11,10)^u_l$	$02^2 \leftarrow 01^1$	Lin01	4638.331 (10)	${}^tR(9,9)$	$02^2 \leftarrow 00^0$	Xu90	7785.701 (10)	${}^tQ(1,0)$	$12^2 \leftarrow 00^0$	McC00
3377.047 (05)	${}^tR(10,3)$	$10^0 \leftarrow 00^0$	Lin01	4641.987 (20)*	${}^tQ(7,3)$	$02^2 \leftarrow 00^0$	Maj89	7789.878 (10)	${}^tR(3,3)$	$12^2 \leftarrow 00^0$	McC00
3380.010 (05)	$R(8,5)^u$	$01^1 \leftarrow 00^0$	Lin01	4661.576 (10)*	${}^nP(7,3)$	$02^2 \leftarrow 00^0$	Maj94	7805.893 (10)†	${}^nP(1,1)$	$12^2 \leftarrow 00^0$	McC00
3381.399 (05)	$R(8,1)^u$	$01^1 \leftarrow 00^0$	Lin01	4664.306 (10)*	${}^tP(3,0)$	$02^2 \leftarrow 00^0$	Xu90	7820.239 (10)	${}^nP(2,2)$	$12^2 \leftarrow 00^0$	McC00
3388.155 (05)	$R(8,2)^l_l$	$02^2 \leftarrow 01^1$	Lin01	4677.273 (15)*	${}^tQ(3,2)$	$02^2 \leftarrow 00^0$	Xu90	7822.375 (10)	${}^tR(2,2)$	$12^2 \leftarrow 00^0$	McC00
3389.119 (05)	$R(9,3)^u_u$	$02^2 \leftarrow 01^1$	Lin01	4685.564 (10)	${}^tR(8,8)$	$02^2 \leftarrow 00^0$	Xu90	7826.739 (10)	${}^nP(3,3)$	$12^2 \leftarrow 00^0$	McC00
3392.547 (05)	$R(8,4)^u$	$01^1 \leftarrow 00^0$	Lin01	4691.962 (100)	${}^tQ(4,2)$	$02^2 \leftarrow 00^0$	Maj89	7833.249 (20)	${}^nP(4,4)^l$	$12^2 \leftarrow 00^0$	McC00
3395.752 (05)	${}^tR(6,1)$	$10^0 \leftarrow 00^0$	Lin01	4700.139 (20)*	${}^nP(4,1)$	$02^2 \leftarrow 00^0$	Maj89	7850.959 (10)	${}^tR(1,1)$	$12^2 \leftarrow 00^0$	McC00
3399.510 (05)	$R(8,3)^u$	$01^1 \leftarrow 00^0$	Lin01	4712.282 (10)*	${}^tQ(5,2)$	$02^2 \leftarrow 00^0$	Maj94	7880.921 (10)	${}^tR(4,3)$	$12^2 \leftarrow 00^0$	McC00
3399.872 (05)	$R(8,8)$	$02^2 \leftarrow 01^1$	Lin01	4721.019 (10)*	${}^nP(4,3)_l$	$03^3 \leftarrow 01^1$	Maj94	7894.711 (10)	${}^nQ(1,1)$	$12^2 \leftarrow 00^0$	McC00
3407.501 (05)	$R(9,6)^u_u$	$02^2 \leftarrow 01^1$	Lin01	4732.041 (10)*	${}^tR(7,7)$	$02^2 \leftarrow 00^0$	Maj94	7898.371 (10)*	${}^nQ(2,1)$	$12^2 \leftarrow 00^0$	McC00
3408.984 (10)	$R(10,7)^u_l$	$02^2 \leftarrow 01^1$	Lin01	4735.941 (100)*	${}^tQ(6,2)$	$02^2 \leftarrow 00^0$	Maj89	7905.717 (10)*	${}^nQ(3,1)$	$12^2 \leftarrow 00^0$	McC00
3411.415 (05)	$R(9,7)^u_u$	$02^2 \leftarrow 01^1$	Lin01	4744.767 (10)*	${}^nP(5,2)^u$	$02^2 \leftarrow 00^0$	Maj94	7912.047 (10)	${}^tR(3,2)$	$12^2 \leftarrow 00^0$	McC00
3411.859 (05)	${}^tR(9,2)$	$10^0 \leftarrow 00^0$	Lin01	4766.167 (100)*	${}^nP(7,4)^l$	$02^2 \leftarrow 00^0$	Maj94	7939.619 (10)	${}^tR(2,1)$	$12^2 \leftarrow 00^0$	McC00
3423.809 (05)	$R(9,9)^u$	$01^1 \leftarrow 00^0$	Lin01	4771.641 (100)*	${}^nP(3,1)$	$02^2 \leftarrow 00^0$	Maj89	7970.413 (10)*	${}^tR(1,0)$	$12^2 \leftarrow 00^0$	McC00
3427.667 (05)*	$R(8,9)$	$02^2 \leftarrow 01^1$	Lin01	4777.226 (10)*	${}^tR(6,6)$	$02^2 \leftarrow 00^0$	Xu90	7998.890 (10)	${}^nQ(2,2)$	$12^2 \leftarrow 00^0$	McC00
3431.295 (05)	$R(9,8)^u$	$01^1 \leftarrow 00^0$	Lin01	4795.030 (10)*	${}^tQ(2,1)$	$02^2 \leftarrow 00^0$	Maj94	8005.582 (30)	${}^tR(4,2)$	$12^2 \leftarrow 00^0$	McC00
3439.825 (05)	$R(11,9)^u_l$	$02^2 \leftarrow 01^1$	Lin01	4804.406 (50)*	${}^tQ(3,1)$	$02^2 \leftarrow 00^0$	Maj89	8007.410 (10)	${}^nQ(3,2)^u$	$12^2 \leftarrow 00^0$	McC00
3441.416 (05)	${}^tR(8,2)$	$10^0 \leftarrow 00^0$	Lin01	4805.287 (20)*	${}^nP(4,2)^u$	$02^2 \leftarrow 00^0$	Maj89	8022.012 (20)	${}^nQ(4,2)^u$	$12^2 \leftarrow 00^0$	McC00
3443.148 (05)	$R(9,7)^u$	$01^1 \leftarrow 00^0$	Lin01	4814.521 (20)*	${}^nP(6,3)$	$02^2 \leftarrow 00^0$	Maj89	8027.840 (20)	${}^tR(3,1)$	$12^2 \leftarrow 00^0$	McC00
3443.466 (10)	${}^tR(7,0)^l$	$11^1 \leftarrow 01^1$	Lin01	4816.353 (10)*	${}^nP(5,3)$	$02^2 \leftarrow 00^0$	Xu90	8037.673 (10)	${}^nR(3,1)^l$	$12^2 \leftarrow 00^0$	McC00
3445.702 (05)	$R(9,1)^u$	$01^1 \leftarrow 00^0$	Lin01	4818.901 (20)*	${}^tQ(4,1)$	$02^2 \leftarrow 00^0$	Maj89	8053.382 (10)*	$P(6,6)$	$21^1 \leftarrow 00^0$	McC00
3448.014 (05)	${}^tR(5,0)$	$10^0 \leftarrow 00^0$	Lin01	4820.598 (10)*	${}^tR(5,5)$	$02^2 \leftarrow 00^0$	Xu90	8071.617 (10)*	${}^nR(1,1)$	$12^2 \leftarrow 00^0$	McC00
3450.711 (05)	$R(9,8)^u_u$	$02^2 \leftarrow 01^1$	Lin01	4839.508 (20)*	${}^tQ(5,1)$	$02^2 \leftarrow 00^0$	Maj89	8089.406 (10)	${}^nQ(4,3)$	$12^2 \leftarrow 00^0$	McC00
3452.852 (05)	$R(9,0)$	$01^1 \leftarrow 00^0$	Lin01	4850.264 (20)*	${}^nP(2,1)$	$02^2 \leftarrow 00^0$	Xu90	8110.069 (10)*	${}^nQ(3,3)$	$12^2 \leftarrow 00^0$	McC00
3455.008 (05)	$R(9,6)^u$	$01^1 \leftarrow 00^0$	Lin01	4859.212 (20)*	${}^tR(8,7)$	$02^2 \leftarrow 00^0$	Xu90	8123.128 (10)	$P(5,5)$	$21^1 \leftarrow 00^0$	McC00
3457.772 (05)	${}^tR(10,2)$	$10^0 \leftarrow 00^0$	Lin01	4861.790 (20)*	${}^tR(4,4)$	$02^2 \leftarrow 00^0$	Xu90	8128.280 (10)	${}^tR(4,1)$	$12^2 \leftarrow 00^0$	McC00
3458.383 (05)	$R(9,3)^l_l$	$02^2 \leftarrow 01^1$	Lin01	4876.938 (10)*	${}^nP(3,2)$	$02^2 \leftarrow 00^0$	Xu90	8162.653 (10)	${}^tR(3,0)$	$12^2 \leftarrow 00^0$	McC00
3461.308 (05)	$R(9,5)^u$	$01^1 \leftarrow 00^0$	Lin01	4895.518 (20)*	${}^tR(7,6)$	$02^2 \leftarrow 00^0$	Xu90	8163.129 (10)*	${}^nR(2,1)$	$12^2 \leftarrow 00^0$	McC00
3461.643 (05)	${}^tR(7,1)$	$10^0 \leftarrow 00^0$	Lin01								

[a] Recommended transition frequency and uncertainties in the last decimal places (in parentheses) in cm^{-1}. Transitions marked with an asterisk were confirmed by combination differences with other transitions.

[b] Recommended assignments using the transition notation defined in Section III.2.

[c] Reference from which the recommended frequency is based. "Carbo" refers to unpublished transitions observed during carbo-cation studies (*51*). Labels defined in Table 1.

† Unusually large deviation from *ab initio* calculations.

‡ Corrected frequency. There was an error in the previously reported value.

‖ Transition not reported in paper, but was identified and measured by us from the original data.

due to a species other than H_3^+. Lines without an asterisk had one or more candidate assignments whose frequency and/or intensity difference from theory was too large to allow a confident assignment.

III.3. Construction of Experimentally Determined Energy Levels

One of the goals of this work was to determine the energy levels from experimental transitions. Constructing all of the relationships between the levels is only possible by combining transitions from different bands. For example, the fundamental band (with the selection rule $\Delta G = 0$) can relate individual J levels within a G "stack" to one another with a combination of P, Q, and R transitions. Relating different G stacks requires transitions with a selection rule other than $\Delta G = 0$. This is the case for overtone and forbidden bands which have the selection rule $\Delta G = \pm 3$. Using a combination of the $\nu_2 \leftarrow 0$, $2\nu_2^2 \leftarrow \nu_2$, and $2\nu_2^2 \leftarrow 0$ transitions, Baw90 and Xu90 experimentally determined the first term values of the ground state in 1990.

We wrote a program to automatically extract from the transition data the relative energies of each level. First, combinations of $\nu_2 \leftarrow 0$, $2\nu_2^2 \leftarrow \nu_2$ and $2\nu_2^2 \leftarrow 0$ bands were used to determine as many ground vibrational state energy relationships as possible. Once this was done, the program examined every transition, searching for transitions whose upper or lower level had already been "determined." The other level in the transition was then calculated. This process was then iterated until no additional levels could be determined. Uncertainties in the transitions were added in quadrature and propagated through the calculation. We performed the entire process twice, once with all of the assigned transitions and once with only the transitions that had been confirmed by combination differences. Levels that were calculated in the first list but not in the second list were necessarily determined by only one transition and are susceptible to mistakes in transition assignments.

At this stage, only the relative values of the energies have been determined and an absolute standard is needed. Additionally, the energy differences between between *ortho* ($G = 3n$) and *para* ($G = 3n \pm 1$) levels are not determined because transitions between them are forbidden. In the past (*21*, *22*), the relationship between *ortho* and *para* levels and the offset from the forbidden level $(J, G) = (0, 0)$ were taken from theoretical calculations. To remain independent from calculations, we instead performed a fit on the ground vibrational state to determine the relationship between the *ortho* and *para* levels as well as their relationship to the (0, 0) level. To do this, we initially computed the absolute values of all of the *ortho* and *para* levels assuming that the lowest populated energy level in each set had zero energy. Next, we performed a least-squares fit of every determined energy level in the ground vibrational state to the following modified symmetric top energy level expression:

$$\begin{aligned} E(J,G) = {} & -E_{1,1} - \delta_{G,3n}E_{o-p} + BJ(J+1) + (C-B)G^2 \\ & - D_{JJ}J^2(J+1)^2 - D_{JG}J(J+1)G^2 - D_{GG}G^4 \\ & - \delta_{G,3}(-1)^J h_3\left\{\frac{(J+3)!}{(J-3)!}\right\} + H_{JJJ}J^3(J+1)^3 \\ & + H_{JJG}J^2(J+1)^2G^2 + H_{JGG}J(J+1)G^4 \\ & + H_{GGG}G^6 + L_{JJJJ}J^4(J+1)^4 \\ & + L_{JJJG}J^3(J+1)^3G^2 + L_{JJGG}J^2(J+1)^2G^4 \\ & + L_{JGGG}J(J+1)G^6 + L_{GGGG}G^8. \end{aligned} \quad [10]$$

The first fitted parameter, $E_{1,1}$, gives the energy of the lowest populated *ortho* level (1,1) relative to the forbidden (0,0) level, and the second parameter, E_{o-p}, gives the energy separation between the (1,1) and the (1,0) levels (the relationship between *ortho* and *para* levels). Each energy level was weighted by the inverse of its uncertainty for the fit. The results of the fit and the 2σ uncertainties in the parameters are listed in Table 6. With this information, we adjusted the absolute value of the $G = 3n$ and $G = 3n \pm 1$ levels by the fit parameters, defining the nonphysical (0,0) level as zero energy. Please note that expression 10 does not behave properly outside of the energy levels used in the fit. As pointed out in Watson *et al.* (*17*), the effective Hamiltonian converges very slowly, making extrapolation difficult. One may be able to overcome this problem by using a

TABLE 6
Determined Molecular Constants for the Ground Vibrational State of H_3^{+a}

$E_{1,1}{}^{\dagger}$	64.1214 (116)
$E_{o-p}{}^{\dagger}$	22.8389 (56)
B	43.5605 (16)
C	20.6158 (20)
D_{JJ}	4.1400 (63) × 10^{-2}
D_{JG}	−0.7496 (14) × 10^{-1}
D_{GG}	0.3700 (14) × 10^{-1}
h_3	−0.4846 (26) × 10^{-5}
H_{JJJ}	0.6745 (86) × 10^{-4}
H_{JJG}	−0.2919 (28) × 10^{-3}
H_{JGG}	0.4145 (38) × 10^{-3}
H_{GGG}	−0.1942 (29) × 10^{-3}
L_{JJJJ}	−0.1015 (36) × 10^{-6}
L_{JJJG}	0.0769 (15) × 10^{-5}
L_{JJGG}	−0.1964 (27) × 10^{-5}
L_{JGGG}	0.1934 (31) × 10^{-5}
L_{GGGG}	−0.0594 (22) × 10^{-5}

[a] All values are in units of cm^{-1}. The numbers in parentheses are the 2σ uncertainties in the last digits. See text for a warning about the use of these values.

† Coefficients used to adjust the absolute energy of the experimental energy levels. These terms in Eq. (10) should be set to zero when the energy structure is simulated with the other coefficients.

Padè-type expression (*57–60*) as done in Ref. (*17*). The energy levels included in the fit, however, do behave properly, justifying our use of expression 10 to determine $E_{1,1}$ and E_{o-p}.

The values of the determined energy levels are listed in Table 3. Levels that were determined using only transitions verified with combination differences are marked with an asterisk. The values in parentheses correspond to the 2σ uncertainty (in the last digits) in the energy of each level due to the uncertainties in the transition frequencies used to construct the level. This can be thought of as the relative uncertainty for each level. There is an additional uncertainty in the systematic shift that must be considered when comparing the absolute energy of each level. The error in the value of the fit parameter $E_{1,1}$ must be included in the uncertainty for every level. The energy values for levels with $G = 3n$ also depend on the fit parameter E_{o-p} which adds an additional uncertainty which must be accounted for. However, the uncertainties in $E_{1,1}$ and E_{o-p} do not affect the calculations of transitions using these energy levels.

IV. APPLICATION OF RESULTS

The comprehensive list of assigned transitions and observed energy levels presented here will find many applications in the theoretical, laboratory, and astrophysical spectroscopy of H_3^+. In this section, we briefly outline two such applications: the search for the "forbidden" rotational spectrum and the evaluation of theoretical energy level calculations.

IV.1 Forbidden Rotational Transitions

At its potential minimum, H_3^+ is a perfect equilateral triangle with no dipole moment and consequently does not possess an allowed pure rotational spectrum. However, as pointed out by Pan and Oka (*61*), the centrifugal distortion of the molecule due to rotation will break its C_3 symmetry and induce a small dipole moment in the plane of the molecule. The resulting dipole moment will give rise to a weak rotational spectrum which obeys the selection rules $\Delta J = 0, \pm 1$ and $\Delta G = \pm 3$. The general theory of forbidden rotational transitions in polyatomic molecules was developed by Watson (*62*). In the case of a nonpolar molecule like H_3^+, the rotational transition $|J, G+3\rangle \leftarrow |J-1, G\rangle$ can be thought of as arising from a mixing between $|J, G+3\rangle$ in the ground state and $|J, G\rangle$ in the ν_2 state, which leads to an intensity borrowing from the allowed rovibrational transition $R(J-1, G)$ of the fundamental band.

The transition dipole of such rotational transitions is proportional to the derivative of the dipole moment with respect to the ν_2 coordinate. This quantity is much larger for H_3^+ than for other molecules—in fact, the line strengths of H_3^+ transitions are orders of magnitude larger than those of CH_4, which have been observed in the laboratory. Although the transition dipole moments are small by the usual standards of rotational spectroscopy (most ranging between 1 and 30 mD), they approach the infrared transition moment (158 mD) at higher J levels. With the rapid development of quantum cascade lasers in the far infrared, the rotational transitions of H_3^+ may soon be detected in the laboratory.

These rotational transitions are also of fundamental importance in the relaxation of H_3^+ in the interstellar medium, where their spontaneous emission lifetimes are shorter than collision times. Black (*63*) has pointed out that the flux of such H_3^+ transitions would be orders of magnitude lower than the thermal continuum from warm dust grains, making their detection infeasible. Draine and Woods (*64*) have suggested that H_3^+ rotational transitions may be observable in X-ray heated regions such as the starburst galaxy NGC 6240. Black (*63, 65*) has further suggested that, under the right conditions, the ${}^tR(3, 1)$ transition could become an astrophysical maser.

In order to enable (laboratory and astronomical) searches for the rotational spectrum of H_3^+, we have estimated the transition frequencies using our experimentally determined energy levels from Table 3. These are given in Table 7, along with the most recent intensity calculations by Neale *et al.* (*56*).

IV.2. Evaluation of Theoretical Calculations

Variational calculations of H_3^+ have substantially improved in recent years with the introduction of adiabatic, relativistic, and nonadiabatic corrections to the theory. The experimentally determined energy levels provide a powerful tool to diagnose the behavior of these calculations, and to compare and contrast the different computational approaches. Before doing so, we give a brief overview of the development of the most recent H_3^+ theoretical calculations.

IV.2.1. Computational Overview

The first calculations to effectively account for non-Born–Oppenheimer behavior did so by taking an *ab initio* potential energy surface (PES) and adjusting its fitting parameters to better match the experimental values. This semi-empirical approach was used by Watson (*55*) using the Meyer–Botschwina–Burton PES (*67*) and similarly by Dinelli *et al.* (*68*) using the Lie and Frye (*69*) PES. Later, Dinelli, Polyanski, and Tennyson (DPT) (*53*) introduced a slightly different approach: a new semiempirical surface is built by adding a purely *ab initio* Born–Oppenheimer PES to another surface (which they call the "adiabatic surface") of the same functional form whose parameters are determined from the fit to experimental data. In their work the PES of Röhse–Kutzelnigg–Jaquet–Klopper (RKJK) (*70*) was used as the Born–Oppenheimer surface. Energy level calculations using Watson's spectroscopically determined potential were reported by Majewski *et al.* (Maj94) (*27*), and Neale *et al.* (*56*) calculated energy levels using the DVR3D (*71*) suite from the DPT surface. The transitions calculated from these energy levels proved to be invaluable in the assignment of laboratory spectra.

The first attempt to calculate the adiabatic effects *ab initio* was by Dinelli *et al.* (Din95) (*72*), who added a mass-dependent function to the RKJK surface, which accounts for the diagonal

TABLE 7
Pure Rotational Transition Frequencies in the Ground Vibrational State Determined from Experimentally Determined Energy Levels

Label[a]	Frequency[b] (cm^{-1})	$\lvert\mu_{ij}\rvert$[c] (mD)	A_{ij}[c] (s^{-1})	Label[a]	Frequency[b] (cm^{-1})	$\lvert\mu_{ij}\rvert$[c] (mD)	A_{ij}[c] (s^{-1})	Label[a]	Frequency[b] (cm^{-1})	$\lvert\mu_{ij}\rvert$[c] (mD)	A_{ij}[c] (s^{-1})
$^tR(3,1)$	7.255 (10)	4.23†	2.78×10^{-9} †	$^nQ(5,3)$	190.756 (13)	17.7	6.80×10^{-4}	$^nR(5,2)$	553.791 (19)	9.24	5.37×10^{-3}
$^tR(6,3)$	9.261 (13)	14.7†	6.22×10^{-8} †	$^nQ(3,3)$	201.524 (09)	5.37	7.40×10^{-5}	$^nQ(7,6)$	555.500 (14)	13.6	9.93×10^{-3}
$^nP(8,7)$	29.655 (18)	22.3	3.59×10^{-6}	$^tR(7,2)$	220.891 (25)	22.7	1.98×10^{-3}	$^nR(7,1)$	568.013 (34)	20.0	2.59×10^{-2}
$^nP(5,5)$	39.453 (12)	8.33	1.10×10^{-6}	$^tR(6,1)$	261.550 (21)	17.3	1.93×10^{-3}	$^nQ(6,6)$	581.450 (11)	6.99	3.00×10^{-3}
$^tR(5,2)$	51.347 (16)	11.3	6.38×10^{-6}	$^nQ(8,4)$	286.320 (42)	29.3	6.35×10^{-3}	$^nR(4,3)$	612.525 (12)	5.86	3.03×10^{-3}
$^nQ(8,2)$	56.563 (47)	32.5	5.94×10^{-5}	$^nQ(7,4)$	298.423 (24)	22.1	4.05×10^{-3}	$^nR(6,2)$	621.074 (25)	13.1	1.47×10^{-2}
$^nQ(7,2)$	58.880 (28)	25.6	4.19×10^{-5}	$^tR(5,0)$	306.088 (14)	17.3	3.18×10^{-3}	$^nQ(8,7)$	666.334 (20)	15.4	2.19×10^{-2}
$^nQ(6,2)$	61.101 (21)	19.4	2.68×10^{-5}	$^nQ(6,4)$	310.199 (19)	15.5	2.25×10^{-3}	$^nR(7,2)$	683.456 (44)	17.4	3.44×10^{-2}
$^nQ(5,2)$	63.197 (16)	13.9	1.53×10^{-5}	$^nQ(5,4)$	321.347 (15)	9.83	1.00×10^{-6}	$^nQ(7,7)$	700.315 (17)	7.95	6.80×10^{-3}
$^nQ(4,2)$	65.107 (13)	9.17	7.27×10^{-6}	$^nR(2,2)$	325.482 (09)	1.52	3.51×10^{-5}	$^nR(6,3)$	743.039 (18)	14.8	3.25×10^{-2}
$^nQ(3,2)$	66.758 (11)	5.33	2.64×10^{-6}	$^nQ(4,4)$	331.549 (12)	4.97	2.81×10^{-4}	$^nR(4,4)$	748.280 (13)	2.16	7.51×10^{-4}
$^nQ(2,2)$	68.062 (07)	2.40	5.66×10^{-7}	$^tR(7,1)$	338.256 (26)	22.6	7.00×10^{-3}	$^nR(5,4)$	811.941 (18)	4.62	4.22×10^{-3}
$^nP(6,6)$	84.606 (10)	10.6	1.81×10^{-5}	$^nR(4,1)$	353.533 (15)	7.58	9.73×10^{-4}	$^nQ(8,8)$	815.622 (20)	8.93	1.35×10^{-2}
$^tR(4,1)$	95.383 (14)	8.07	2.16×10^{-5}	$^nR(3,2)$	405.563 (12)	3.47	3.23×10^{-4}	$^nR(6,4)$	870.172 (23)	7.69	1.41×10^{-2}
$^tR(7,3)$	100.112 (15)	21.5	1.65×10^{-4}	$^nQ(8,5)$	406.002 (31)	25.7	1.38×10^{-2}	$^nR(7,4)$	922.999 (41)	11.3	3.58×10^{-2}
$^nR(1,1)$	105.173 (04)	0.84	4.26×10^{-7}	$^nQ(7,5)$	423.844 (24)	18.3	8.00×10^{-3}	$^nR(5,5)$	950.783 (17)	2.34	1.75×10^{-3}
$^nP(7,7)$	128.566 (15)	13.1	9.85×10^{-5}	$^nR(5,1)$	429.493 (19)	11.1	3.62×10^{-3}	$^nR(6,5)$	1003.537 (23)	4.98	9.00×10^{-3}
$^tR(6,2)$	138.350 (20)	16.8	2.70×10^{-4}	$^nQ(6,5)$	441.343 (19)	11.7	3.72×10^{-3}	$^nR(7,5)$	1050.737 (30)	8.22	2.57×10^{-2}
$^tR(3,0)$	141.847 (10)	7.20	5.97×10^{-5}	$^tR(7,0)$	455.294 (20)	30.5	3.15×10^{-2}	$^nR(6,6)$	1146.211 (12)	2.48	3.34×10^{-3}
$^nP(8,8)$	170.887 (18)	15.7	3.40×10^{-4}	$^nQ(5,5)$	458.093 (13)	6.00	1.08×10^{-3}	$^nR(7,6)$	1189.072 (16)	5.22	1.63×10^{-2}
$^nQ(7,3)$	178.278 (19)	34.6	2.13×10^{-3}	$^nR(4,2)$	481.837 (15)	6.05	1.57×10^{-3}	$^nR(7,7)$	1336.994 (19)	2.57	5.61×10^{-3}
$^tR(5,1)$	180.395 (16)	12.4	3.36×10^{-4}	$^nR(6,1)$	501.093 (25)	15.2	1.05×10^{-2}				
$^nR(2,1)$	190.662 (09)	2.41	1.76×10^{-5}	$^nQ(8,6)$	533.460 (17)	21.0	2.09×10^{-2}				

[a] Labels for pure rotational transitions using the transition notation defined in Section III.2.
[b] Transition frequencies using energy data from Table 3. Reported uncertainty in the last digits (in parenthesis) is the quadrature sum of the uncertainties from Table 3.
[c] Dipole moments and Einstein coefficients from Ref. (*56*) except when marked otherwise.
† Dipole moment and Einstein coefficient taken from (*66*). The error in the reported values of A_{ij} and μ_{ij} have been corrected as pointed out in Ref. (*19*).

adiabatic contributions. Energy levels were calculated from the modified surface using the TRIATOM program suite (*73*). Results of these calculations gave the best *ab initio* values at the time, but were still inferior to the calculations using the fitted potentials.

Three years later Cencek, Rychlewski, Jaquet, and Kutzelnigg (CRJK) calculated a new *ab initio* PES (*12*), taking into account both the diagonal adiabatic and relativistic corrections, and claimed an accuracy of a few hundredths of a cm^{-1}. Jaquet *et al.* (Jaq98) (*74*) then calculated energies from this surface using TRIATOM. Jaquet *et al.* considered the different choices of mass: the average mass (proton mass plus 2/3 electron mass denoted **NU23**), nuclear mass (**NU**), atomic mass (**AT**), and reduced mass (**RE**). Using the same PES and DVR3D, Polyansky and Tennyson (Pol99) (*75*) calculated energy levels but attempted to simulate the nonadiabatic effects by using a different mass for rotational and vibrational motion. The rotational masses in their work were set to the nuclear value and the vibrational masses were set to a scaled atomic mass. Similarly, Jaquet (*15*) (Jaq99) calculated energies of the CRJK PES using NU23 masses for motion along the $R(\mathrm{H{-}H_2})$ and $r(\mathrm{H_2})$ coordinates and NU masses for motion along the $\theta(R, r)$ coordinate (Jacobi-type scattering coordinates), which he denotes as **NUVR**.

The coordinate systems used in Watson's and in TRIATOM and DVR3D calculations cannot handle the kinetic energy singularity that occurs at the barrier to linearity ($\sim$10,000 cm^{-1}) when using the usual Morse oscillator basis functions.[5] In 1989, Whitnell and Light (*79*) introduced hyperspherical coordinates, which properly treat the linear regions of the potential, to the calculations of H_3^+. Their methodology limited the calculations to $J = 0$ levels, but this limitation was later overcome by Bartlett and Howard (*80*). Initially, calculations using hypershperical coordinates were performed on the MBB PES (*79–82*) but later used the more accurate RKJK surface (Ali95) (*83*) and very recently the CRJK surface (Ali01) (*84*). Ali95 and Ali01 were

[5] At the barrier to linearity one of the moments of inertia vanishes, causing some of the terms in the kinetic energy Hamiltonian to become singular. The terms that become singular depend on the coordinate system used. These singularities impose boundary conditions on the basis functions which are not met when using the common coordinate systems with the convenient Morse oscillators. Instead, artificial barriers must be applied to the potential to keep the calculations from diverging (consequently these calculations are expected to give poor results at energies near and above the the barrier to linearity) (*52*), or alternative basis functions such as spherical oscillators (which are much harder to make converge) are used (*56*). References (*76–78*) discuss this computational problem in more detail.

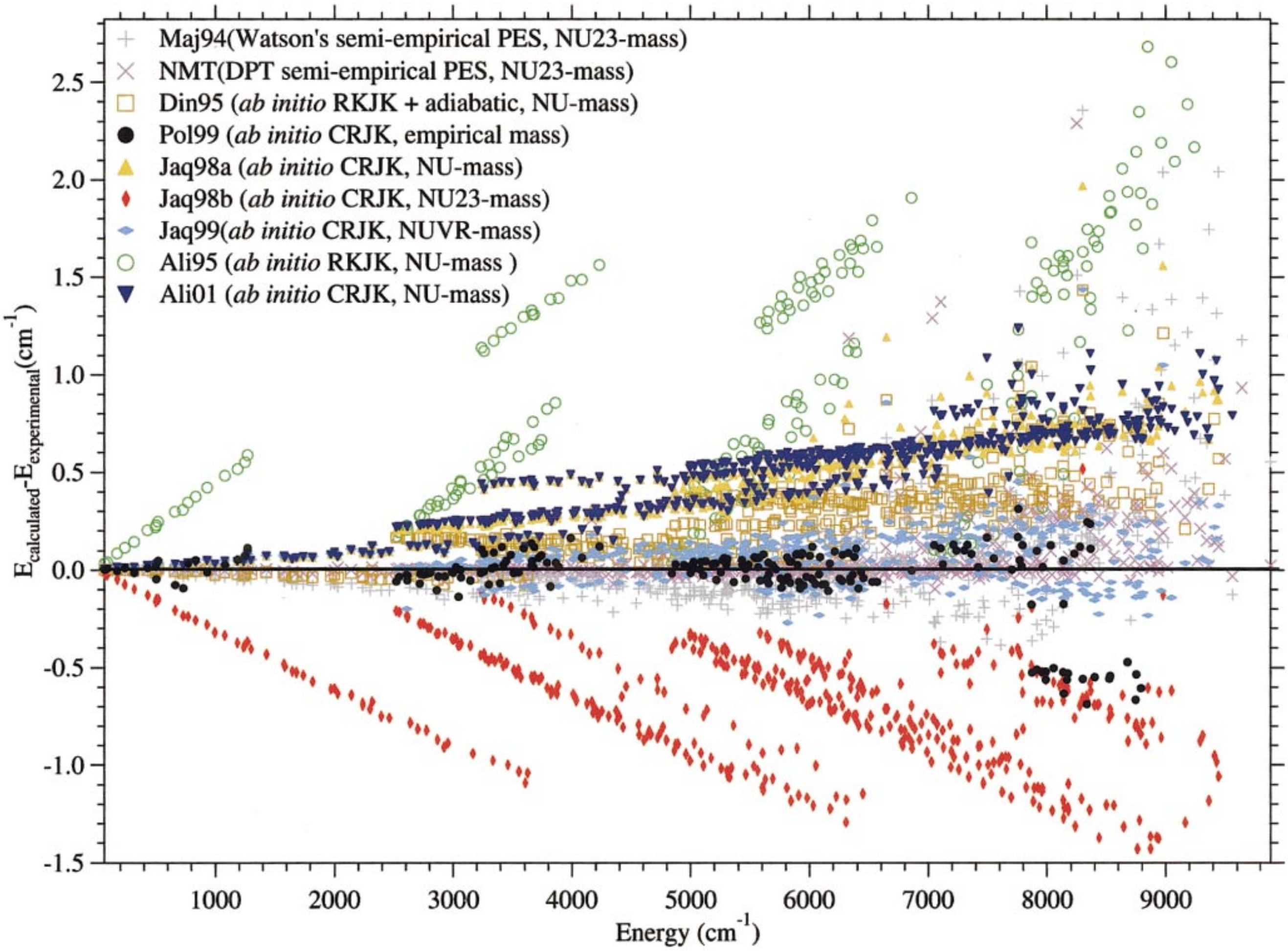

FIG. 3. Comparison of the latest calculated energy levels to experiment. Labels used in the legend are defined in Section IV.2. A printable color version of this figure is available online (*39*).

performed using nuclear masses, and in Ref. (*13*) the authors discuss the merits of this approach.

IV.2.2. Qualitative Comparison

To evaluate each of the calculations, we have plotted the difference in the calculated and experimental values for all experimentally determined levels (Fig. 3). This diagram clearly depicts the dependence of each calculation on vibrational state, rotational energy, and general scatter, which is useful in analyzing the effects of the various theoretical approaches. While a detailed analysis of each of these calculations is beyond the scope of this paper, we would like to make several qualitative remarks that are apparent from our comparison to experimental data:

1. Semiempirical vs ab initio approaches. The semiempirical calculations give the most accurate results at energies where data were available at the time of the fit. At higher energies, where experimental data was sparse, the agreement is considerably poorer. In these cases, *ab initio* calculations perform better due to their more systematic residuals.

2. PES and non-BO corrections. There is considerable difference between Din95 and Ali01 (and Jaq98a) which both use NU-mass, but use different PESs. This suggests that the introduction of relativistic effects (as done in CRJK, but not in RKJK + adiabatic) may increase the energy residuals or that the diagonal adiabatic contribution is treated differently in the two calculations.

3. Choice of mass. The large rotational dependence of the residuals of Jaq98b implies that NU23 calculations produce too large a moment of inertia and consequently underestimates the rotational dependence of the the energies. While the scaled mass systems (NUVR and empirical mass) give smaller residuals and a flatter rotational dependence, the NU-mass calculations seem to give much more systematic residuals. We cannot rule out the possibility that the scatter in Pol99 and Jaq99 is due to convergence problems.

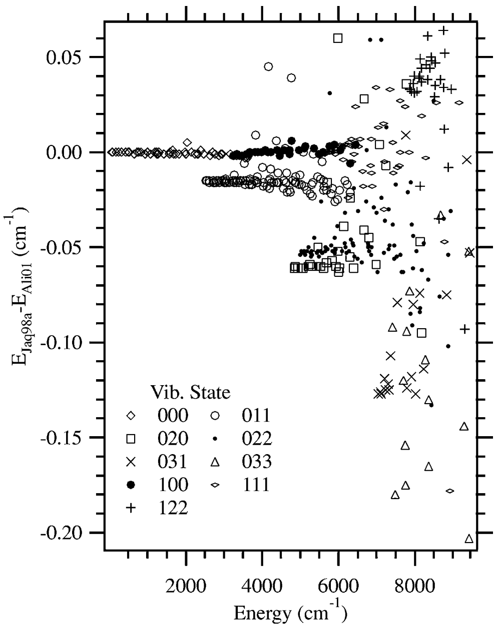

FIG. 4. Comparison of the energy level calculations of Ali95 and Jaq98a versus energy. Labels are defined in Section IV.2.

4. Differences in similar approaches. To verify that the observed differences in calculations are indeed due to the different approaches (and not simply due to variances from one group's calculation to another) we compared Ali01 and Jaq98a which use the same choice of mass and same PES. Their results compared quite nicely, confirming that the differences in each of the other calculations are significant. Upon close inspection, the differences between Ali01 and Jaq98a show a slight dependence on the vibrational state (see Fig. 4). This difference is on the order of 0.05 cm^{-1} and is significant when compared to the most accurate calculations of Pol99 and Jaq99. The source of this vibrational dependence is unclear, but may be due to the choice of coordinate system and/or basis set.

It is difficult to pinpoint the source of the differences in results between each computational approach due to the limited amount of computational data available. Further "experiments on the calculations" need to be performed—systematic comparisons of the energies calculated with different coordinate systems, basis sets, mass choices, and non-BO corrections will be necessary to iron out the remaining discrepancies. The experimentally determined energy levels will be instrumental in this endeavor as a powerful tool to probe the rotational, vibrational, and energy dependencies, as well as the general scatter of the various computational methodologies.

V. CONCLUSION

This work represents the end of a chapter in the laboratory spectroscopy study of H_3^+. Energy levels for nearly every vibrational band below the barrier to linearity have been probed and determined experimentally, many of them up to $J = 9$. Almost all of the observed lines have been assigned, and those that have not are probably due to species other than H_3^+ or have an error in the frequency measurement. While there are still transitions to be measured in this energy regime—higher J transitions in the $2\nu_2$ and $3\nu_2$ bands should be achievable with the better diode lasers and higher sensitivity available today—these will likely not lead to a better understanding of H_3^+ behavior at low energies or produce a qualitatively better diagnostic tool for theoretical calculations.

The next step for laboratory work is to make observations of states above the barrier to linearity, where some of the theoretical calculations are expected to break down. This is also the regime where the approximate quantum numbers begin to fail, and a new formalism may need to developed to describe such levels. Such experiments are currently underway in Chicago where the $5\nu_2 \leftarrow 0$ band is being studied with a high-power Ti:Sapphire laser.

ACKNOWLEDGMENTS

We gratefully acknowledge T. Oka for his assistance and encouragement during the course of this work. We also acknowledge J. K. G. Watson, J. Tennyson, R. Jaquet, and A. Alijah for many helpful conversations about theoretical calculations and for supplying us with their transition and energy level lists, in several cases before publication. Additionally, we appreciate their comments on an early version of the manuscript. B.J.M. wishes to thank the Fannie and John Hertz Foundation for their financial support. This work was also supported by NSF Grant PHYS-9722691 and NASA Grant NAG5-9583.

REFERENCES

1. B. J. McCall and T. Oka, *Science* **287,** 1941–1942 (2000).
2. T. Oka, *Phys. Rev. Lett.* **45,** 531–534 (1980).
3. T. R. Geballe and T. Oka, *Nature* **384,** 334–335 (1996).
4. B. J. McCall, T. R. Geballe, K. H. Hinkle, and T. Oka, *Astrophys. J.* **522,** 338–348 (1999).
5. B. J. McCall, T. R. Geballe, K. H. Hinkle, and T. Oka, *Science* **279,** 1910–1913 (1998).
6. L. Trafton, D. F. Lester, and K. L. Thompson, *Astrophys. J.* **343,** L73–76 (1989).
7. P. Drossart *et al. Nature* **340,** 539–541 (1989).
8. T. R. Geballe, M. F. Jagod, and T. Oka, *Astrophys. J.* **408,** L109–112 (1993).
9. L. M. Trafton, T. R. Geballe, S. Miller, J. Tennyson, and G. E. Ballester, *Astrophys. J.* **405,** 761–766 (1993).
10. J. E. P. Connerney and T. Satoh, *Philos. Trans. R. Soc. London A* **358,** 2471–2483 (2000).
11. K. H. Hinkle, R. R. Joyce, N. Sharp, and J. A. Valenti, *Proc. SPIE* **4008,** 720–728 (2000).
12. W. Cencek, J. Rychlewski, R. Jaquet, and W. Kutzelnigg, *J. Chem. Phys.* **108,** 2831–2836 (1998).
13. J. Hinze, A. Alijah, and L. Wolniewicz, *Polish J. Chem.* **72,** 1293–1303 (1998).
14. A. Aguado, O. Roncero, C. Tablero, C. Sanz, and M. Paniagua, *J. Chem. Phys.* **112,** 1240–1254 (2000).
15. R. Jaquet, *Chem. Phys. Lett.* **302,** 27–34 (1999).
16. T. Oka, *Phil. Trans. R. Soc. London A* **303,** 543–549 (1981).

17. J. K. G. Watson, S. C. Foster, A. R. W. McKellar, P. Bernath, T. Amano, F. S. Pan, M. W. Crofton, R. S. Altman, and T. Oka, *Can. J. Phys.* **62,** 1875–1885 (1984).
18. W. A. Majewski, M. D. Marshall, A. R. W. McKellar, J. W. C. Johns, and J. K. G. Watson, *J. Mol. Spectrosc.* **122,** 341–355 (1987).
19. W. A. Majewski, P. A. Feldman, J. K. G. Watson, S. Miller, and J. Tennyson, *Astrophys. J.* **347,** L51–L54 (1989).
20. T. Nakanaga, F. Ito, K. Sugawara, H. Takeo, and C. Matsumura, *Chem. Phys. Lett.* **169,** 269–273 (1990).
21. M. G. Bawendi, B. D. Rehfuss, and T. Oka, *J. Chem. Phys.* **93,** 6200–6209 (1990).
22. L.-W. Xu, C. M. Gabrys, and T. Oka, *J. Chem. Phys.* **93,** 6210–6215 (1990).
23. S. S. Lee, B. F. Ventrudo, D. T. Cassidy, T. Oka, S. Miller, and J. Tennyson, *J. Mol. Spectrosc.* **145,** 222–224 (1991).
24. L.-W. Xu, M. Rösslein, C. M. Gabrys, and T. Oka, *J. Mol. Spectrosc.* **153,** 726–737 (1992).
25. B. F. Ventrudo, D. T. Cassidy, Z. Y. Guo, S. Joo, S. S. Lee, and T. Oka, *J. Chem. Phys.* **100,** 6263–6266 (1994).
26. D. Uy, C. M. Gabrys, M.-F. Jagod, and T. Oka, *J. Chem. Phys* **100,** 6267–6274 (1994).
27. W. A. Majewski, A. R. W. McKellar, D. Sadovskií, and J. K. G. Watson, *Can. J. Phys.* **72,** 1016–1027 (1994).
28. A. R. W. McKellar and J. K. G. Watson, *J. Mol. Spectrosc.* **191,** 215–217 (1998).
29. S. Joo, F. Kühnemann, M.-F. Jagod, and T. Oka, The Royal Society Discussion Meeting on Astronomy, Physics, and Chemistry of H_3^+, London, February 9–10, 2000, poster.
30. B. J. McCall and T. Oka, *J. Chem. Phys.* **113,** 3104–3110 (2000).
31. C. M. Lindsay, R. M. Rade, Jr., and T. Oka, *J. Mol. Spectrosc.* **210,** 51–59 (2001).
32. L. Kao, T. Oka, S. Miller, and J. Tennyson, *Astrophys. J. Suppl. Ser.* **77,** 317–329 (1991).
33. B. M. Dinelli, L. Neale, O. L. Polyansky, and J. Tennyson, *J. Mol. Spectrosc.* **181,** 142–150 (1997).
34. J. K. G. Watson, *J. Mol. Spectrosc.* **103,** 350–363 (1984).
35. I. R. McNab, *Adv. Chem. Phys.* **89,** 1–87 (1995).
36. E. Teller, *Hand Jahrb. Chem. Phys.* **9,** 43–188 (1934).
37. J. T. Hougen, *J. Chem. Phys.* **37,** 1433–1441 (1962).
38. L. D. Landau and E. M. Lifshitz, "Quantum Mechanics (Non-relativistic Theory)," 3rd ed. Pergamon, Oxford, 1977.
39. Energy level figures and tables of the transitions, energy levels, labels, and unassigned lines are available at the authors' Web site (http://h3plus.uchicago.edu) and on IDEAL (http://www.idealibrary.com).
40. B. J. McCall, *Philos. Trans. R. Soc. London A* **358,** 2385–2401 (2000).
41. A. Carrington, J. Buttenshaw, and R. A. Kennedy, *Mol. Phys.* **45,** 753–758 (1982).
42. A. Carrington and R. A. Kennedy, *J. Chem. Phys.* **81,** 91–112 (1984).
43. A. Carrington, I. R. McNab, and Y. D. West, *J. Chem. Phys.* **98,** 1073–1092 (1993).
44. F. Kemp, C. E. Kirk, and I. R. McNab, *Phil. Trans. R. Soc. London A* **358,** 2403–2418 (2000).
45. G. Herzberg, *Trans. R. Soc. Can.* **5,** 3–36 (1967).
46. A. S. Pine, *J. Opt. Soc. Amer.* **66,** 97–108 (1976).
47. R. C. Woods, *Rev. Sci. Instr.* **44,** 282–288 (1973).
48. Y. Endo, K. Nagai, C. Yamada, and E. Hirota, *J. Mol. Spectrosc.* **97,** 213–219 (1983).
49. C. S. Gudeman, M. H. Begemann, J. Pfaff, and R. J. Saykally, *Phys. Rev. Lett.* **50,** 727–31 (1983).
50. S. Miller and J. Tennyson, *J. Mol. Specrosc.* **128,** 530–539 (1988).
51. T. Oka, *in* "Frontiers of Laser Spectroscopy of Gases" (A. C. P. Alves, J. M. Brown, and J. M. Hollas, Ed.) Vol. 234, pp. 353–377. Kluwer Academic, Amsterdam, 1988.
52. J. K. G. Watson, *Can. J. Phys.* **72,** 238–249 (1994).
53. B. M. Dinelli, O. L. Polyansky, and J. Tennyson, *J. Chem. Phys.* **103,** 10433–10438 (1995).
54. J. K. G. Watson, personal communication.
55. J. K. G. Watson, *Chem. Phys.* **190,** 291–300 (1995).
56. L. Neale, S. Miller, and J. Tennyson, *Astrophys. J.* **464,** 516–520 (1996).
57. S. P. Belov, A. V. Burenin, O. L. Polyansky, and S. M. Shapin, *J. Mol. Spectrosc.* **90,** 579–589 (1981)
58. A. V. Burenin, O. L. Polyanskii, and S. M. Shchapin, *Opt. Spektrosk.* **53,** 666–672 (1982).
59. A. V. Burenin, T. M. Fevral'skikh, E. N. Karyakin, O. L. Polyansky, and S. M. Shapin, *J. Mol. Spectrosc.* **100,** 182–192 (1983).
60. A. V. Burenin, O. L. Polyanskii, and S. M. Shchapin, *Opt. Spektrosk.* **54,** 436–41 (1983).
61. F.-S. Pan and T. Oka, *Astrophys. J.* **305,** 518–525 (1986).
62. J. K. G. Watson, *J. Mol. Spectrosc.* **40,** 536–544 (1971).
63. J. H. Black, *Philos. Trans. R. Soc. London A* **358,** 2515–2521 (2000).
64. B. T. Draine and D. T. Woods, *Astrophys. J.* **363,** 464–479 (1990).
65. J. H. Black, *Faraday Discuss.* **109,** 257–266 (1998).
66. S. Miller and J. Tennyson, *Astrophys. J.* **335,** 486–490 (1988).
67. W. Meyer, P. Botschwina, and P. Burton, *J. Chem. Phys.* **84,** 891–900 (1986).
68. B. M. Dinelli, S. Miller, and J. Tennyson, *J. Mol. Spectrosc.* **163,** 71–79 (1994).
69. G. C. Lie and D. Frye, *J. Chem. Phys.* **96,** 6784–6790 (1992).
70. R. Röhse, W. Kutzelnigg, R. Jaquet, and W. Klopper, *J. Chem. Phys.* **101,** 2231–2243 (1994).
71. J. Tennyson, J. R. Henderson, and N. G. Fulton, *Comput. Phys. Comm.* **86,** 175–198 (1995).
72. B. M. Dinelli, C. R. Le Sueur, J. Tennyson, and R. D. Amos, *Chem. Phys. Lett.* **232,** 295–300 (1995).
73. J. Tennyson, S. Miller, and C. R. Le Sueur, *Comput. Phys. Comm.* **75,** 339–364 (1993).
74. R. Jaquet, W. Chencek, W. Kutzelnigg, and J. Rychlewski, *J. Chem. Phys.* **108,** 2837–2846 (1998).
75. O. L. Polyansky and J. Tennyson, *J. Chem. Phys.* **110,** 5056–5064 (1999).
76. J. R. Henderson and J. Tennyson, *Chem. Phys. Lett.* **173,** 133–138 (1990).
77. S. Carter and W. Meyer, *J. Chem. Phys.* **96,** 2424–2425 (1992).
78. J. R. Henderson, J. Tennyson, and B. Sutcliffe, *J. Chem. Phys.* **96,** 2426–2427 (1992).
79. R. M. Whitnell and J. C. Light, *J. Chem. Phys.* **90,** 1774–1786 (1989).
80. P. Bartlett and B. J. Howard, *Mol. Phys.* **70,** 1001–1029 (1990).
81. S. Carter and W. Meyer, *J. Chem. Phys.* **93,** 8902–8914 (1990).
82. L. Wolniewicz and J. Hinze, *J. Chem. Phys.* **101,** 9817–9829 (1994).
83. A. Alijah, J. Hinze, and L. Wolniewicz, *Ber. Bunsenges. Phys. Chem.* **99,** 251–253 (1995).
84. A. Alijah and P. Schiffels, in preparation.